Molecular Rods and Stars through Cross-Coupling Reactions

Inauguraldissertation

zur
Erlangung der Würde eines Doktors der Philosophie
vorgelegt der
Philosophisch-Naturwissenschaftlichen Fakultät
der Universität Basel
von

David Muñoz Torres
von Spanien

Basel, 2013

Genehmigt von der Philosophisch-Naturwissenschaftlichen Fakultät der Universtität Basel auf Antrag von

Prof. Dr. Marcel Mayor

Prof. Dr. Edwin Constable

Basel, den 11.12.2012

Prof. Dr. Jörg Schibler

Original spanish version:

Caminante, son tus huellas
el camino, y nada mas;
caminante, no hay camino,
se hace camino al andar.
Al andar se hace camino,
y al volver la vista atras
se ve la senda que nunca
se ha de volver a pisar.
Caminante, no hay camino,
sino estelas en la mar.

English translation:

Wanderer, your footsteps are
the road, and nothing more;
wanderer, there is no road,
the road is made by walking.
By walking one makes the road,
and upon glancing behind
one sees the path
that never will be trod again.
Wanderer, there is no road,
only wakes upon the sea.

Antonio Machado
from "Proverbios y cantares" in Campos de Castilla. 1912

Acknowledgment

I wish to express my sincere gratitude to Prof. Dr. Marcel Mayor for allowing me total freedom to work during the last four years in his group. I also want to thank Prof. Dr. Edwin Constable for the co-examination of this thesis. A special thank goes to Thomas Eaton, Kathiresan Murugavel and Lukas Jundt for proofreading this manuscript. I am also thankful to the Swiss National Foundation and the University of Basel for their financial support.

I also take the opportunity to thank past and present colleagues for their synthetic assistance and fruitful discusions: Thomas Eaton, Carla Cioffi, Kathiresan Murugavel, Umut Soydaner, Nicolas Weibel, Lucas Jundt, Srboljub Vujovic, Adnan Ganic, Anne-Florence Stoessel, Silvia Bellotto, Yann Leroux and Sandro Gabutti.

In the everyday life of a chemist the work cannot be done alone and I want to thank the people, who helped me in my research: Daniel Haussinger and his team for some NMR measurments, Heinz Nadig for the mass spectrometry measurements and Werner Kirsch for elemental analysis.

Teaching to students in the lab courses has always been a pleasure and I want to thank Prof. Antoinette Chougnet for giving me this opportunity. Brigitte Howald is also thanked for her administration work as well as the Werkstatt with a special thank to Francis Cabrera and Manuel Hermida. For her enthusiasm during the unisport courses, I want to thank Monica Dressler and for the nice chats before and after the sport lessons I send my thanks to Roger Clerc.

Having done part of my studies in Fribourg I want to express my gratitude to some former colleagues and friends: Karin Marxer, Ursula Streit, Gaetan Gozel, Michael Bersier, Nicolas Fragnière, Patrick Tondo, Daniella Bossi, Roger Mafua, Martine Poffet, Isak Alimi, Cédric Bürki.

Finally I send a warm thanks to Sandra Staudacher and Luca Preite, to my girlfriend Barbara Cecil, to my brother Iván and my parents.

Abstract

In the quest of smart electronic devices the society faces the challenge of miniaturization. Chemists, who know how to manipulate the smallest but still diverse bricks of the matter, namely the molecules, have the adequate tools for this challenge. A better understanding of the rules applying in the nanoworld is essential to build any functional molecular device construction. In this work three different approaches to answer these questions were followed.

The first one is the synthesis of a molecule suited to integrate a junction of two nanotube electrodes. When a voltage is applied the molecular bridge emits a characteristic light. The originality of this approach lies in the particularity of having an electroluminescence produced by a single molecule. Several molecular rods suiting this set-up were synthesized.

The second approach deals with surface functionalization. A surface network with hexagonal cavities is filled with three-arm star shaped molecules with different sizes and functionalities. The structures of these targets had to be adapted to solve size matters as well as their behavior in the cavities. The dimensions of the stars were successively reduced in order to match the pore size and in a second step decorated with hydroxy groups to slow down or ideally stop their rotation in the hexagonal pores.

To explore the potential and the limitation of molecules as electronic devices, a two terminal electronic component was targeted. The third approach describes indeed the synthesis of a molecule that acts as a single molecular diode meant to have the same properties as the macroscopic one, namely it lets circulate the current in only one direction. These rectification properties were studied by bridging two gold electrode with the molecular diodes.

These three projects geared towards the design of physical properties on a single molecule level, demonstrate the scientific challenges as well as the potential of tailor-made molecular building blocks in future molecular devices.

Résumé

La société actuelle est en quête d'objets intelligents toujours plus petits et performants tels des téléphones ou autres ordinateurs. Pour y parvenir, les outils de fabrication dont nous disposons aujourd'hui vont trouver leur limites et le développement d'une nouvelle génération d'outils est inévitable. Pour afronter ce défit le chimiste possède les outils adéquats car il sait manipuler les plus petites briques de la matière, les molécules. Avant d'être capable de construire un objet intelligent avec ces briques que sont les molécules il doit d'abord comprendre les règles de fonctionnement dans ce monde de l'infiniment petit. Dans l'optique d'accroître nos connaissance en la matière, ce travail décrit trois différentes approches.

Dans un premier temps nous avons choisi de fabriquer une molécule pensée pour former une jonction moléculaire. Cette unique molécule connecte deux électrodes de nanotubes de carbone et émet de la lumière si une différence de potentiel est appliquée. L'originalité de cette approche réside dans la mesure d'une l'électroluminescence émanant d'une unique molécule.

Le deuxième sujet d'étude décrit dans ce travail traite de fonctionnalisation de surfaces. En effet, nous avons produit une série de molécules en forme d'étoile à trois branches ou quatre branches qui s'intègrent dans un réseau fait de pore hexagonaux sur une surface. Ce réseau est construit par l'assemblage de deux sortes de molécules liées entre elles par des pont hydrogène. La série de molécule produite est constituée de molécules de différentes tailles et fonctionnalités afin de trouver le meilleur candidat pour intégrer les pores et étudier leur comportement sur la surface.

Finalement, en s'inspirant de la composant électroniques qu'est la diode, nous avons produit son équivalent moléculaire. En plaçant cette molécule entre deux electrodes nous avons étudié sa capacité à se comporter comme une diode, c'est à dire à ne conduire le courant que dans une seule direction.

Tous ces sujets d'études ont pour point commun de vouloir augmenter notre connaissance sur la matière avec l'espoir de voir dans un futur proche des molécules comme composantes à part entière de circuits électroniques.

List of abbreviations

CPDIPSA: [(3-cyanopropyl)diisopropylsilyl]acetylene
CPDMSA: [(3-cyanopropyl)dimethylsilyl]acetylene
DABCO: 1,4-diazabicyclo[2.2.2]octane
DME: 1,2-dimethoxyethane
DMF: dimethylformamide
r.t.: room temperature
GPC: gel permeation chromatography
MAOS: microwave-assisted organic synthesis
OPE: oligo(phenylene ethynylene)
OPV: oligo(phenylene vinylene)
PTCDI: perylene tetracarboxylic diimide
PTLC: preparative thin layer chromatography
rec-GPC: recycling gel permeation chromatography
SAMs: self-assembled monolayers
SMNs: supramolecular networks
SWNTs: single walled carbon nanotubes
TBAF: tetra-n-butylammonium fluoride
TBME: tert-butyl methyl ether
THF: tetrahydrofuran
TIPSA: triisopropylsilylacetylene
TLC: thin layer chromatrography
TMEDA: N,N,N',N'-tetramethyl-ethane-1,2-diamine
TMS: trimethylsilane
TMSA: trimethylsilylacetylene
Tr: triphenylmethyl
UPD: underpotential deposition
UHV: ultra high vacuum

Contents

Part I

General Introduction

Chapter 1

Aim of the Work

The original question that we asked ourselves in the early days of this research work was not "How can we build a device that has molecules as functional units?" rather "How do molecules behave at the nanoscopic scale, why do they behave that way and is it possible to integrate them in nanoscopic devices?" As matter architects, chemists have the tools to answer these questions by designing and synthesizing new molecules tailor made for specific functions. Their close collaboration with physicists allows them to investigate molecular properties at the nanoscale, and their precious feed-backs about possible improvements drives them towards success.

The quest of understanding the relations between the structure of a molecule and its properties is at the core of this PhD dissertation. This work describes the design and synthesis of several molecular architectures used in various set-ups to study their properties. During the four years of research several projects were carried out covering different approaches to the same question. The synthesis of several molecular architectures was initiated or completed. Amongst them are a molecular rod meant to transport electrons through a membrane bilayer, a fully conjugated molecular rod used in a single molecular junction, a star shaped molecule meant to bridge a three electrode set-up, a macrocycle, a molecular rod for electroluminescence experiment in a nanotube junction, a star-shaped molecule for a host-guest surface network and a molecular rectifier. In a desire for clarity, only the last three projects mentioned above will be discussed in this dissertation.

These investigations proceeded between October 2008 and September 2012. The syntheses were performed by the author and all the set-up investigations were accomplished by our collaborators around the world.

Chapter 2

Chemistry: Architecture of the Nanoworld

2.1 Cross-Coupling Reactions: Ideal Tools for the Synthesis of Molecular Rods and Stars

Metal catalyzed cross-coupling reactions have become one of the most powerful methods for the formation of C-C bonds in organic chemistry. This family of reactions includes metal catalyzed couplings of two different moieties. These reactions are nowadays widely employed for numerous applications.[1] Three pioneers in this field, namely Ei-ichi Negishi, Akira Suzuki and Richard F. Heck, were awarded with the Nobel Prize in Chemistry in 2010 "for palladium-catalyzed cross-couplings in organic synthesis". Palladium is nowadays the most versitile metal catalyst for its numerous advantages over the other metals for its greater reactivity, selectivity and functional group tolerance. Here are listed some examples of metal catalyzed cross-coupling reactions:

Kumada (1972): $R^1MgX + R^2X \xrightarrow{NiL_n} R^1R^2$

Heck (1972): $ArX + RCH{=}CH_2 \xrightarrow[base]{PdL_n} ArCH{=}CHR$

Sonogashira (1975): $ArX + RC{\equiv}CH \xrightarrow[base]{PdL_n,\ Cu(I)} ArC{\equiv}CR$

Negishi (1977): $R^1{-}X + R^2{-}Zn{-}X \xrightarrow{PdL_n \text{ or } NiL_n} R^1{-}R^2$

Stille (1978): $RCH{=}CHOTf + R^1R^2C{=}CSnR^3_2 \xrightarrow{PdL_n} RCH{=}CHCH{=}CR^1R^2$

Suzuki(1979): $Ar^1X + Ar^2B(OH)_2 \xrightarrow[\text{base}]{PdL_n} Ar^1Ar^2$

Buchwald-Hartwig (1994): $ArX + R^1NHR^2 \xrightarrow[\text{base}]{PdL_n} Ar^1NR^1R^2$

The present chapter focuses on the two most important metal catalyzed cross-coupling reactions in the synthesis of molecular rods and stars, namely the Sonogashira and Suzuki reactions.

2.1.1 Sonogashira Cross-Coupling Reaction

One of the most powerful methods to introduce a C≡C bond in a molecule is the Sonogashira cross-coupling reaction published in 1975 by Kenkichi Sonogashira.[2] Since its discovery, it has found applications in different fields such as total synthesis[3,4] and molecular electronics[5] amongst many others. In total synthesis, the Sonogashira reaction is particularly used for the synthesis of 1,5-diyn-3-ene moieties, a structure found in many anticancer antibiotics.[6] This method has also been used to build complex conjugated architectures[7] such as shape persistent macrocycles[8] and molecular wires.[9] Recently a review focusing particularly on the construction of nanoscale structures using the powerful versatility of Sonogashira reaction was published.[10]

The Sonogashira cross-coupling reaction is a combination of two other cross-coupling reactions, namely Castro-Stephens coupling[11] and Heck alkynylation.[12] An advantage of this reaction is the formation of a new sp^2–sp bond under milder conditions, tolerating a wide range of functional groups. It is widely used due to higher conversions and its ease of use. Since its discovery in 1975, many developments have been made but the most commonly used system to date is a slightly modified version of the original procedure:

$$PhI + HC{\equiv}CH \xrightarrow[Pd(PPh_3)_2Cl_2,\ CuI]{Et_2NH} PhC{\equiv}CPh$$

Although many catalytic systems have been developed during the intervening years, most of the synthetic procedures reported in the literature involve an aryl bromide or iodide, a terminal alkyne (often a protected acetylene), an amine base such as Et_3N, Et_2NH or $^iPr_2NH$, $Pd(PPh_3)_2Cl_2$ or $Pd(PPh_3)_4$ as a catalyst, CuI as a co-catalyst and THF as a solvent:

$$ArI + RC{\equiv}CH \xrightarrow[Pd(PPh_3)_2Cl_2 \text{ or } Pd(PPh_3)_4,\ CuI]{Et_3N,\ Et_2NH \text{ or } {}^iPr_2NH} ArC{\equiv}CR$$

What comes now is a selection of important aspects of the Sonogashira

reaction, notably its mechanism, the reactivity and chemoselectivity of the moieties to be coupled and the different acetylene protecting groups available. These aspects have been the subject of many studies summarized in excellent reviews.[13–15]

Mechanism

The mechanism of the reaction is not yet completely understood and is subject to many discussions. Different mechanisms are possible depending on the system used, but the commonly accepted one contains two cycles involving a palladium catalyst and a copper co-catalyst.

The main cycle (A in scheme 2.1) involves a palladium catalyst and has three steps: oxidative addition, transmetalation, reductive elimination. The rate determining step of the reaction is either the oxidative addition or the transmetalation depending on the nature of the aryl halide and the acetylene involved in the reaction.The catalyst active in the cycle is a 14 e^- complex of Pd(0) formed after reduction of $[Pd(II)L_n]$ in $[Pd(0)L_2]$. Oxidative addition to Pd(0) complex by aryl halide ArX gives $[Pd(II)ArL_2X]$ followed by transmetalation where the halide is replaced by the acetylide coming from the copper co-catalyst cycle giving $[Pd(II)(C{\equiv}CR)ArL_2]$. The next step is the

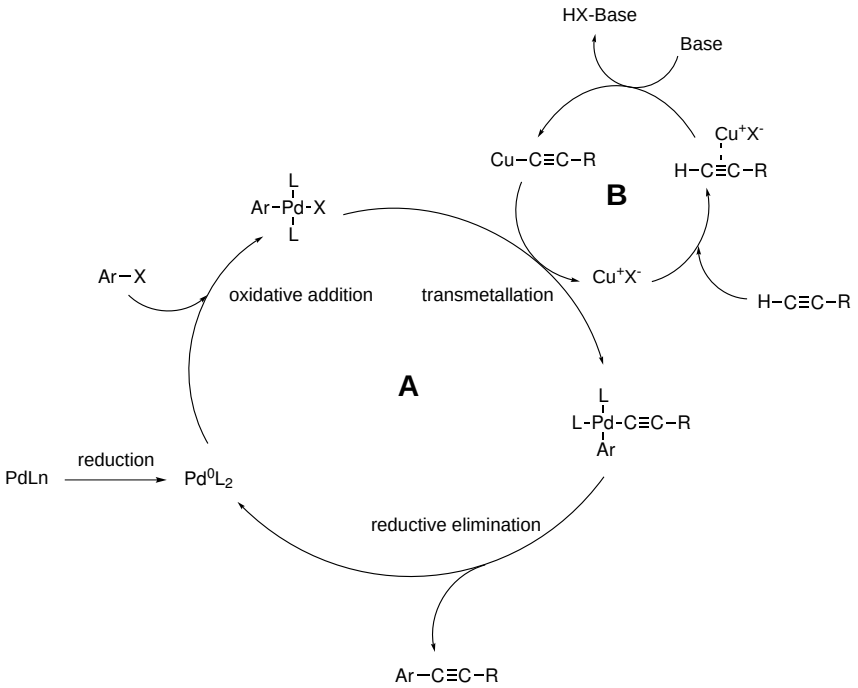

Scheme 2.1: Mechanism of the Sonogashira reaction

reductive elimination of Pd(II) to Pd(0), the later starting a new catalytic cycle and releasing the desired product ArC≡CR. The copper cycle (B in scheme 2.1) plays an important role in the deprotonation of acetylene since the base is not strong enough. Cu(I) complexes to the triple bond yielding a more acidic acetylene proton which is removed by the base (in general an amine).

A second [Cu–C≡CR] complex might be involved in the transmetalation step which would form [Pd(II)$(C{\equiv}CR)_2L_2$] releasing the active catalyst [Pd(0)L_2] and a homocoupled product RC≡C–C≡CR. The latter is a major side product in Sonogashira cross-couplings and a major product in Glaser coupling mediated by Cu(I) in the presence of O_2.[16]

Reactivity and Chemoselectivity

Although there are no general rules to predict the reactivity of two moieties in a Sonogashira reaction, one can draw certain trends based on the rate and efficiency of the reaction as it depends on many influencing factors such as the catalytic cycle, nature of both the ArX reagent and Pd ligands. Other factors like the nature of the base or the presence of a co-solvent can also influence the evolution of the reaction. The nature of the ArX bond in general dictates the rate of the reaction since it strongly influences the oxidative addition which is the rate limiting step in most cases. The oxidative addition of ArX to palladium is strongly dependent on the strength of the Ar–X bond. The stronger this bond, the slower will be the oxidative addition. In general ArI can be inserted at room temperature, ArBr needs higher temperatures and cross-coupling with ArF are rare and need very particular catalysts. Aryl substituents also play an important role in the oxidative addition since electron withdrawing groups increases the reaction rate compared to electron donating groups. Another important effect is the steric bulk at the 2,6 positions. Aryl halides substituted at these positions show slower reaction rates due to a greater difficulty for the palladium to insert at such "hindered" position.

Although an extensive work has been done and is still on-going to find the ligand giving the best results, PPh_3 is by far the most prevalent for palladium catalysts. Their relative low price, direct availability from chemical providers and efficiency in most common reactions are certainly the main reasons. Other commonly used ligands are N-heterocyclic carbenes (NHC), amines or palladacycles. Studies have shown that bulky and electron rich ligands (e.g. $P(tBu)_3$, $P(Cy)_3$) give better yields and have greater reaction rates, probably due to the formation of a [Pd(II)ArL_1X] complex that favors the reaction.[17,18]

Other factors including the nature of the base or the solvent have a minor influence in the catalytic cycle. The most common used bases are Et_3N, Et_2NH and $^{i}Pr_2NH$ but some stronger bases like piperidine or pyrrolidine are also reported. Solvents (THF, DMF and toluene) do not influence the evolution of the reaction in a significant way, although positive effects have been shown when a solvent is used in combination with the amine, generally explained by a solubility factor. The order of reactivity summarized below doesn't have to be taken as a rule applicable for each reaction but more like a general tendency:

Ar–X (bond strength): Ar–I > Ar–Br = Ar–OTf > Ar–Cl > Ar–F
Ar–X (substituents): EWG > H > EDG
R–C≡C–X (substituents): EDG > H > EWG
Ar–C≡C–H (substituents): EWG > H > EDG
PdL_n (electronic effect of ligands): e^- rich > e^- rich
PdL_n (size of ligands): bulky > not bulky

Most Common Protected Acetylenes

Probably the most important reason for the revival of acetylene chemistry is that protected acetylenes are commercially and readily available. These are processable building blocks while acetylene gas tends to explode, and is very difficult to handle. Therefore they are very handy tools to introduce triple bonds in chemical compounds.

There is a variety of protecting groups,[19] the most common ones being (trimethylsilyl)acetylene (TMSA) and its polar analogue [(3-cyanopropyl)-dimethylsilyl]acetylene (CPDMSA)[20] which are deprotected under mild basic conditions, in general K_2CO_3 or KOH in the presence of H_2O or MeOH. Another method is by using a F^- source such as TBAF in THF. A more robust couple of protected acetylene is (triisopropylsilyl)acetylene (TIPSA) and its polar analogue [(3-cyanopropyl)diisopropylsilyl]acetylene (CPDIPSA)[21] which are usually deprotected with TBAF in THF. An alternative to the silyl protected acetylene, the hydroxy protected acetylenes like (hydroxymethyl)-acetylene (HOMA) are deprotected with MnO_2 and KOH and (2-hydroxy-propyl)acetylene (HOPA) are deprotected by heating with alkali metal hydroxides or hydrides in refluxing toluene. Furthermore polar acetylenes such as CPDMSA, CPDIPSA, HOMA and HOPA have the advantage to facilitate chromatographic purifications since the coupled product has a different polarity than the starting compound.

In the synthetic route of OPE conjugated rods, the moities often have to be functionalised with two protected acetylenes. The orthogonality of those protecting groups is fundamental to obtain selective reactions. Silyl protect-

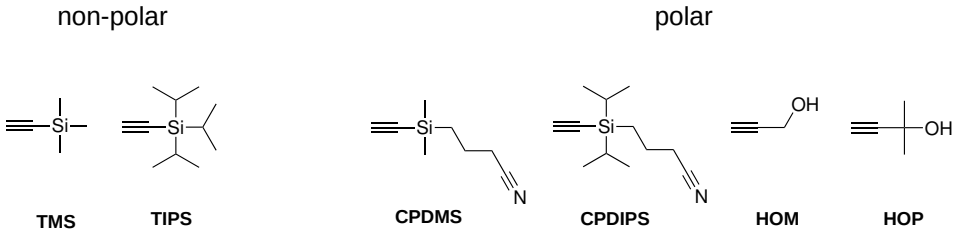

Scheme 2.2: Common protected acetylenes used in organic synthesis

ing groups (TIPS, TMS, CPDMS, CPDIPS) are orthogonal with hydroxy protecting groups (HOM, HOP). If two silyl protecting groups are chosen they sequential lability might be of great use. This is only the case if the TMS acetylene is deprotected before the TIPS acetylene with basic conditions (e.g. K_2CO_3 or KOH). If a fluorine source would be used, both groups would be deprotected.

If orthogonal protecting groups cannot be introduced in a specific situation, a way to overcome this problem is to use a statistical deprotection. Although this method leads in general to a mixture of starting compound, monodeprotected and the doubly deprotected products which decrease significantly the yields, it has proven to be a good alternative in the synthesis of a giantocycle.[22]

Alternatives for Difficult Cases

When the adjustments of the parameter influencing the catalytic cycle do not lead to the desired effects there are still alternatives to perform the coupling. Examples that have proven to give good results are the copper free reaction, the Negishi reaction, the in situ acetylene deprotection, or the microwave assisted Sonogashira reaction (section 2.2).

One of the major causes of low yields in Sonogashira reactions are alternative reactions like the diacetylene coupling (Glaser type reaction). The presence of copper in the reaction mixture and molecular oxygen O_2 are responsible for this side product formation. To disable this reaction, it can be performed under oxygen free atmosphere and "copper free"medium. Examples of copper free reactions have been reported, but the results are still under debate since it has been proven that traces of copper are often present in the palladium catalyst. The copper free reactions performed would be in fact reactions with extremely low copper loadings. However what has been shown is that bulky palladium ligands favor copper free reactions. To have an oxygen free atmosphere, a particular care has to be taken in degassing the reaction mixture. One of the most efficient method is known as freeze-

pump-thaw. In this method, the solvent is frozen with liquid nitrogen, the air is then removed by a HV pump for a couple of minutes and the flask is warmed to room temperature. This cycle is repeated three times and finally the reaction mixture is filled by an inert gas (e.g. nitrogen).

Negishi cross-couplings are also an interesting alternative since alkynylzinc are less prone to homodimerization and are also suited for steric demanding cases. A representative example is shown in the synthesis of hexaethynylbenzene where Negishi and Sonogashira cross-coupling reactions are used in combination.[23]

$$\mathrm{Ar{-}X + R{-}C{\equiv}C{-}Zn{-}X \xrightarrow{PdL_n} Ar{-}C{\equiv}C{-}R + ZnX_2}$$

A concentration decrease of the reacting free acetylene can diminish the formation of dyines and therefore increase the yields of Sonogashira reactions. The first way to do so is by adding slowly the acetylene into the reaction mixture which "forces" it to react with the aryl iodide. An alternative is the formation of the free acetylene in the reaction mixture by an in situ deprotection. Shultz et al. applied this method to synthesize a bisporphyrin[24] and haley et al. also used in situ deprotections in the synthesis of nanostructures for the formation of diacetylene macrocycles.[25] The same technique has been used in the one pot symmetrical diaryl synthesis, named "sila"-Sonogashira, developed by Brisbois and Grieco[26] using the DBU/water couple to in situ deprotect the acetylene. This approach also avoids the TMS-alkyne deprotection and purification steps.

$$\mathrm{Ar{-}X + (CH_3)_3Si{-}C{\equiv}C{-}H \xrightarrow[Pd(PPh_3)_2Cl_2,\ CuI]{DBU,\ H_2O} Ar{-}C{\equiv}C{-}Ar}$$

Other methods for acetylene formation

The introduction of the triple bonds in organic synthesis is generally done using the previously mentioned Sonogashira cross-coupling reaction of halides with commercially available protected acetylenes. When for some reason the acetylene cannot be inserted by this method an alternative strategy is its formation by transformation of a functional group. Their formation from alkylhalides by double elimination,[27] from alkenes by halogenation and double elimination,[27] by hydrox-(oxophosphoryl) elimination[27] or from an aldehyde by Ohira-Bestmann modification of the Seyfert-Gilbert homologation[28] have been reported. These methods are often not appropriate for the synthesis of OPEs. Below are described two transformations commonly used in the synthesis of conjugated molecular rods:

A modification of the Corey-Fuchs reaction[29] transforms an aldehyde into a TMS protected acetylene via the formation dibromoalkene.

$$\mathrm{Ar{-}CHO} \xrightarrow[\mathrm{CH_2Cl_2,\ 0\ ^\circ C\ to\ r.t.}]{\mathrm{CBr_4,\ PPh_3}} \mathrm{Ar{-}C{=}CBr_2} \xrightarrow[\mathrm{THF,\ -78\ ^\circ C\ to\ r.t.}]{\mathrm{LDA,\ TMSCl}} \mathrm{Ar{-}C{\equiv}C{-}TMS}$$

The transformation of an acetyl aryl to a protected acetylene was used for the formation of long OPEs.[9] Here the acetyl forms the enolate with LDA followed by the addition of diethyl chlorophosphonate wich forms a strong O-P bond. Subsequent addition of LDA followed by TMSCl forms the protected acetylene.

$$\mathrm{Ar{-}C(O)CH_3} \xrightarrow[\mathrm{3.\ LDA;\ 4.\ TMSCl}]{\mathrm{1.\ LDA;\ 2.\ (C_2H_5O)_2P(O)Cl}} \mathrm{Ar{-}C{\equiv}C{-}TMS}$$

2.1.2 Suzuki Cross-Coupling Reaction

Another very important palladium catalyzed cross-coupling reaction is the Suzuki reaction.[30,31] In this reaction, an 1-alkenylboron reacts with an organic electrophile.

$$\mathrm{R^1{-}X{+}R^2{-}CH{=}CH{-}B(OR)_2} \xrightarrow[\mathrm{PdL_n,\ NaOH\ or\ K_2CO_3}]{\mathrm{THF/H_2O,\ toluene/EtOH\ or\ DMF}} \mathrm{R^2{-}CH{=}CH{-}R^1}$$

This type of reaction has been used in areas such as total synthesis where it is often used to form conjugated dienes of high stereoisomeric purity.[3] The Suzuki coupling was used by Nicolaou in an important step toward the synthesis of vancomycin[32,33] which is an antibacterial agent. In polymer science, this reaction has been first used by Schülter et al. to synthesize poly(p-phenylenes).[34] This method of Suzuki polycondensation was then extensively applied.[35]

In the following paragraphs, important aspects of the Suzuki reaction will be discussed. To obtain a deeper view on the use of this cross-coupling reaction of organoboron derivatives with organic electrophiles the reader is referred to excellent reviews.[36–38]

Mechanism

The mechanism of the Suzuki reaction is similar to any other metal catalyzed cross-coupling reaction. Accordingly all the discussion done in the subsection dedicated to the Sonogashira reaction (subsection 2.1.1) applies also here. The following reactivity series applies also here, starting with

the more reactive: Ar–I > Ar–Br = Ar–OTf > Ar–Cl > Ar–F. Electron withdrawing groups (EWG) on the ArX increase their reactivity. Palladium complexes such as $Pd(PPh_3)_4$, $Pd(PPh_3)_2Cl_2$ or $Pd(OAc)_2$ are used as catalyst and when these complexes bear bulky ligands the reactivity is again increased. The first step of the catalytic cycle is the oxidative addition of PdL_2 with ArX. This step is followed by the transmetalation step where the organoboronic acid or boronate replaces the halide of the PdL_2ArX complex to form PdL_2ArR that liberates the product by reductive elimination. The active palladium catalyst is reformed and can start another cycle (scheme 2.3). The catalytic cycle is often influenced by factors such as the nature of the base or the steric hindrance in the boronic acid or boronate. Boranes are not very nucleophilic and hence a base is needed. When stronger bases (e.g. NaOH, NaOMe) are used, the reaction works better with THF/water as solvent but when weaker bases (e.g. K_2CO_3 or K_3PO_4) are employed DMF suits better as solvent. The base plays a particularly important role in the transmetalation step of the catalytic cycle since it activates the borate by coordination.[39,40] Moreover the steric hindrance caused by substituents at the ortho position of the aryl boronic acids slow down the transmetalation step. Anhydrous condition are required for such cases.

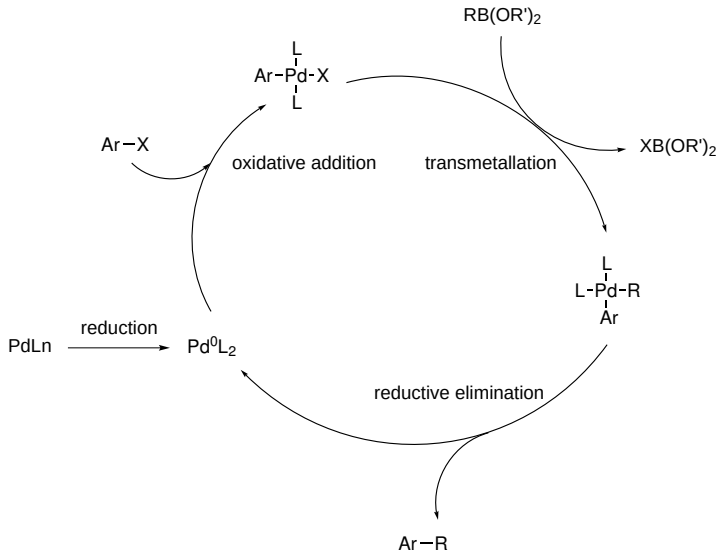

Scheme 2.3: Mechanism of Suzuki cross-coupling reaction

2.2 Microwave Assisted Organic Synthesis

2.2.1 Basic Principles

Since the late 90s, the amount of publications of microwave-assisted organic synthesis (MAOS) has increased exponentially. At present, MAOS has become a common tool in organic chemistry research labs.[41–43] It is used in the synthesis of natural products or material science and has been the topic of several books.[44,45]

Kappe et al. demonstrated that MAOS offers various advantages over traditional oil bath synthesis by reducing significantly the reaction times, delivering cleaner reaction mixtures, increasing overall yields and improving reproducibility.[41] Many studies have been made to understand the differences observed between traditional heating (oil bath) with microwave heating. It is commonly agreed by the scientific community that the rate enhancement observed with MAOS is purely a thermal/kinetic effect coming from the rapid heating of the reaction mixtures and the higher temperatures (above boiling point) that can be reached. The ability of the medium to absorb microwaves and therefore to heat is given by the loss tangent : $\tan\,\delta = \varepsilon''/\varepsilon'$ with ε'' the dielectric loss (efficiency of the electromagnetic radiation conversion into heat) and ε' the dielectric constant (polarizability of the molecule). Solvents with high loss tangent convert more rapidly the electromagnetic wave into heat. The absorption can be classified as follows: high ($\tan\,\delta > 0.5$)(e.g. ethylene glycol, ethanol, DMSO, methanol), medium ($0.1 < \tan\,\delta < 0.5$)(e.g. 1,2-dichlorobenzene, acetic acid, DMF, water, 1,2-dichloroethane), and low ($\tan\,\delta > 0.1$)(e.g. $CHCl_3$, ethyl acetate, THF, CH_2Cl_2, toluene, hexane). Even solvents with low $\tan\,\delta$ are permitted in microwave reactions since often polar reagents or catalysts absorb the microwaves producing heat.

2.2.2 Microwave Assisted Cross-Coupling Reactions

Microwave assisted cross-coupling reactions are one of the most important and most studied reaction using MAOS. Amongst others the Sonogashira and Suzuki cross-coupling are particularly adapted for this method.[46]

Sonogashira

Typical procedure for microwave assisted Sonogashira reactions involves DMF as solvent, Et_2NH as base, $Pd(PPh_3)_4$ and copper iodide as catalysts.[47]

$$\mathrm{Ar{-}X + R{-}C{\equiv}C{-}H \xrightarrow[\mathrm{DMF,\ Et_2NH,\ 5\ min,\ MW\ 120\,^\circ C}]{\mathrm{Pd(PPh_3)_2Cl_2,\ CuI}} Ar{-}C{\equiv}C{-}R}$$

Swager and coworkers have used MAOS for the synthesis of rotaxane conjugated sensor polymers[48] reducing the reaction time from 2 days to less than 1h. Khan and Hecht used microwave assisted Sonogashira coupling in the synthesis of poly(meta-phenyleneethynylene)s[49] by a water/DBU insitu deprotection.

Suzuki

Microwave assisted Suzuki reactions were used for the synthesis of a fluorescent dye[50] or in the synthesis of a polymer[51] amongst many other examples. This method is suited for difficult cases where high temperature are needed like reacting on a Ar−F. This reaction succeeded under microwave irradiation at 150 °C for 15 min.[52] A typical procedure for a Suzuki reaction in the microwave is described here:

$$\mathrm{Ar_1{-}X + Ar_2{-}B(OR)_2 \xrightarrow[\mathrm{toluene,\ EtOH,\ 10\ min,\ MW\ 120\,^\circ C}]{\mathrm{Pd(PPh_3)_2Cl_2,\ K_2CO_3}} Ar_1{-}Ar_2}$$

2.3 Purification and Optical Methods

Recycling Gel Permeation Chromatography

Gel permeation chromatography (GPC) also named sized exclusion chromatography is a method that separates a mixture of compounds based on their sizes. This technique is often used in the analyses of polymers who differ greatly in size but for the purification of smaller compounds this method is less appropriate since the size differences are not sufficient to reach a good separation. Indeed, in normal GPC the compound runs once through the column and is collected in several fractions directly after it.

If the system is closed after the injection, letting the mixture of compounds run through the column several times, after each run, the compounds in the mixture are more distant from each other affording a better separation. This improved method, named recycling GPC (recGPC), is an automated purification which gives a better separation without wasting any solvent. This method of separation is not yet widely used, although it is extremely powerful and yields pure compounds with minimal loss. It is particularly suited for the separation of long nanostructures.[53]

As shown in the second part of this dissertation (part II) this method has proven to be essential in the synthesis of molecular rods and stars to separate the desired target from the different side products formed during the reactions. Traditional purification lab methods based on polarity (column chromatography on silica gel or reverse phase) or on solubility (recrystallization) were less successful in the purification of such structures.

Absorption and Fluorescence Spectroscopy

The excitation of a molecule by light can promote electrons to an excited state (absorption from ground state to higher energy levels: $S_1 \leftarrow S_0$). The release of this energy can follow various radiative mechanisms (fluorescence, phosphorescence) or non-radiative mechanisms (internal conversion, intersystem crossing, vibrational relaxation). Fluorescence emission occurs when the electrons relax from an excited singlet state to the ground singlet state $S_1 \rightarrow S_0$ and phosphorescence emission occurs when the electrons relax from an excited triplet state to the singlet ground state $T_1 \rightarrow S_0$. Jablonski diagrams (scheme 2.4)[54] show different electronic transitions between the energy level S_0(ground state), S_1, S_2 and T_1. Each energy level is formed by a series of vibrationally excited levels (indicated by 0, 1 and 2). The different electronic energy levels are described with a number in subscript and the vibrational energy levels of each electronic energy level are described with a number in superscript.

After the absorption of light, electrons are promoted from the ground state S_0^0 to the different vibrational excited states (S_1^0, S_1^1, S_1^2, S_2^0, S_2^1, ...etc.).

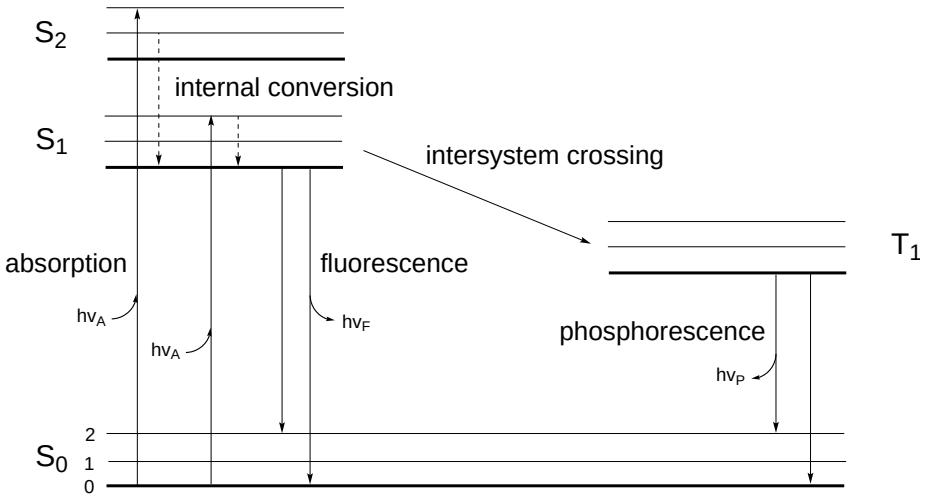

Scheme 2.4: One form of a Jablonski diagram[54]

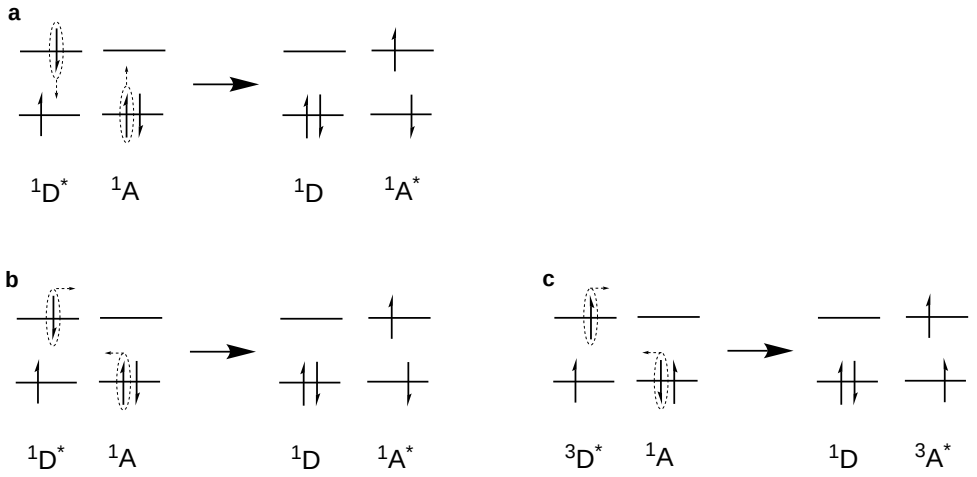

Scheme 2.5: Forster and Dexter energy transfers. Two molecular orbitals (HOMO and LUMO) are represented for an donor (D) and an acceptor (A) before (left) and after (right) the energy transfer. **a.** singlet-singlet Forster energy transfer, **b.** singlet-singlet Dexter energy transfer, **c.** triplet-triplet Dexter energy transfer. Singlet and triplet states are shown with numbers one and three as superscript and excited states are show with an asterisk as superscript

Since the internal conversion mechanism is faster than the fluorescence mechanism, the electrons relax to the lowest energy vibrational state of S_1 and fluorescence occurs from S_1^0 to the vibrationally excited ground states (S_0^0, S_0^1, S_0^2, S_0^3, ...etc.). The distance between the vibrational energy levels of the excited states is similar to that of the ground state. This results in the symmetry between the absorption and the fluorescence spectra.

Quenching can be caused by energy transfers between two separated molecules or two parts of the same molecule named donor and acceptor. Two types of energy transfers will be described, the Förster and the Dexter energy transfers (see scheme 2.5). In the first one, also named resonance energy transfer (RET) or Förster resonance energy transfer (FRET), an excited electron of the donor relaxes to the ground state and transfers its energy to the acceptor that promotes one electron to the excited state. If the acceptor is fluorescent the energy is released as light, if not it is dissipated as heat. This energy transfer is a long range dipole-dipole interaction between donor and acceptor (r=10-100 Å).

The second energy transfer occurs in short range (r=5-10 Å) and needs the overlap of the involved orbitals. Excited donor and ground state acceptor have to be close enough to process this non-radiative energy transfer. An excited electron of the donor is transferred to the acceptor that transfers

an electron back from its ground state to the donor ($^1D^*+{}^1A \rightarrow {}^1D+{}^1A^*$). A similar process is possible for the triplet state of a donor ($^3D^*+{}^1A \rightarrow {}^1D+{}^3A^*$).

Quantum Yield Calculations

A fluorescence quantum yield is a fundamental property for any photoluminescent species. It gives an indication of the emission efficiency of a fluorophore and is defined as follows:[54]

$$\Phi = \frac{number\ of\ photons\ emitted}{number\ of\ photons\ absorbed} \tag{2.1}$$

It is calculated by measuring the absorbance and fluorescence of a substance with known quantum yield and repeating these measurements with the compound of unknown quantum yield applying the same experimental parameters. The data are then integrated in equation (2.2) having I for the integrated emission intensity, A for the absorbance at the excitation wavelength and n for the refractive index of the solvent. If the same solvent is used to dissolve the sample and the reference the fraction with the refraction index can be ignored. The values for the reference substance are indicated with the subscript R.

$$\Phi = \Phi_R \left(\frac{I}{I_R}\right)\left(\frac{A_R}{A}\right)\left(\frac{n^2}{n_R^2}\right) \tag{2.2}$$

Measuring the emission of the sample at different concentrations permits a more accurate determination of the quantum yield. Indeed, this is done by integrating the emission peak for an absorbance at a certain concentration and repeating this process for different concentrations (at least five different concentrations with an absorbance lower than 0.1 to avoid inner filter effects). The values of the integrated fluorescent intensities (y axis) are plotted against the value of the absorbance at a certain concentration (x axis)(see figure 2.6). A linear regression of these points gives a straight line with slope Δ. The same process is repeated to obtain the graphic for the standard. Then the quantum yield can be calculated using equation 2.3 with Φ_R for the know quantum yield of the reference, Δ_R for the slope given by the plot of the standard and Δ for the slope given by the plot of the compound with unknown quantum yield.

$$\Phi = \Phi_R \left(\frac{\Delta}{\Delta_R}\right)\left(\frac{n^2}{n_R^2}\right) \tag{2.3}$$

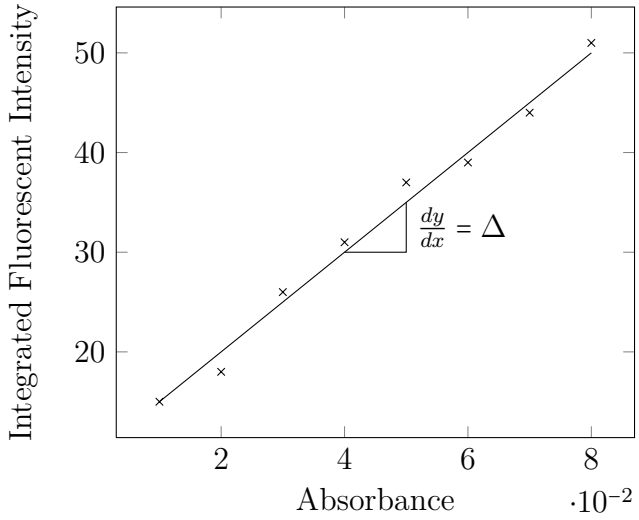

Scheme 2.6: Integrated fluorescent intensity as function of the absorbance at a certain concentration measured for one compound at different concentrations. The slope of this plot gives the delta value for equation 2.3.

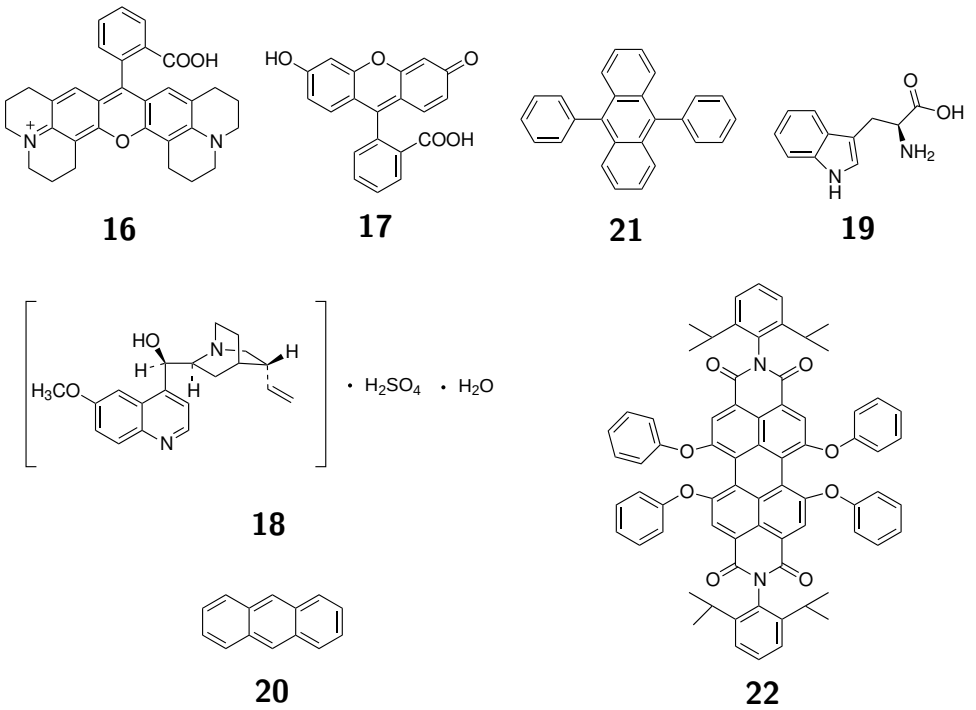

Scheme 2.7: Common standards for quantum yield measurements

The most commonly used standards in quantum yield measurements (scheme 2.7) are:[55] Rhodamine 101 (**16**), fluorescein (**17**), quinine sulfate (**18**), tryp-

tophan (**19**), anthracene (**20**), 9,10-diphenylanthracene (**21**) and *N,N'*-bis(2,6-diisopropylphenyl)-1,6,7,12-tetraphenoxyperylene-3,4,9,10-tetracarboxylic acid bisimide (also know as "perylene red" or "fluorescent red", **22**).

As shown in table 2.1, the brightest emissions are displayed by substances such as rhodamines with values approaching unity. The choice of the appropriate quantum yield is made by matching its emissions wavelength with the range given in table 2.1. Compound **22** is generally used to measure the quantum yield of NDIs by Würthner et al.[56,57]

Standard	Solvent	Lit. Φ_f	Range [nm]	Ref.
16	Ethanol + 0.01% HCl	1.00	600-650	[58]
17	0.1M NaOH	0.79	500-600	[59]
18	0.1M H_2SO_4	0.54	400-600	[60]
19	Water, pH 7.2, 25 $^\circ$ C	0.14	300-380	[61]
20	Ethanol	0.27	360-480	[60]
21	Cyclohexane	0.90	400-500	[62]
22	CH_3Cl	0.96	400-550	[63,64]

Table 2.1: Standards materials for quantum yield experiments[55]

Chapter 3

Looking into the Nanoworld: a Multidisciplinary Task

Since the development of the first electronic devices, advances have been made on different aspects such as efficiency, speed and size. Due to the importance of miniaturization, the integration of molecules as the smallest functional units in electronic circuits has always been an issue.

How electron transport through molecules occurs, and what are the mechanical stabilities of such molecular devices are amongst many others important questions asked to scientists. These questions bring together experts from different disciplines such as chemists, physicists, electronic engineers, theorists, etc... A close team work between these scientists and a good understanding of each others challenges and difficulties is crucial to make advances in the understanding and the control of such complexes systems.

3.1 Connecting Electrodes with Molecules

3.1.1 Molecular Junction Techniques

The techniques employed to integrate molecules in electronic circuits are diverse and follow two approaches, either the electrodes are connected by a monolayer of molecules or by single molecules. The first one includes techniques such as crossed-wire junction or mercury droplet junction and will not be discussed in this section. The reader is referred to the corresponding literature.[65–67] Three techniques of the second approach will be described here, namely STM junctions, AFT junctions and mechanically controllable break junction.

Scanning Tunneling Microscope Junctions

Scanning tunneling microscopy (STM) is a technique for surface imaging using a quantum tunneling of electrons through the vacuum between the surface and the STM tip when a bias is applied. In STM molecular junctions the molecule under investigation is bound to the surface. When it meets the tip a variation of the tunneling current is recorded. In contrast to the techniques described below where the molecule is attached to both the electrodes, in a STM junction the molecule is never in direct contact with the tip and the effect recorded is only a tunneling phenomena. This technique was used to measure an oligophenylene ethynylene molecule bound to a gold surface with a thiol linker and surrounded by shorter alkylthiols. When the tip scans through the surface and passes on the OPE, an increase in conductance is recorded.[68,69]

Atomic Force Microscope Junctions

Atomic force microscope (AFM) is an imaging technique that scans surfaces with the sharp tip of a cantilever. When in STM measurments a tunneling effect is recorded, in AFM the topography of the surface is measured by contact. Different molecular junctions use this imaging technique. In conducting probe atomic force microscope (cpAFM) one side of the molecule under investigation is bound to the surface and the other side to a gold nanoparticle.. Besides it is surrounded by a self-assembled monolayer (SAM). This technique was for the first time used to measure the conductance of alkanedithiolates.[70] The investigation of transport characteristics of conjugated oligophenyleneimine (OPI) wires[71] is another example. In direct contact conducting probe atomic force microscopy (direct cpAFM) the tip is directly bound to the molecule under investigation without the use of a goldnanoparticle. A bias is applied between a gold coated conductive cantilever and a gold substrate. This technique was recently used to simultaneously investigate the conductance and the breaking mechanism of a metal-molecule junction.[72]

Mechanically controllable break junctions

The mechanically controllable break junction (MCBJ) uses a notched metallic wire attached to a flexible substrate that can be bent until the wire breaks at the notch. The gap formed in this way can be adjusted to allow deposited molecules to bridge the two sides. This metal-molecule-metal junction was used to demonstrate that aromatic π-π coupling between adjacent molecules allows the formation of a bridge between the two electrodes.[73,74]

3.1.2 Areas of Investigations

In the search of the best candidates for integrating molecules in electronic circuits different aspects have to be taken into consideration like molecular structure (length, conformation, anchoring group), the number of molecules in the junction, as well as the type of electrode-molecule connection. It is well know that π-π conjugated molecule have a greater conductivity and it was shown that oligo(phenylene vinylene) OPV have slightly higher conductance than OPE oligo(phenylene ethynylene).[75]

One of the difficulties with molecular junctions is to determine with precision how many molecules are involved in the junction. To have a better understanding of this phenomena an asymmetrical molecule was used in a MCBJ. The asymmetry of the molecule was reflected in the current-voltage measurement showing the probable presence of a single molecule in the junction.[74] The influence of torsion angle between two phenyl ring was also investigated using a molecular junction.[76] The metal-molecule connection is of great importance and the choice of the most suited anchoring group is challenging. A variety of anchoring groups have been studied: thiols[77] (or acetyl protected thiols[78]), methyl thiol,[79,80] nitrile,[81] pyridine,[82] ... etc.

3.2 Molecular Organisations on Surfaces

The organization of molecules on surfaces is of great importance for applications in nanotechnology. The so called "bottom-up" approach (in contrast to the "top down" technique such as lithography) takes full advantage of the ability that allows molecules to organize in an ordered way on a surface due to intermolecular interactions (van der Walls, hydrogen bond dipole-dipole). In this section, we describe two different methods of organizing a molecule on surfaces, namely the self-assembled monolayers and the creation of porous surface networks.

3.2.1 Self-Assembled Monolayers

Self-assembled monolayer (SAMs) are organized arrangement of molecules adsorbed on a solid surface forming an ordered structure due to intermolecular van der Waals interactions. Most often SAMs are formed from chemisorption of organic molecules with anchor groups (e.g. thiols, phosphonates) on noble metallic surfaces (e.g. gold). They find applications in systems and devices in the field of nanotechnology such as in corrosion prevention,[83] sensing,[84–86] and molecular electronics[68,87] and in particular for the stabilization

of gold nanoparticles.[88] Other SAMs application can be found in two excellent review[89,90] treating of SAMs formation of thiols on gold surfaces, which is the most common example of SAMs.

3.2.2 Nanoporous Networks on Surfaces

The formation of ordered structures on surfaces is a key aspect of the "bottom-up" approach in nanotechnology. Controlling the organization on the surface allows the formation of ordered systems for a variety of applications. Using intermolecular van der Waals interactions or hydrogen bonding to create networks on surfaces opens the door for future devices built starting from the very elemental building blocks that are the molecules. The creation of ordered structure with nanoscale precision over large areas is still very challenging.

Two dimensional porous systems can be used as templates to functionalize specific regions of the surface. Indeed controlling substrate composition and functionality is of major interest and molecules are the favorite building blocks to decorate, structure, and functionalize surfaces. The tools of supramolecular chemistry provide the guidelines to design molecular building blocks in order to obtain the appropriate networks for the desired application.

Organisation on surfaces can be obtained by simple molecules adsorbed on the surface forming an organised pattern such as star-shaped oligophenylenes on graphite[91] but if the molecules are well chosen the organisation of the molecules on the surface can produce a nanoporous network. Covalent nanoporous network are obtained by preformed cavity molecules such as crown-ethers[92,93] or shape-persistent macrocycles.[94] Another example shows how the same compound can adopt two different orientation depending on the type of surface used for the absorption.[95] Self-assembled nanoporous networks are formed *in situ* by intermolecular interactions between rigid structures on the surface. A recent review describes various nanoporous networks on surfaces by supramolecular self-assembly.[96]

A system of different molecules self-assembling in a supramolecular network has been investigated by Beton *et al.* They deposit in UHV (ultra high vacuum) perylene tetra-carboxylic di-imide (PTCDI) and melamine and used the network cavities to host fullerenes.[97] In further studies, they investigated the formation of the network on different surfaces[98–102] as well as other networks[103,104] in detail.

Manfred Buck and coworkers have been investigating surface functionalization by a template network made up of PTCDI (perylene tetracarboxylic diimide) and melamine (figure 3.1). The method used by Buck to form the network on the surface is solution based[105] in contrast to ultra-high vacuum

(UHV) method use by P.H. Beton.[97] Buck's method has two advantages over UHV deposition. A broader choice of molecules (e.g. non-sublimable molecules) can be used as guest molecules and this technique produces less waste which matters since the valuable material used comes from multi-step synthesis. Then self-assembled monolayers (SAMs) are formed by adsorbing thiols into the pores of the network. Electrochemistry with such hybrid structures was investigated by underpotential deposition (UPD) of copper leading to the intercalation of copper between SAM and gold altering the thiol/gold bond enhancing SAM stability.[106] In a later work, Buck and coworkers use the supramolecular network as sacrificial mask for the generation of a nanopatterned binary SAM.[107] By the modification of the network substituting PTCDI by two adamantanes Manfred Buck investigated the effect of the modification on the adsorption of C_{60} guest molecules.[108]

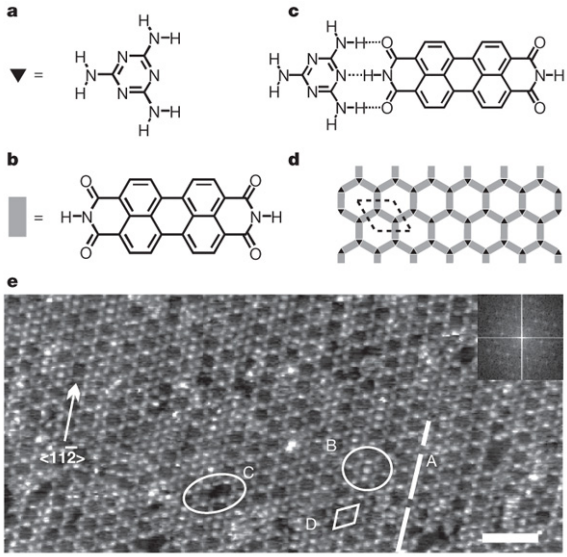

Figure 3.1: Supramolecular network of melamine-PTCDI self-assembled on Au(111)[105]

Host-Guest Network on Surfaces

The main application for nanoporous networks on surface is to host molecules in their cavities. Despite some exceptions where the flexible network readjusts to receive the guest molecules,[109,110] in most of the cases the network forms fixed cavities and only guests fitting in them are accepted. Very often the guest of choice is C_{60}. The adsorption of C_{60} in Fe-TPA networks on Cu(100) was demonstrated.[111]

The PTCDI-melamine network described above has also been used by Beton *et al.* to trap C_{60} on silver-terminated silicon surface[97] (figure 3.2) and on Au(111)[100,102] under UHV conditions. The use of the solution based conditions by Buck *et al.* offers a broader choice of molecules for the adsorption and the cavities can be filled by different thiols[105–107,112] or C_{60}.[112]

Dynamic behaviors such as free rotation of the guests in the cavities were also studied for a star shaped molecule[113] or for porphyrin in a porphyrin network, where the guest (a self-trapping porphyrin) could also be individually switched by the STM tip.[114]

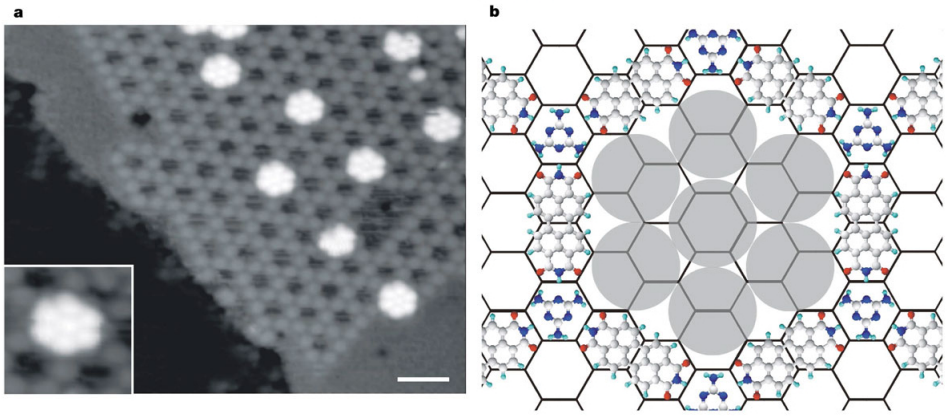

Figure 3.2: **a.** STM image of C_{60} heptamers on a PTCDI-melamine network. **b.** Schematic diagram of a C_{60} heptamer.[97]

Part II

Applications of Conjugated Molecules

Chapter 4

Electroluminescence in a Carbon Nanotube Junction

4.1 Project Description

This project was developed in a fruitful collaboration with Sergio Grunder (Mayor group, University of Basel, Switzerland), Alfred Blaszczyk (Mayor group, Karlsruhe Institute of Technology, Germany) and Prof. Ralph Krupke and his group (Karlsruhe Institute of Technology, Germany).

Electronic transport properties of molecules have been widely studied in molecular junctions. Optical signals have rarely been recorded from molecular junctions and the only examples reported used STM setups.[115,116] In this project the synthesis of a tailor made molecule for electroluminescence of a nanotube-molecule-nanotube junction is reported. Electroluminescence is observed when an electric current passes though a material which emits light in response. In this set-up a single tailor-made molecule connected to two SWNT electrodes under a difference of potential emits fluorescent light, indicating its presence in the junction. This junction (scheme 4.1) is composed of two palladium electrodes bridged by a carbon nanotube after dielectrophoretic deposition. The nanotube standing freely above a trench in silicon oxide is cut by an electrical breakdown leaving a gap of about 5 nm. Dielectrophoretic deposition of the polarizable molecule from solution forms the molecular junction. When a voltage is applied between the electrodes an emission of light is observed. For a deeper insight into the experimental set-up the reader is referred the first paper we published in Nature Nanotechnology that describes this nanotube-molecule-nanotube junction.[117]

This project was started by Alfred Blaszczyk and Segio Grunder who synthesized a variety of molecular rods of different sizes with a fluorescence emis-

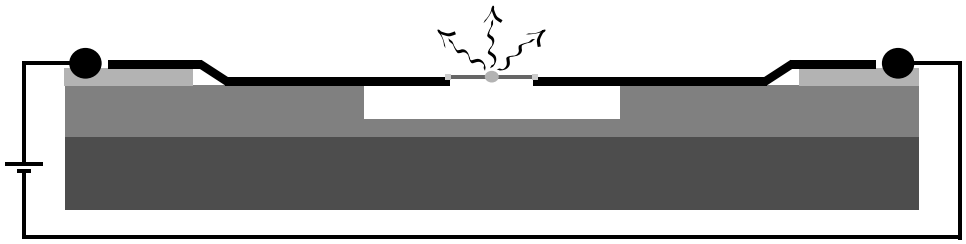

Scheme 4.1: Electroluminescence from a molecular rod in a nanotube-molecule-nanotube junction.[117] The molecule is deposited on the cut nanotube bridging the two ends. When a voltage is applied the junction emits a characteristic light, depending on the deposited molecule.

sion at 638 nm.[118] After their optimizations, a good candidate was obtained and its emissive properties was studied in the carbon nanotube junction.[117] The design and the synthesis of a new series of molecular rods having different emission wavelengths for investigations in a carbon nanotube junction is reported in this chapter, in addition to their optical properties.[118]

4.2 Molecular Design and Synthetic Strategy

The design and the strategy of the new series of targets were based on the work of Alfred Blaszczyk and Segio Grunder.[118] The NDI core substitution was changed to obtained different emissive properties but the general structure of the rods were kept unchanged.

Molecular Design

The suitable molecule for the nanotube molecular junction is composed of two parts: a chromophore that give its emissive properties to the molecule, connected to the nanotube electrodes by two conjugated branches with their anchor groups (scheme 4.1). A fine tuning of the structure of each part is a prerequisite to achieve the desired set-up. The electrostatic deposition of the molecule in the junction requires a rod-like polarizable structure longer than 5 nm bearing a flat conjugated system at each end to bind to the SWNTs by π-π-interactions. The choice was directed to phenanthrene since it proved to be a good candidate in previous studies.[118] As polarizable part, a linear π-conjugated oligo(phenylene ethynylene) (OPE) bearing solubilizing side chains was chosen. Naphthalene diimides (NDI) are good candidates as central chromophores since their fluorescence signals depend on the chemical nature of the core substituents.[119] This ability to emit different wavelength

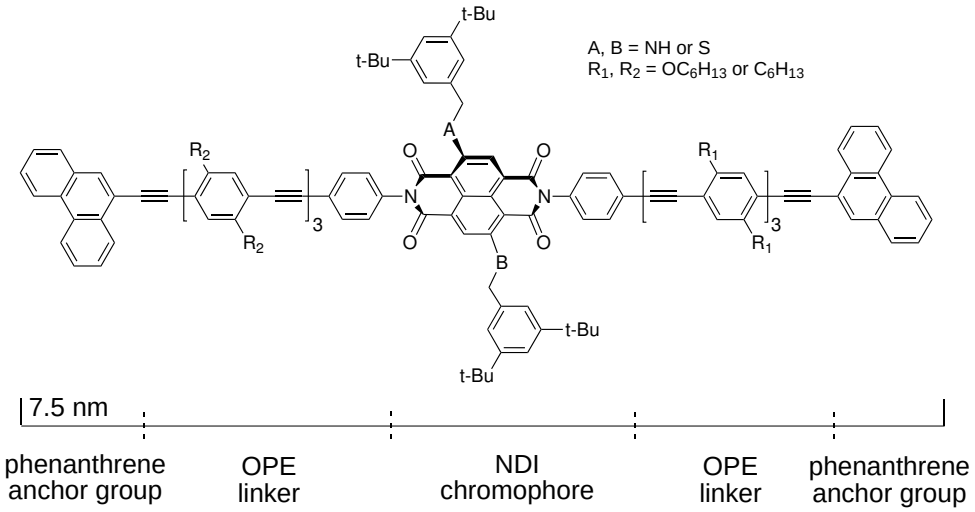

Scheme 4.2: Model compound for the molecular junction

depending on the substitution pattern on the core of the NDI permits to obtain different readily accessible rods for the molecular junction. The perpendicular angle at both imide positions between OPE and NDI is ideal to increase the emissive charge recombination of the electrons and the holes on the chromophore.

Synthetic Strategy

A convergent strategy offering in general higher overall yields and better modularity is the most suited route to build such symmetric rigid molecular rods. Most disconnections in the retrosynthetic analysis rely on the synthesis of molecular wires where sequences of Sonogashira cross-couplings yield the targets (scheme 4.3). The first disconnection was made between the NDI and the OPE which allows a parallel synthesis of the chromophore and the conjugated branches. The NDI subunit is further disconnected at the benzylic substituents to allow a straightforward access to different chromophores by core substitution, the emission properties being strongly correlated to the substitution pattern.[119] The unsubstitued NDI is further disconnected at the imide positions giving an aniline derivative and a naphthalenetetracarboxylic acid bisanhydride derivative. The latter is formed in four steps as reported in the literature.[120] The OPE subunit was disconnected in positions where the product is made accessible by sequences of Sonogashira cross-couplings and acetylene deprotections. This sequence of reactions was started from the commercially available 9-bromophenanthrene and continued taking a particular care in having only one reaction site, except for the last coupling where

a statistical reaction with dihexyldiiodobenzene is necessary.

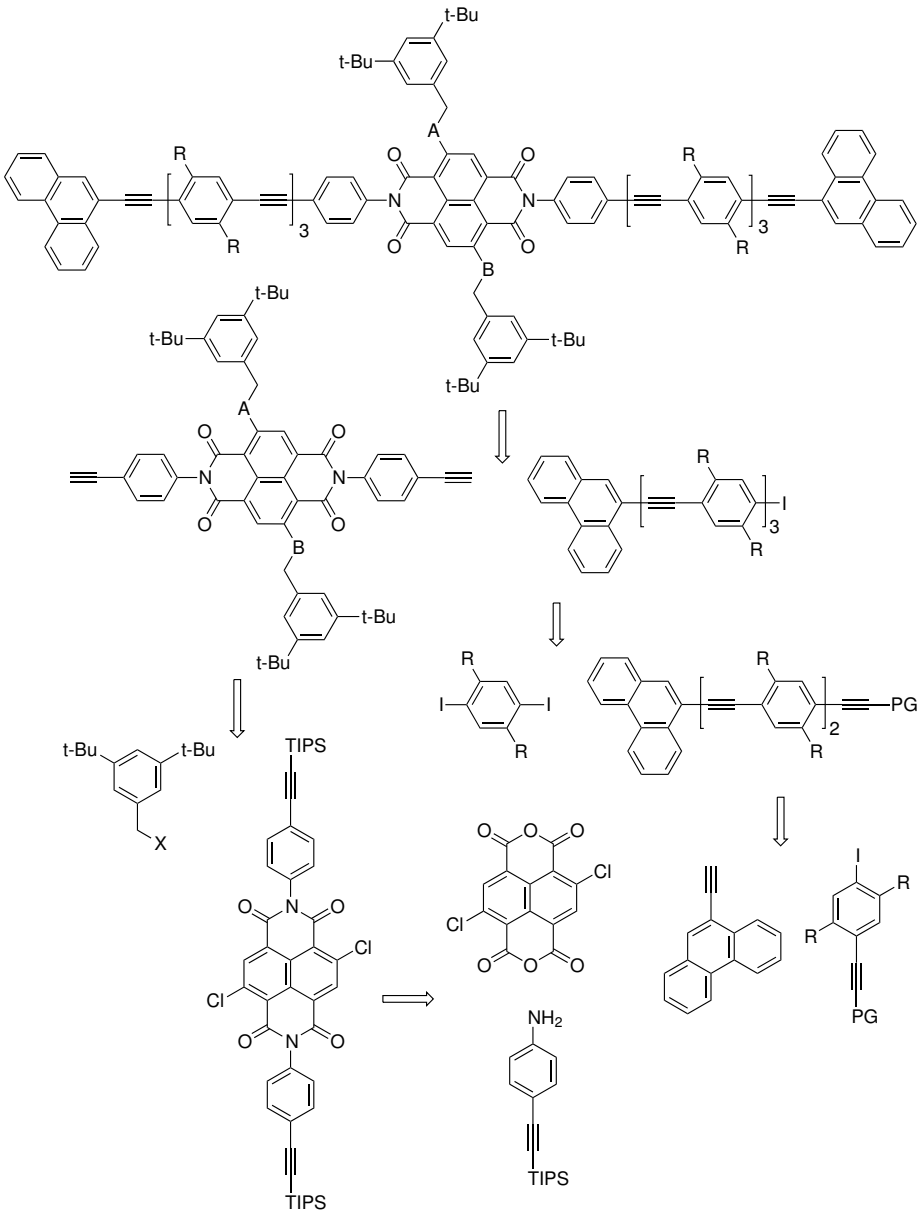

Scheme 4.3: Retrosynthetic analysis for the target structure

4.3 Synthesis and Characterization

The synthesis of the OPE subunit (scheme 4.4) was started by a Kumada reaction between 1,4-dichlorobenzene and hexylmagnesium bromide

giving the product as a colorless oil after a Kugelrohr distillation in an excellent yield. The iodination of this compound[121,122] afforded 1,4-dihexyl-2,5-diiodobenzene **23** as white needles in moderate yield after the removal of the remaining I_2 and two recrystallisation in EtOH. The polar silyl protected acetylene [(3-cyanopropyl)diisopropylsilyl]acetylene (prepared according to a literature procedure[20]) was then used for a statistical Sonogashira reaction with the diiodo derivative to give **24** as well as the doubly coupled product. Both were easily separated by column chromatography taking great advantage of the polarity of the protecting group. The ethynyldihexyliodobenzene **24** was then coupled with 9-ethynylphenanthrene **25** (obtained in two steps from the commercially available 9-bromophenanthrene and TMS acetylene). The resulting OPE **26** was elongated following a sequence of two Sonogashira cross-couplings, one with **24** and the second one with 1,4-dihexyl-2,5-diiodobenzene **23** in a statistical reaction resulting in compound **27** and the doubly coupled product. Surprisingly the statistical Sonogashira reactions of the diiodo derivatives with the acetylene give always the doubly coupled product in a non negligible amount, even if a large excess of the diiodo derivative is used. The coupling with the first acetylenic branch seems to enhance the reactivity of the product which reacts more rapidly with the free acetylene than the diiodo derivative. The OPE bearing alkoxy side chains **38**

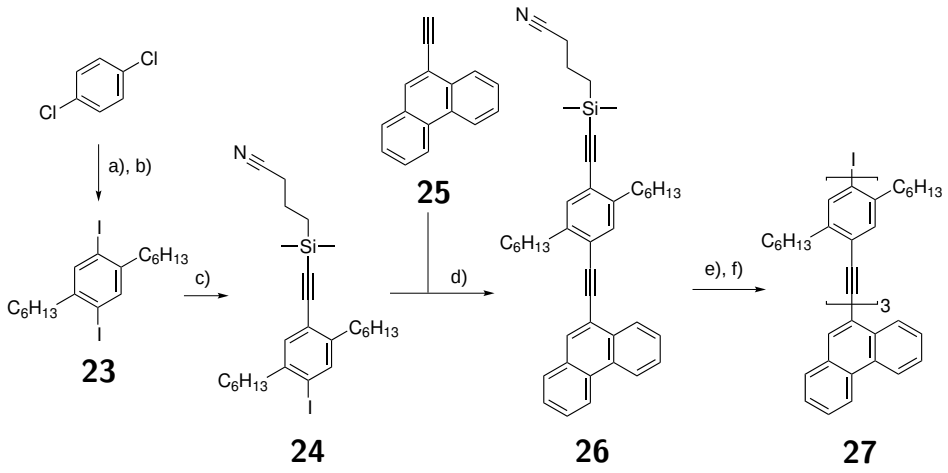

Scheme 4.4: Synthesis of building block **27**. Reagents and conditions: a) $C_6H_{13}Br$, Mg, [dppp]$NiCl_2$, Et_2O, 95%; b) I_2, KIO_3, H_2SO_4, H_2O, AcOH, 120 °C, 18h, 52%; c) CPDMSA, $Pd(PPh_3)_2Cl_2$, CuI, PPh_3, piperidine, r.t., 16h, 52%; d) $Pd(PPh_3)_4$, CuI, $^iPr_2NH$, THF, 45 °C, 16h, 96%; e) 1. K_2CO_3, THF, MeOH, 0 °C, 1h, 83%, 2. $Pd(PPh_3)_4$, CuI, $^iPr_2NH$, THF, 45 °C, 16h, 83%; f) 1. K_2CO_3, THF, MeOH, 0 °C, 2h, 86%, 2. $Pd(PPh_3)_4$, CuI, $^iPr_2NH$, THF, 60 °C, 16h, 37%.

(scheme 4.5) was similarly obtained by Sergio Grunder.[118,123]

The synthesis of the NDI subunit (scheme 4.5) was started with the coupling of the commercially available bromoaniline and triisopropylsilylacetylene (TIPSA) giving compound **28** in good yield without having to protect the aniline.[124] The latter was then reacted with 2,6-dichloro-1,4,5,8-naphthalene tetracarboxylic acid anhydride **29** to obtain compound **30**. In this reaction the nucleophilic substitution of the aniline derivative at the core of the desired product **30** forms a red side product that was separated by chromatography from the yellow desired product. Generally the purification by column chromatography of colored NDI compounds is easy since the monitoring of the separation can be done by the naked eye. On the other hand, probably due to strong π-π interactions between the different products, two columns are often needed to have a pure compound since several mixed fractions are obtained. The NDI core substituents, either the thiol or the amine, were obtained from commercially available 1-(bromomethyl)-3,5-di-tert-butylbenzene through a Gabriel or Delépine reaction for the amine **32** or via a nucleophilic substitution with potassium thioacetate for the thiol **33**. The chlorines of the naphthalene diimide **30** were either substituted at room temperature with the thiol **33** giving the red sulfur substituted protected NDI subunit, or at 60 °C with the amine **32** giving the blue nitrogen substituted protected NDI subunit. The amine is less reactive than the thiol at the chlorine positions and therefore it needs higher temperatures. Probably due to this reason, better yields are obtained when the chlorines of the NDI are substituted by sulfur than when they are substituted by nitrogen. Their difference in nucleophilicity was furthermore used to obtain the mixed sulfur-nitrogen core substituted NDI subunit. The 2,6 dichloro compound **30** was first reacted with the less nucleophilic amine **32** at 40 °C for six hours. This mono-substituted product was then isolated by column chromatography and reacted with the more nucleophilic thiol **33**. Removal of the TIPS protecting groups were performed with TBAF at 0 °C in each case. For the statistical deprotection yielding **34**, the evolution of the reaction was followed by TLC until the amount of mono deprotected product was considered sufficient.

The deprotected compounds **35**, **36** and **37** were coupled with **38** through Sonogashira reactions giving the molecular rods **2**, **3** and **4**. In this reaction, a particular care has to be taken to work in an oxygen free atmosphere since the chromophore bearing two free acetylenes has a high tendency to homocouple following a Glaser type reaction. In the case of the asymmetrical molecular rod **1** the monodeprotected NDI **34** was first coupled with **27** followed by deprotection of the second acetylene with TBAF. Successive coupling with **38** afforded the rod **1** as a green solid.

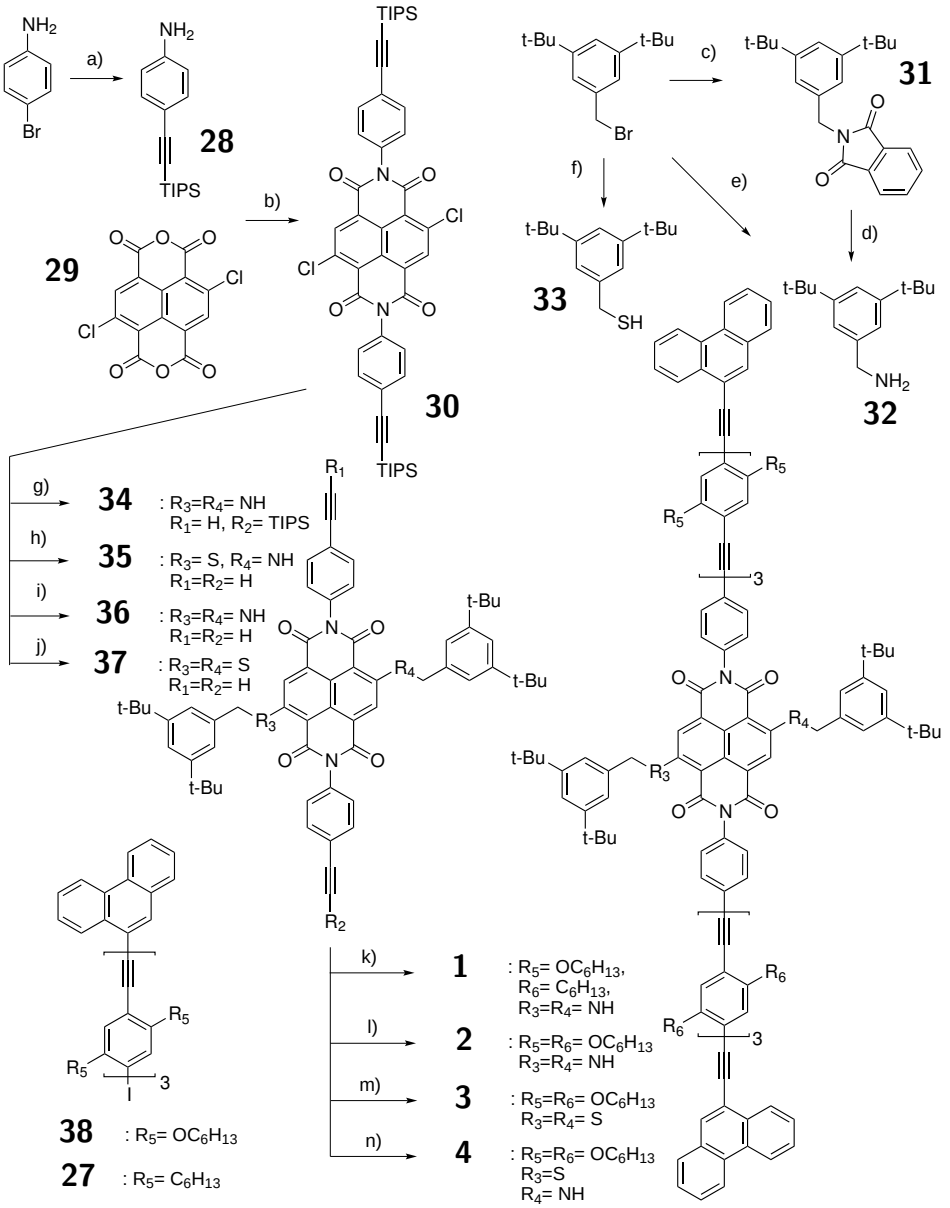

Scheme 4.5: Reagents and Conditions: a) TIPSA, $Pd(PPh_3)_2Cl_2$, CuI, THF, Et_3N, r.t., 5h, 80%; b) AcOH, 120 ° C, 30 min., 62%; c) phthalimide, K_2CO_3, DMF, r.t., 16h, quant.; d) $NH_2NH_2{\cdot}H_2O$, THF, 70 ° C, 3h, 90%; e) 1. urotropine, NaI, EtOH; 2. HCl, MeOH; 3. NaOH 79%; f) 1. KSAc, THF, r.t., 1h, 2. K_2CO_3, MeOH, r.t., 1h, 72%; g) **32**, K_2CO_3, DMF, 70 ° C, 16h, 29%, 2. TBAF, THF, 0 ° C to r.t., 4h, 62%; h) 1.**32**, K_2CO_3, DMF, 40 ° C, 6h, 58%; 2. **33**, K_2CO_3, DMF, r.t., 16h, 86%; 3. TBAF, THF, r.t., 3h, 58%; i) 1. **32**, K_2CO_3, DMF, 60 ° C, 16h, 31%, 2. TBAF, THF, 0 ° C, 2h, 70%; j) 1. **33**, K_2CO_3, DMF, r.t., 16h, 93%; 2. TBAF, THF, r.t., 2h, 75%; k) 1. **27**, $Pd(PPh_3)_4$, CuI, $^iPr_2NH$, THF, r.t., 4h, 35%; 2. TBAF, THF, 0 ° C to r.t., 4h, 77%; 3. **38**, $Pd(PPh_3)_4$, CuI, $^iPr_2NH$, THF, 45 ° C, 6h, 45%; l) **38**, $Pd(PPh_3)_4$, CuI, $^iPr_2NH$, THF, r.t, 23h, 95%; m) **38**, $Pd(PPh_3)_4$, CuI, $^iPr_2NH$, THF, r.t, 15h, 37%; n) **38**, $Pd(PPh_3)_4$, CuI, $^iPr_2NH$, THF, r.t., 21h, 29%.

4.4 Optical Properties

UV/Vis and Fluorescence

Absorption and emission spectra of compounds **2**, **3** and **4** were recorded in CH_2Cl_2 at room temperature. Figure 4.1 shows the absorption of the three compounds with their OPE absoption band at 415 nm and their NDI absoption at 530 nm (**3**), to 567 nm (**4**) and 609 nm(**2**). The shift in absorption is due to the different substituents at the NDI core.[119]

The emission spectra of compound **2** and its precursors is shown in figure 4.2. The OPE building block shows an emission at 449 nm upon excitation at 415 nm and NDI building block show an emission at 638 nm when excited at 609 nm and no emission when excited at 415 nm. The rod **2** shows an intense emission at 637 nm when the NDI subunit is excited at 609 nm. When the OPE subunit is excited at 415 nm, an intense emission at 637 nm is also observed demonstrating an efficient energy transfer from the OPE to the NDI subunits.

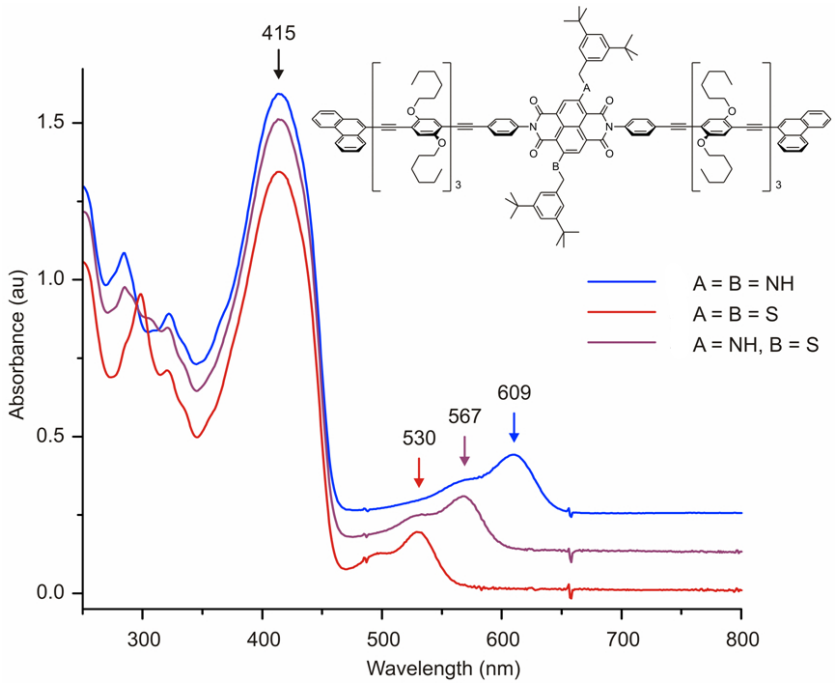

Figure 4.1: Absorption spectra of compounds **2** (blue line), **3** (red line) and **4** (purple line) recorded at room temperature in CH_2Cl_2(10^{-5} M). OPE absorption at 415 nm for the three rods and NDI absorption at 530 nm, 567 nm and 609 nm for the rods **3**, **4** and **2** respectively.

The decrease in the emission intensity in the series of compounds **2**, **3** and **4** is shown in figure 4.3. A strong fluorescence is observed for the nitrogen substituted NDI **2** and almost no fluorescence for the sulfur substituted NDI **3**. As predicted, the intensity as well as the wavelength fluorescence signal of the mixed rod **4** is somewhere between the emission of the nitrogen substituted NDI rod and the sulfur substituted NDI rod.

Quantum Yields

A fluorescence quantum yield is a fundamental property for any photoluminescent species. It gives an indication of the emission efficiency of a fluorophore (see 2.3). Quantum yields of the fluorescence were determined in $CHCl_3$ by the "optical dilution method"[54] by using *N,N'*-bis(2,6-diisopropylphenyl)-1,6,7,12-tetraphenoxyperylene-3,4,9,10-tetracarboxylic acid bisimide excited at 575 nm as reference ($\Phi_f = 0.96$, $CHCl_3$).[63,64] The given quantum yields were averaged from values obtained at five different concentrations all with absorbances below 0.1 at the excitation wavelengths. Long NDI rods

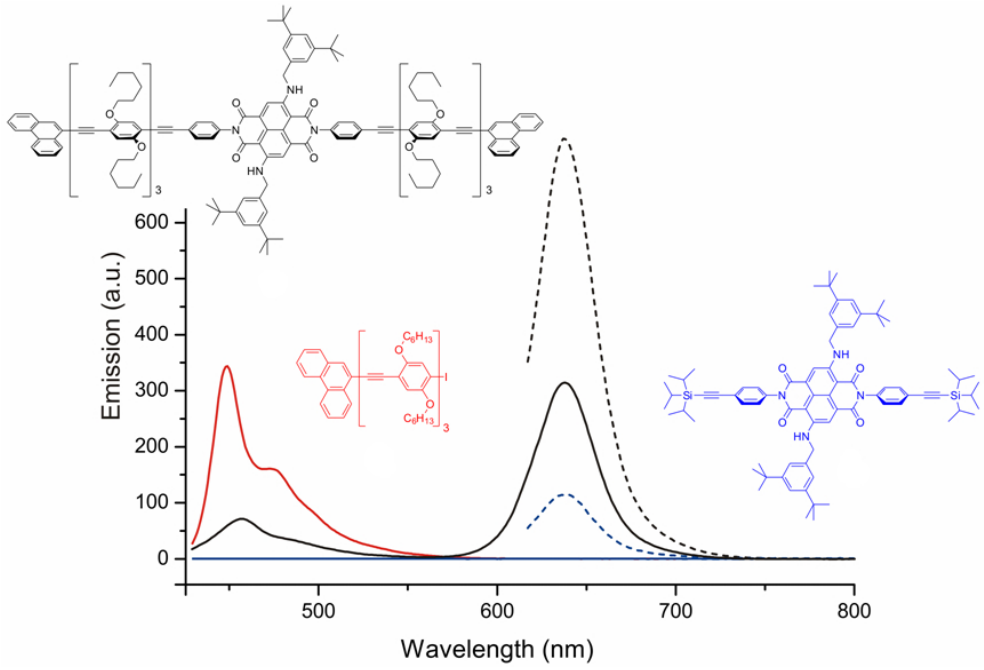

Figure 4.2: Emission spectra at room temperature of rod **2** (6.5×10^{-7} M in CH_2Cl_2) and the NDI precursor (red line)(2.2×10^{-6} M in CH_2Cl_2) and the OPE precursor (blue line)(1.2×10^{-6} M in CH_2Cl_2). Solid lines upon excitation at 415 nm and dashed lines upon excitation at 609 nm.

2, **3**, and **4** were excited at 609, 530 and 567 nm, respectively. While a quantum yield of $\Phi_f = 0.31$ was measured for **2**, the quantum yield of **4** was with $\Phi_f = 0.02$ more than one order of magnitude smaller. Within the concentration range required for the "optical dilution method", the emission peak of **3** could not be distinguished from the noise of the spectrum. These measured quantum yields confirmed the decrease in fluorescence intensity from **2** over **4** to **3**, which was already observed by the naked eye. While **2** was an intensely shining compound under the UV lamp, the emission of **4** was much less intense, while that of **3** could hardly be detected. The loss of fluorescence intensity by substituting benzylamino-core substituents with benzylsulfanyl substituents reflects the increased efficiency of the latter in quenching of the NDI excited state due to its larger number of electrons. This loss of fluorescence intensity with core substituents of increasing atomic weight has already been observed for NDI chromophores.[119]

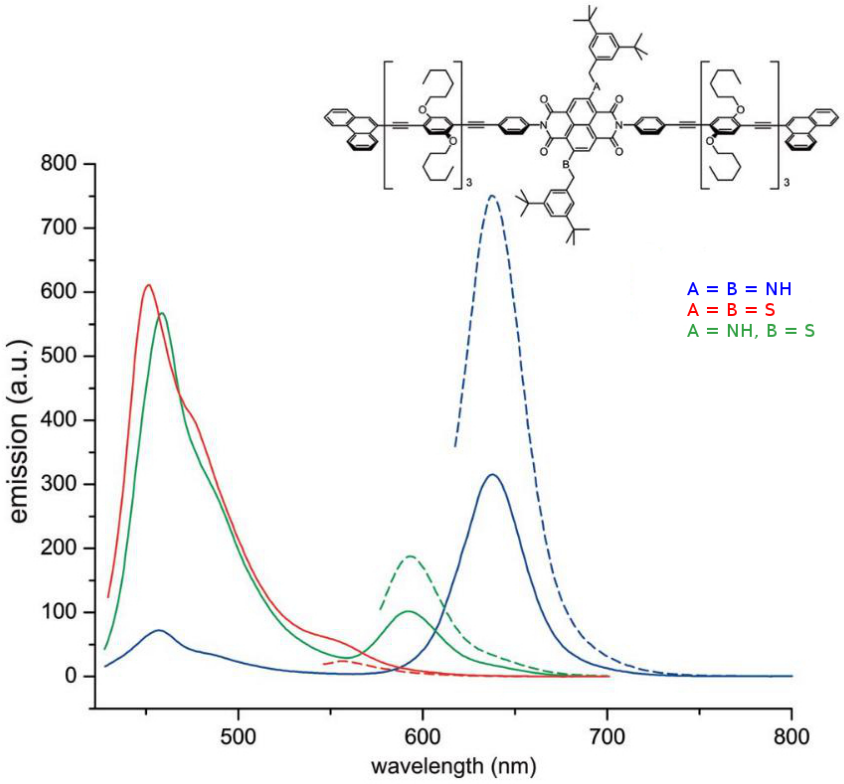

Figure 4.3: Emission spectra of compounds **2**, **3** and **4** recorded at room temperature in CH_2Cl_2($6.5x10^{-7}$ M). Solid lines upon excitation at 415 nm and dashed lines upon excitation at 609 nm for **2** (blue lines), at 530 nm for **3** (red lines) and at 567 nm for **4** (green lines).

Molecular junctions studies

Electroluminescence studies were performed in the nanotube-molecule-nanotube junction with molecular rods **2**, **3** and **4**. Nitrogen core substituted rod **2** showed a strong emission and its presence in the junction was detected. Since this rod was synthesized by Sergio Grunder and Alfred Blaszczyk the junction results won't be discussed here and the reader is referred to the corresponding literature.[117] In contrary to the first rod, the sulfur substituted rod **3** and mixed nitrogen-sulfur rod **4** show weaker emissions and therefore their presence in the junction could not be recorded. This result was in agreement with the emission experiments performed in solution as well as with the calculated quantum yields that show a great difference between the doubly nitrogen substituted rod **2** and the two other rods.

4.5 Conclusion and Outlooks

The synthesis of tailor-made molecules to function in a unique new type of molecular junction measuring optical signals from single molecules was reported. Indeed a series of four naphthalene diimide rods differing from their chromophore or from their oligo(phenylene ethynylene) linkers were synthesized by a convergent strategy through Sonogashira cross-coupling reactions sequences. An asymmetric rod **1** has also been successfully synthesized and is still under investigation in the molecular junction. The deposition of these molecular rods in a carbon nanotube junction and their electroluminescence

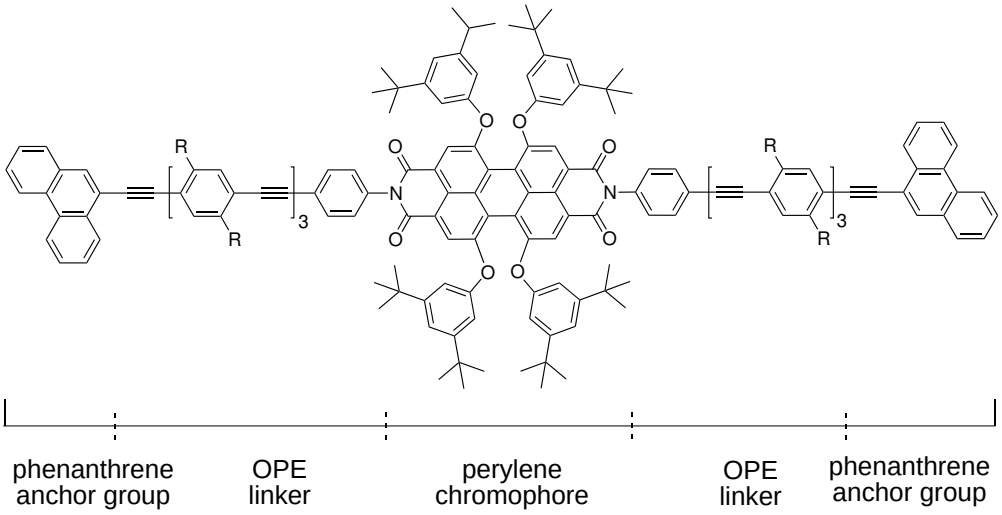

Scheme 4.6: Proposed perylene analog of naphthalene rod **2**

was investigated. These results have been partially published[117] as well as their synthesis and optical properties.[118]

The investigation of luminescence in the nanotube molecular junction could be continued by depositing molecular rods emitting at other wavelengths. Perylenes are good candidate since they provide a strong fluorescence emission[125] measurable in the junction set-up. A perylene equivalent of the strongly fluorescent naphthalene rod **2** is depicted in scheme 4.6.

Chapter 5

Star Shaped Molecules for Surface Functionalization

5.1 Project Description

This work is the product of a fruitful collaboration with Thomas Eaton (University of Basel, Switzerland) who did a part of the synthesis described below and Prof. Manfred Buck's group (University of St Andrews, Scotland) who performed the surface investigations.

This project addresses the challenge of surface functionalization at the single molecular level by using a supramolecular porous network as a template to deposit tailor-made molecules. Scheme 5.1 represents schematically the different units forming the surface network. The solution based deposition of this network on a Au(111) surface was developed by Manfred Buck.[105] Perylene tetracarboxylic diimide (PTCDI, in blue) and melamine (in purple) form the honeycomb structure of the network by hydrogen bonding. The cavities of this network are well suited for a host-guest system. The design and synthesis of the guest molecules are described in the next sections. Following a process of optimization, the proposed candidates were tuned in size and functionalities to control their deposition on the surface and allow the study of their dynamic behavior.

5.2 Molecular Design and Synthetic Strategy

Molecular Design

The surface cavities of the perylene tetracarboxylic diimide (PTCDI) and melamine supramolecular network are rigid structures that form very ordered

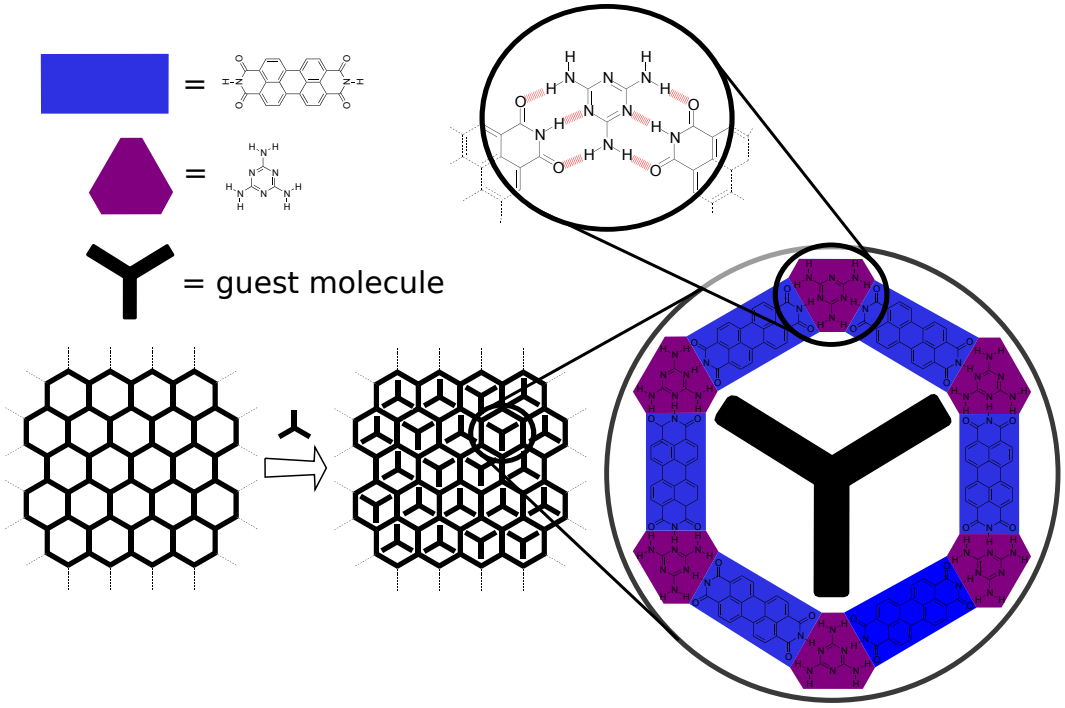

Scheme 5.1: Schematic representation of the perylene tetracarboxylic diimide (PTCDI, blue) and melamine (purple) supramolecular network before and after deposition of the guest molecule. The guest molecules are randomly orientated in the hexagonal cavities in two possible positions.

arrangements. In order to remain organized, the cavities of the network cannot be subjected to deformations. The molecule that acts as a guest must be perfectly adapted to the space available in the cavity created by the host. Ideally its structure is modular to allow a fine tuning of its size and functionalities. A flat aromatic structure formed either by phenylacetylene, stilbene or biphenyl subunits (scheme 5.2) is ideal since it gives the desired modularity. Indeed the size of the subunits decrease in the given order and by choosing carefully the subunits, the appropriate guest size can be precisely adjusted. Furthermore flat aromatic molecules are known to be ideal for surface deposition due to the π-π interaction between the molecule and the surface that favor the adsorption. The hexagonal geometry of the host suggests a star-shaped molecule as an ideal guest candidate. Having a benzene as the central subunit, the star can bear from three to six branches, pointing at one of the six melamine subunits forming each pore of the supramolecular network. All the branches of the star can be identical or not, permitting less symmetrical guests. The stars can moreover be decorated with hydroxy or amine groups to allow the branches to bind to the host by hydrogen bonds.

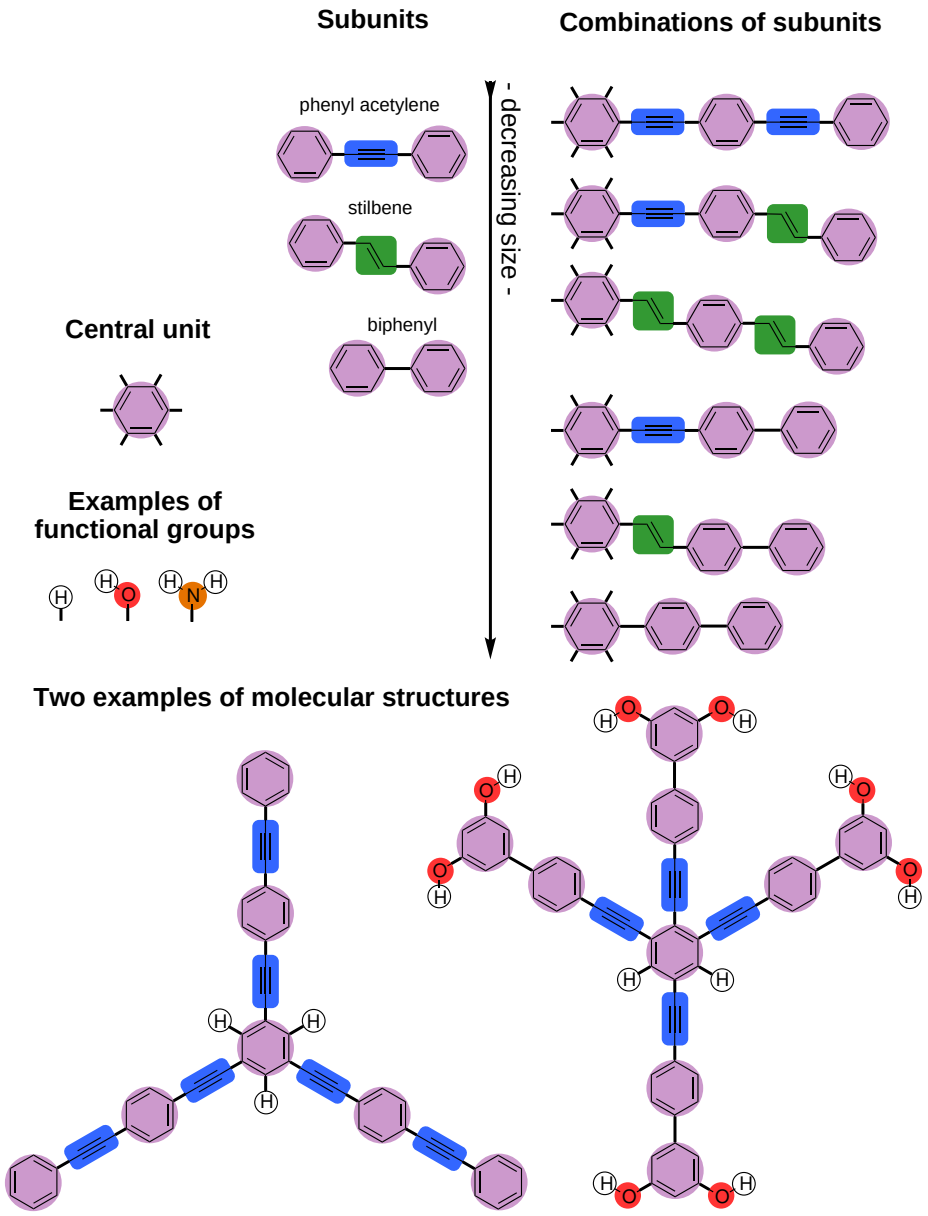

Scheme 5.2: Molecular design for the targeted architectures. The modular approach allows access to a variety of guest molecules having different sizes and functionalities.

Our modular approach allows access to a variety of compound bearing a different number of functional groups. The behavior of the star in the cavities can therefore be controlled by molecular design in a very precise way.

Synthetic Strategy

To obtain a molecular star formed by either phenylacetylene, stilbene or biphenyl subunits, three synthetic routes were considered. The three routes are depicted in scheme 5.3 for the larger star, but remain valid for shorter targets (stilbene or biphenyl stars). Either the star is built from its edges (route 1), or from its center (route 3), or from the edged and the center at the same time (convergent, route 2). The different subunits can be connected by cross-coupling reactions (Suzuki, Sonogashira, Heck) or by Wittig reactions. The first route, purely linear, starts from the edges of the star and reaches

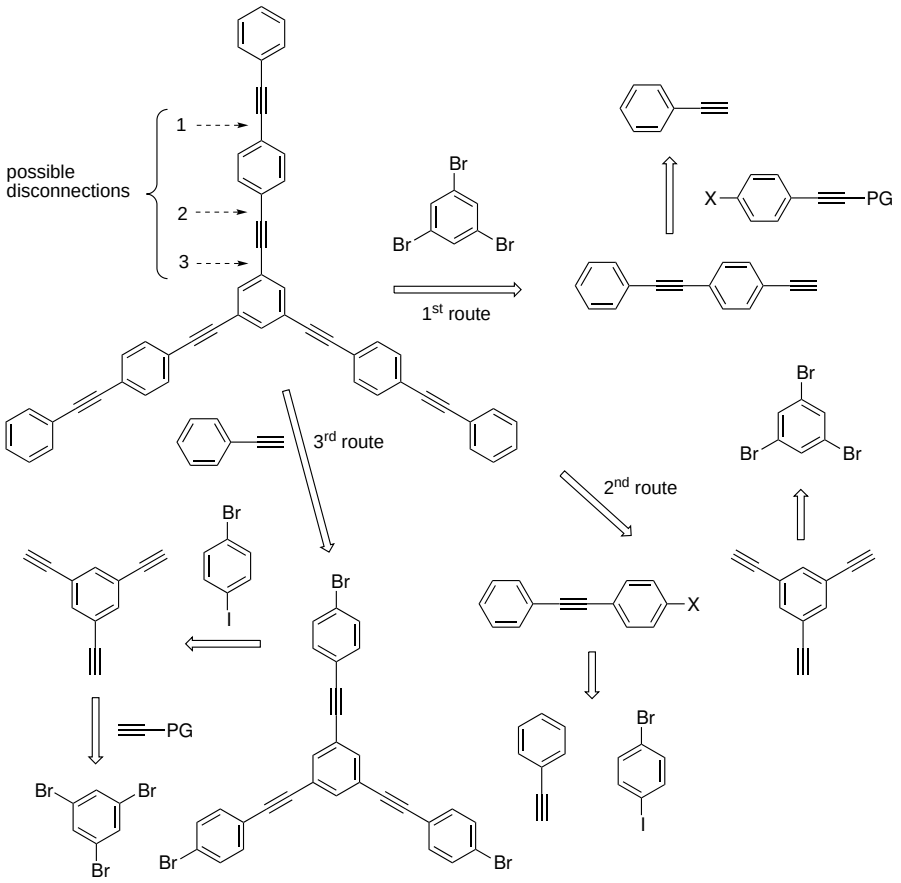

Scheme 5.3: Three synthetic routes to the larger star. These routes are also valid for stars with reduced dimensions.

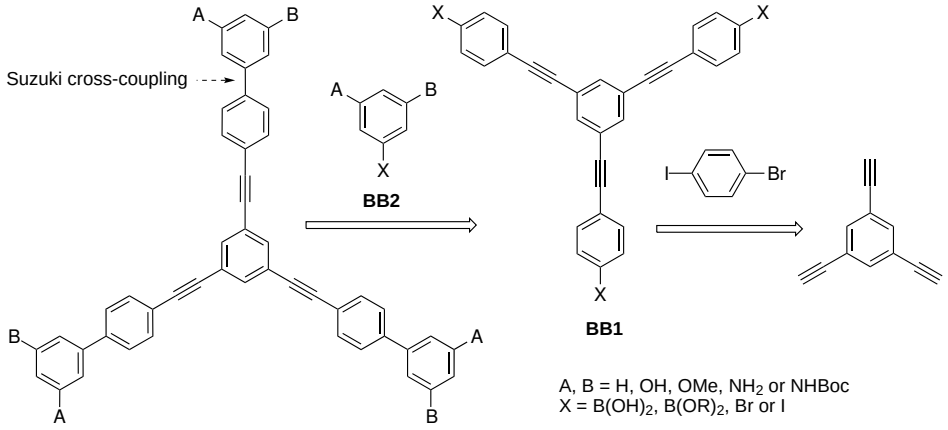

Scheme 5.4: Route to a library of compounds readily accessible by simply coupling subunit **BB1** with different edge subunits **BB2**

the target by a final coupling with tribromobenzene. The second route follows a convergent strategy were the synthesis of the star is simultaneously started from the edges and from the center. In this route the partially formed branch would be coupled with triethynylbenzene in the last step. The third route, purely linear, forms the star starting from its center performing three couplings at each step bearing the danger of yield lose. On the other hand, the third strategy has the advantage of being more modular since if the edges have to be redesigned to change the functionalities of the star, a complete rebuild of the star from the beginning is not necessary. By simply coupling the prebuilt subunit with different edge subunits, a variety of targets can be readily obtained (scheme 5.4).

5.3 Synthesis and Surface Investigations

In this section the synthesis and surface investigations of the different targeted guest molecules are described. The proposed candidates are tuned in size and functionalities thanks to the feedback coming from St Andrews where the surface investigations were performed.

The Three-Arm Phenylacetylene Star 5

The first targeted three-arm star was synthesized following a linear strategy (scheme 5.5). In a one pot reaction, 1-bromo-4-iodobenzene was first coupled at room temperature to TIPS acetylene followed by phenylacetylene at 80 ° C. This reaction takes advantage of the preferred reactivity of the free

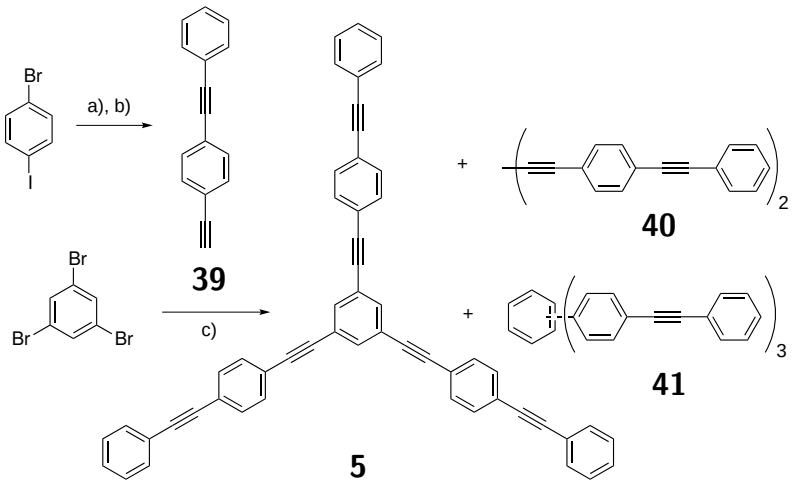

Scheme 5.5: Reagents and conditions: a) 1. TIPSA, $Pd(PPh_3)_2Cl_2$, CuI, THF, $^iPr_2NH$, 40 ° C, 3h; 2. phenylacetylene, 80 ° C, 16h, quant.; b) TBAF, THF, 0 ° C, 88%; c) $Pd(PPh_3)_4$, CuI, THF, $^iPr_2NH$, 60 ° C, 7h, 26%.

acetylene to aryliodides in a Sonogashira reaction. Indeed the TIPS acetylene reacts only at the iodine position of the 1-bromo-4-iodobenzene if exactly one equivalent of TIPSA is use. The bromo position remained untouched (no product bearing two TIPS acetylenes was observed). When the temperature of the reaction mixture was increased from 40 ° C to 80 ° C, phenylacetylene was added to the reaction mixture and it reacted at the bromo position. Performing two reactions in one pot with good yields was a serious advantage since it avoids purification steps. Subsequent TBAF deprotection and coupling of **39** with 1,3,5-tribromobenzene afforded the desired three-arm star **5**. This reaction was first performed at 80 ° C in toluene. After purification by column chromatography, the product was analysed by MALDI-TOF MS showing the presence of three compounds. The mass of the desired product was found with the mass of the homocoupled product **40**. The third mass found in the MALDI-TOF MS was attributed to the three-arm star **41** formed by the coupling of the homocoupled product with free acetylene **39**. The same reaction was repeated using THF as solvent, decreasing the temperature to 60 ° C and keeping a strict oxygen free atmosphere but the same side products were obtained. Other reaction conditions could have been tried such as a copper free reaction or changing the palladium catalyst, but the decision was made to work on the purification of the mixture containing the desired product. The chemical properties of the different components of this mixture were similar which rendered the purification steps troublesome. Indeed conventional purification methods like column chromatography (silica

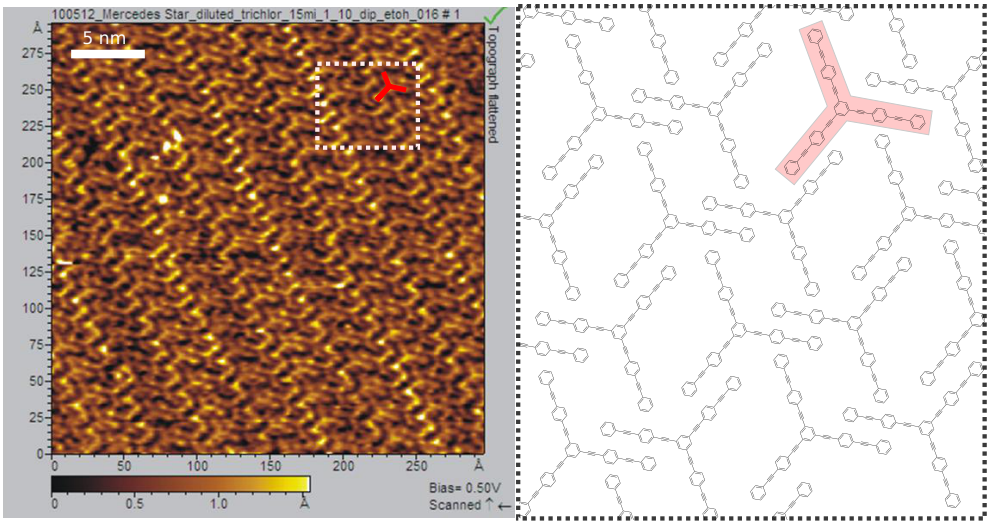

Figure 5.1: Left: room temperature STM pictures of the phenylacetylene star **5** on a naked Au(111) surface. Right: schematic representation of the surface organization

gel) or recrystalizations were unsuccessful. Taking advantage of their little but sufficient difference in size, a recycling gel permeation chromatography (rec-GPC) was finally the method of choice to obtain a clean product (in 26% yield).

Having the first star model in hand, the molecule was deposited on a Au (111) surface in order to determine whether the molecule is adsorbed on the surface. The STM pictures (figure 5.1) revealed a nice organization of the phenylacetylene stars on the surface. This observation was encouraging to continue the investigations on the network functionalized surface. The star was therefore deposit on a Au(111) surface previously functionalized with the PTCDI-melamine supramolecular network. The star guest molecule **5** was then deposit in solution on the same surface. The STM pictures (scheme 5.2 **a-c**) show the co-deposition of the star and the PTCDI-melamine network on the gold surface. The hexagonal structures of the network remains unchanged if no star molecule is present in the cavity. When the star molecule is present in the cavity, its hexagonal structure is subjected to deformation (figure 5.2 **d**). The size of the star is clearly too big to fit in the cavities and it breaks the hydrogen bonds between the PTCDI and the melamine units. The molecular modeling of the phenylacetylene star **5** in the PTCDI-melamine cavity (figure 5.2 **e**) confirmed this observation although this calculation is only an approximation since the length of the hydrogen bonds between the PTCDI and the melamine subunits of the cavities are not known with precision. Therefore,

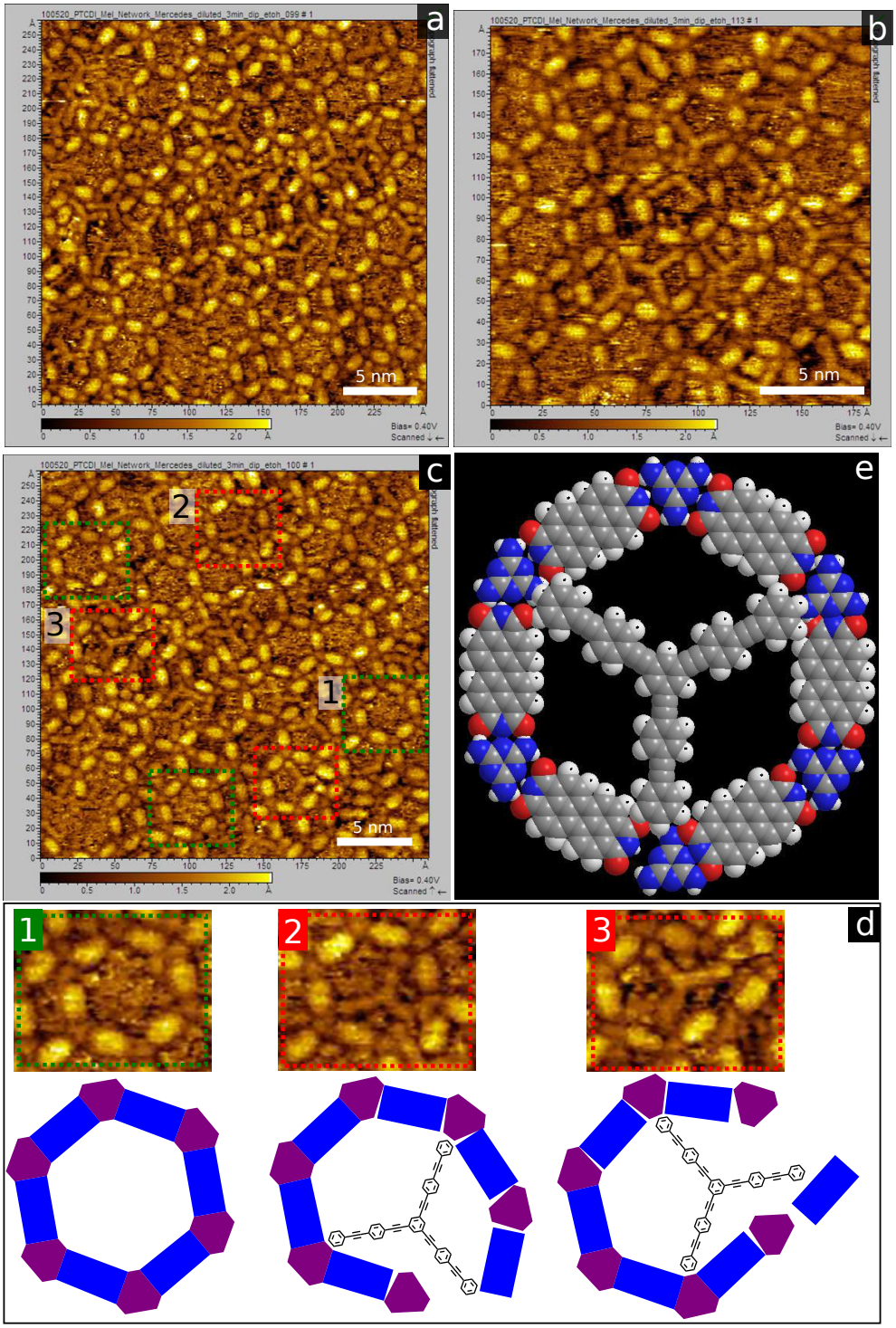

Figure 5.2: **a-c:** STM pictures of phenylacetylene star **5** and the PTCDI-melamine network on a Au(111) surface. Some cavities host a star (red) and some others remain empty (green). **d:** Magnifications and scheme of some hexagonal cavities of picture **c**. **e:** Molecular modeling of an PTCDI-melamine cavity hosting the star.

only by systematically modifying the size of the star molecule an appropriate guest can be found.

The Three-Arm Stilbene Star 6 and Biphenyl Stars 7

The STM observations demonstrated that the phenyl acetylene **5** is not a good candidate to act as a guest in the supramolecular network but our structure design goes in the right direction and a small size readjustment could provide the right guest. The arms of the star were therefore modified to obtain shorter targets by replacing one acetylene by an olefin (stilbene star **6**) or connecting the two phenyls directly (biphenyl star **7**). To accomplish this task, a more convergent route was developed. This new route helped also to overcome some purification difficulties encountered in the synthesis of the first star. In the previous route, the last connection was made between the free acetylenes OPE rod and the central tribromobenzene. In

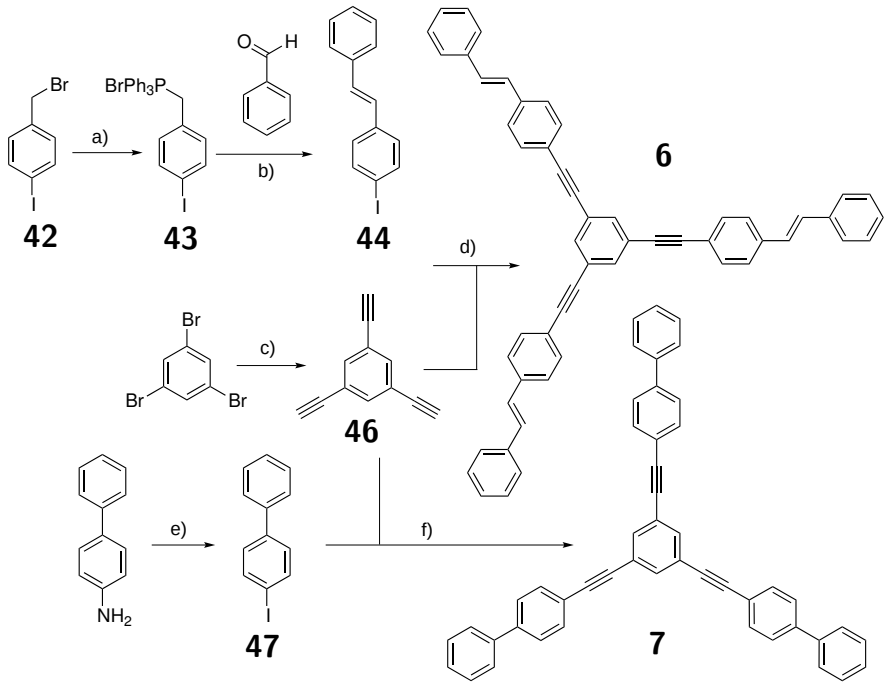

Scheme 5.6: Reagents and conditions: a) PPh_3, 85 °C, 1h, 76%; b) 1. ^{t}BuOK, toluene, 0 °C, 1h30; 2. r.t., 16h, 77%; c) 1. TMSA, CuI, $Pd(PPh_3)_2Cl_2$, THF, $^i Pr_2NH$, 60 °C, 16h, quant.; 2. K_2CO_3, THF, MeOH, r.t., 6h, quant.; d) $Pd(PPh_3)_4$, CuI, THF, $^i Pr_2NH$, r.t., 16h, 49%; e) 1. pTsOH·H_2O, $NaNO_2$, KI, CH_3CN, H_2O, 15 °C, 10 min.; 2. 20 °C, 2h, 71%; f) $Pd(PPh_3)_4$, CuI, THF, $^i Pr_2NH$, r.t., 16h, 83%.

this new route the free acetylenes are borne by the central unit and the arms bear the halide. This route can possibly form side products (homocoupling of triethynylbenzene) but they are expected to be easily separated from the desired compound by straightforward purification methods (e.g. column chromatography, recrystalization).

The stilbene star was obtained by first converting 1-(bromomethyl)-4-iodobenzene **42** into the phosphonium ylide **43** in good yield (scheme 5.6). This product was then reacted with benzaldehyde to give the mixed E and Z stilbene products via a Wittig reaction. The product was first obtained performing this reaction in CH_2Cl_2 with an aqueous NaOH solution as base (yield of 35%). The reaction was optimized by using dry toluene as solvent and potassium tert-butoxide as a base. By this modification the yield was significantly increased to 77%. The E/Z mixture of products was refluxed in toluene with traces of iodine delivering only the E form. The parallel synthesis of the central subunit was started by the coupling of tribromobenzene and TMSA, followed by the cleavage of the protecting groups under basic conditions. Both reaction afforded the product in quantitative yields. The obtained 1,3,5-triethynylbenzene **46** was coupled in a Sonogashira reaction with the iodo stilbene **44** giving the desired stilbene star **6**. Having the free acetylenes in the central unit was a successful route since the star was obtained in fair yields (49%) but the removal of the side products was not troublesome and a conventional purification method (column chromatography) was sufficient.

The biphenyl three-arm star was obtained following the same route (scheme 5.6). A Sandmeyer reaction on commercially available 4-aminobiphenyl formed the iodobiphenyl **47**. The latter was coupled in a Sonogashira reaction with 1,3,5-triethynylbenzene **46** affording the biphenyl star **7** in good yields after silica gel column chromatography (a mixture of cyclohexane and CH_2Cl_2 as eluent). The similar reaction with the bromo equivalent of **47** did not lead to the desired biphenyl star **7** probably due to the lower reactivity of the bromo equivalent towards Sonogashira reactions. The products formed are assumed to be a mixture of homocoupled compounds that precipitate.

The surface investigations of the stilbene star **6** (which are not depicted here) show, as for the phenylacetylene star **5**, that the star is too big to act as a guest in the PTCDI-melamine hexagonal cavity. This observation was again supported by the molecular modeling of the star (figure 5.3). The STM measurements of the biphenyl star **7** (figure 5.4 **a**) show the perfect hexagonal structures of the network with most of the cavities filled with a guest molecule. In contrast to the broken network seen for the phenylacetylene **5**, here the network remains intact after the co-depostionn of the star molecules which demonstrates the perfect insertion of the star in the

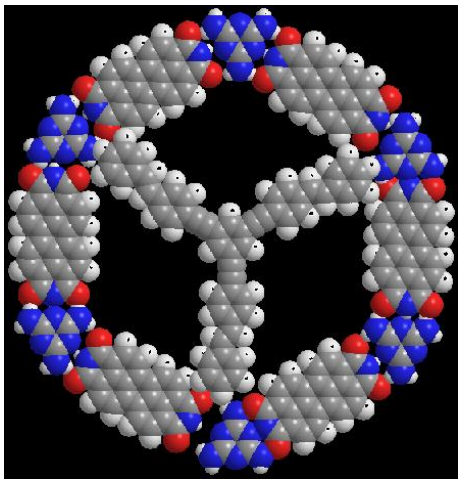

Figure 5.3: Molecular modeling of the stilbene star **6**.

supramolecular cavities. The size of the star is now optimal to act as a guest in the PTCDI-melamine network. This observation was supported by the molecular modeling (figure 5.4 **b**). In the STM pictures, most of the pores contain six protrusions (magnified in figure 5.4 **c**) which could mean that two molecules lay on top of each other, but this hypothesis was ruled out since the STM tip would be able to distinguish the difference between one or two molecules in each cavity (the height of the STM tip would be different). The second hypothesis is that the biphenyl stars rotate in the cavities and what is seen on the pictures is a time-averaged image of the different positions (at t_0 and t_1 in figure figure 5.4 **c**). In order words, the time needed to record an image is longer than the rotation of the molecule which make two position of the same molecule visible in one image. To confirm the hypothesis that the star rotates on the time scale of the STM investigation in the cavities, the set-up can be cooled down to slow down the molecular motion. This option is limited by the solvent used for the deposition. The second option is to add molecular interactions between the network and the star (e.g. hydrogen bonds). The formation of new hydrogen bonds between the network and the star would decrease the free rotation of the latter in the hexagonal cavity and allow dynamic investigations (scheme 5.7).

The Three-Arm Hydroxy and Dihydroxy Biphenyl Stars 8 and 9

The STM pictures revealed that the biphenyl star has the perfect size to act as a guest in the supramolecular network. Therefore this structure was chosen to continue the investigations on the host-guest system. To precisely control the free rotation of the biphenyl star, the addition of new hydrogen

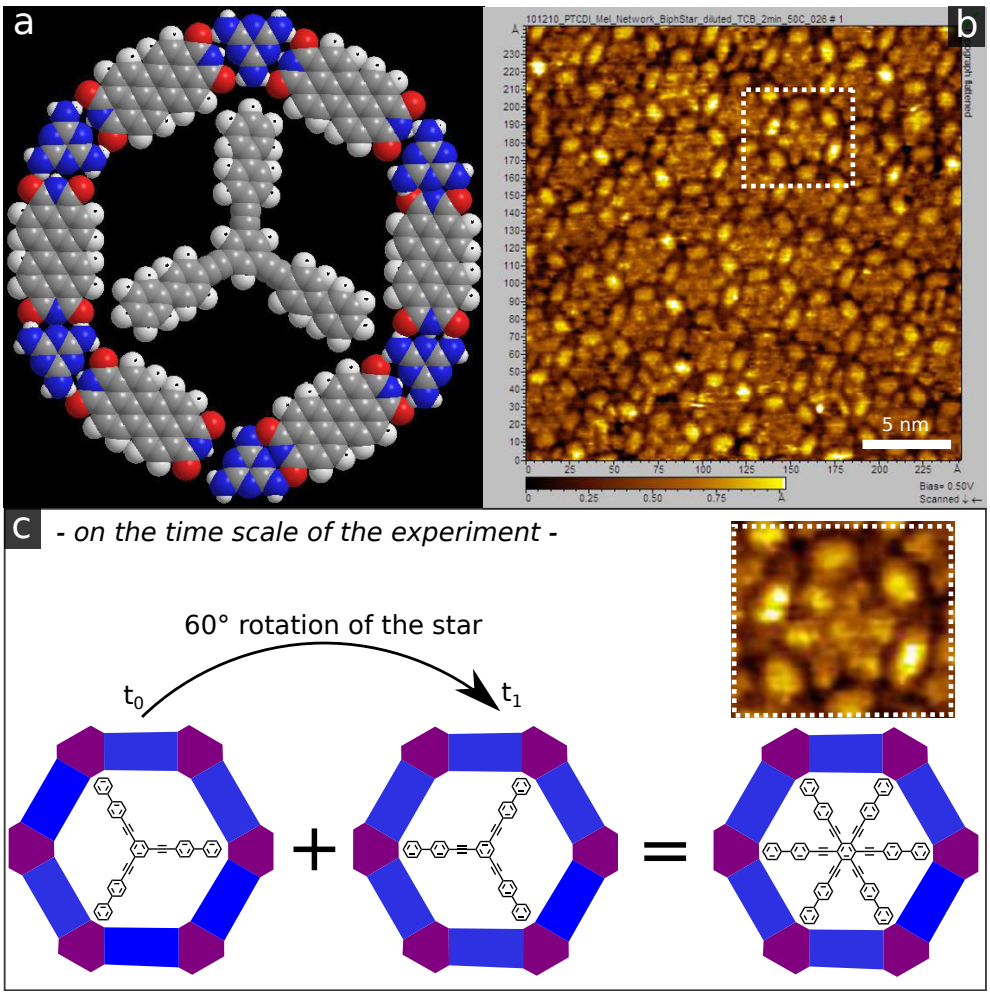

Figure 5.4: **a**: Molecular modeling of the biphenyl star **7**. **b**: Room temperature STM picture of the biphenyl star **7** on a Au(111) surface previously functionalized with the PTCDI-melamine network. **c**: Magnification of an hexagonal cavity containing six protrusions corresponding to the superposition of two orientations of the same molecule at different times (t_0 and t_1); the two different orientations cannot be distinguished on the time scale of the experiment and the STM picture shows the appearance of both positions of the star in the cavity.

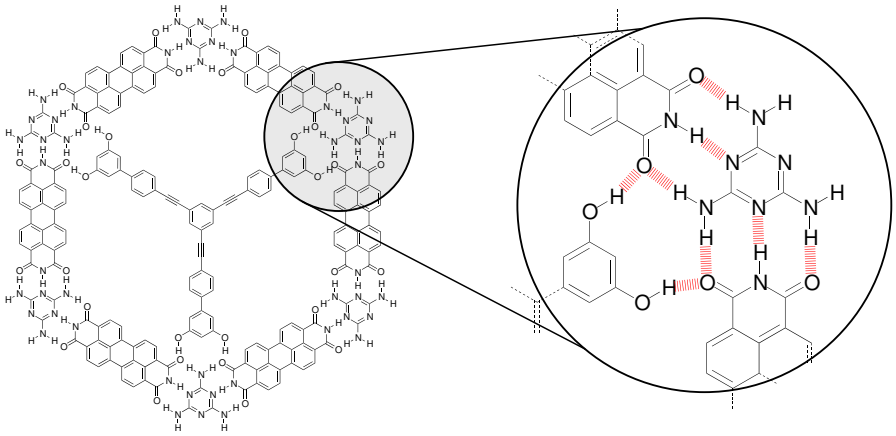

Scheme 5.7: Schematic representation (with magnification) of the hydrogen-bonds between the dihydroxy biphenyl star **9** and the PTCDI-melamine network.

bonds between the host and the guest was envisaged to act as anchor groups and therefore slow down or stop the motion of the star (scheme 5.7). The star was therefore functionalized with hydroxy groups. The later was preferred over amine groups since R_1–OH···OR_2 hydrogen bonds are stronger than the R_1–NH_2···OR_2 ones. Two hydroxy functionalized three-arm star shaped structures were imagined. The first one bears one hydroxy group per branch with a total of three new possible interactions with the host cavity. The second candidate bears two hydroxy groups per branch giving a total of six new hydrogen bonds with the host.

The control of the rotation requires a fine tuning of the star structure and to do so a library of compounds having different numbers of hydroxy (or ev. amine) groups is ideal to find the best candidate. A more modular and straightforward route was proposed to obtain this library of compounds in a more rapid way (scheme 5.8).

This route was started with the coupling of 1,3,5-triethynylbenzene and 1-bromo-4-iodobenzene affording in good yields the desired 1,3,5-tris((4-bromophenyl)ethynyl)benzene **48**.[126] This reaction takes advantage of the chemoselectivity of Sonogashira reactions to perform the coupling of the free acetylene only at the iodo position of 1-bromo-4-iodobenzene, leaving the bromo position untouched. Indeed, no mixed products were observed. This new building block is very handy for a modular route where readily or commercially available compounds can be coupled to have a library of compounds bearing different functionalities without having to rebuild the whole star structure from the beginning for every target. An example is the microwave assisted Suzuki coupling of compound **48** to the commercially available (3-

hydroxyphenyl)boronic acid giving the three hydroxy star **8** in an very low yield (5%) which can be explained by the poor solubility of the product in $CHCl_3$ which was the solvent used in the rec-GPC. The real yield is probably higher since the majority of the crude remained insoluble. The possibility to purify the rest of the crude by reverse phase chromatography was envisaged but the amount of pure product cleaned by rec-GPC was sufficient to perform the surface investigations and no further attempts to have more product were accomplished. Compound **48** was coupled in a similar manner with 3,5-dimethoxyphenylboronic acid leading to the protected version of the star **9** but its deprotection by BBr_3 was never complete due probably to the limited solubility of the partially deprotected intermediate. Since the dihydroxy biphenyl star **9** was targeted in parallel via its synthesis through a Sonogashira coupling with a unprotected dihydroxy building block, no other deprotection systems (solvents, deprotection agents) were tested.

Having a compound that needs deprotection in the very last step was an unappropriate route to the target and this strategy was abandoned to focus on the strategy that proved its success in the synthesis of the previous stilbene star **6** and biphenyl star **7**, namely the coupling of the triethynylbenzene with the corresponding hydroxy biphenyl. This synthesis was started by the statistical Suzuki coupling of 3,5-dimethoxyphenylboronic acid and 1,4-dibromobenzene which formed the 4'-bromo-3,5-dimethoxy-1,1'-biphenyl in moderate yields (48%). The losses in yield can be explained by the formation of a non negligible amount of the dehalogenated product 3,5-dimethoxy-1,1'-biphenyl (31%). The coupling on both bromo position of 1,4-dibromobenzene was not observed and the dehalogenation pathway was preferred. The reaction conditions were not optimized at that stage since the quantities obtained were sufficient to go on with the synthesis. The deprotection of the 4'-bromo-3,5-dimethoxy-1,1'-biphenyl was performed with BBr_3 in CH_2Cl_2 at -78 °C giving the doubly deprotected product **49** in fair yields (68%) and the monodeprotected product (20%). The reaction conditions were not further optimized and compound **49** was coupled to 1,3,5-triethynylbenzene without resulting in the desired product. The low reactivity of the bromine **49** as well as the probable instability of the free hydroxy groups at elevated temperature were probably the causes. To overcome these difficulties the iodo analog **51** was synthesized to offer a more reactive reagent for the coupling. The first route tried was coupling 3,5-dimethoxyphenylboronic acid with 1,4-diiodobenzene in a similar statistical reaction than the one described above, but this route led to major amounts of the doubly coupled product although a large excess of 1,4-diiodobenzene was used. The decision was then made to "mask" one of the two iodines in 1,4-diiodobenzene by a triazene to perform the coupling only once on each aryl. Therefore iodoaniline was

transformed into the corresponding triazene **50** in fair yields followed by the coupling with 3,5-dimethoxyphenylboronic acid in a Suzuki reaction giving the biphenyl product in a yield of 56%. Heating this compound in a sealed vial with MeI at 130 ° C afforded the corresponding iododimethoxybiphenyl that was deprotected with BBr_3 in a excellent yield giving compound **51**. The final coupling of 1,3,5-triethynylbenzene with compound **51** yielded to the desired dihydroxy biphenyl star **9** in 63% yield after troublesome purification steps. Indeed compound **9** could not be purified by recycling GPC like star **8** for solubility reasons. Indeed $CHCl_3$ is the solvent used in our recycling GPC system and this solvent is not appropriate to dissolve the hy-

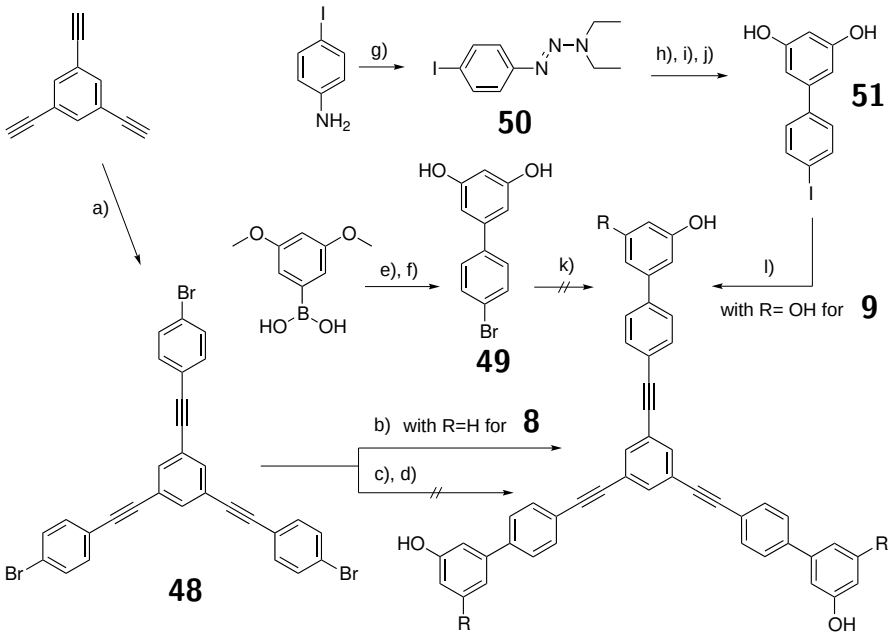

Scheme 5.8: Reagents and conditions: a) 1-bromo-4-iodobenzene, $Pd(PPh_3)_2Cl_2$, CuI, THF, $^iPr_2NH$, r.t., 5h, 79%; b) 3-hydroxyphenylboronic acid, $Pd(PPh_3)_2Cl_2$, K_2CO_3, toluene, EtOH, MW 110 ° C, 30 min, 5%; c) 3,5-dimethoxyphenylboronic acid, $Pd(PPh_3)_2Cl_2$, K_2CO_3, toluene, EtOH, MW 110 ° C, 20 min, 67%; d) 1. BBr_3, CH_2Cl_2, -78 ° C, 2h; 2. r.t., 16h, -%; e) $Pd(PPh_3)_2Cl_2$, K_2CO_3, toluene, EtOH, 80 ° C, 20h, 48%; f) 1. BBr_3, CH_2Cl_2, -78 ° C, 2h; 2. r.t., 16h, 68%; g) 1. H_2O, $NaNO_2$, HCl; 2. K_2CO_3, Et_2NH, 53%; h) 3,5-dimethoxyphenylboronic acid, $Pd(PPh_3)_4$, K_2CO_3, toluene, EtOH, 80 ° C, 56%; i) MeI, 130 ° C, 90%; j) BBr_3, CH_2Cl_2, -78 ° C, 97%; k) 1,3,5-triethynylbenzene, $Pd(PPh_3)_4$, CuI, DMF, $^iPr_2NH$, 60 ° C, 5h30, -%; l) 1,3,5-triethynylbenzene, $Pd(PPh_3)_4$, CuI, DMF, $^iPr_2NH$, 45 ° C, 16h, 63%.

droxy functionalized star. Therefore compound **9** was purified with success by repeated reverse phase chromatographies in a mixture of MeOH/H_2O as eluents.

The STM pictures of hydroxy biphenyl star **8** are depicted in figure 5.5 **a-d**. In some cavities the three arms of the stars are clearly visible which could mean that it is not rotating anymore on the time scale of the experiment. In some other cavities, six protrusion are seen which means that in that cavity the star rotates in a time scale faster than the scan rate of the STM imaging and what is observed in the STM image is a superposition of two orientations of the star. The same phenomena was described for the biphenyl star **7** in figure 5.4. In some other cases, the stars seem at the edge of the time scale. A schematic representation of three cavities of figure 5.5 **d** are shown in figure 5.5 **e**.

The Four-Arms Dihydroxy Biphenyl Star 10

In our attempt to control the behavior of the star on the surface, the fine adjustment of the molecular structure is a key point. The three-arm stars allows the introduction of a maximum of six hydroxy groups, two per branch. To introduce more hydroxy groups, a fourth arm had to be added to the star. A straightforward route meeting the strategy yielding to the three-arm hydroxy biphenyl stars was followed. In this approach a central unit bearing four free acetylenes is coupled with the dihydroxy biphenyl subunit previously used in the synthesis of the three-arm star. The dihydroxybiphenyl was chosen since it offers the maximum number of new hydrogen bonds.

The synthesis of the four-arms star (scheme 5.9) followed the successful strategy previously used in the route of the three-arm stars. It requires a central phenyl substituted by four bromines or iodines in positions 1,2,3 and 5. A straightforward route to obtain such structure was to synthesize 2,4,6-triiodoaniline via the iodination of aniline with ICl.[127] In this reaction, the purification of the crude was troublesome and the triiodoaniline was finally obtained in 22% yield after several consecutive recrystalizations in EtOH. A Sandmeyer reaction[128] with 2,4,6-triiodoaniline **52** afforded 1,2,3,5-tetraiodobenzene **53** in a moderate yield. The higher reactivity of aryl iodides over aryl bromides in Sonogashira reactions implies that 1,2,3,5-tetraiodobenzene **53** may be the best candidate for the formation of the four branched star. However other alternatives where considered to overcome the moderate to low yield obtained in the synthesis of this compound. Therefore the commercially available 2,4,6-tribromoaniline was subjected to a Sandmeyer reaction giving 1,3,5-tribromo-2-iodobenzene **55** in 68% yield, which is a satisfactory yield for a Sandmeyer reaction known to rarely give very

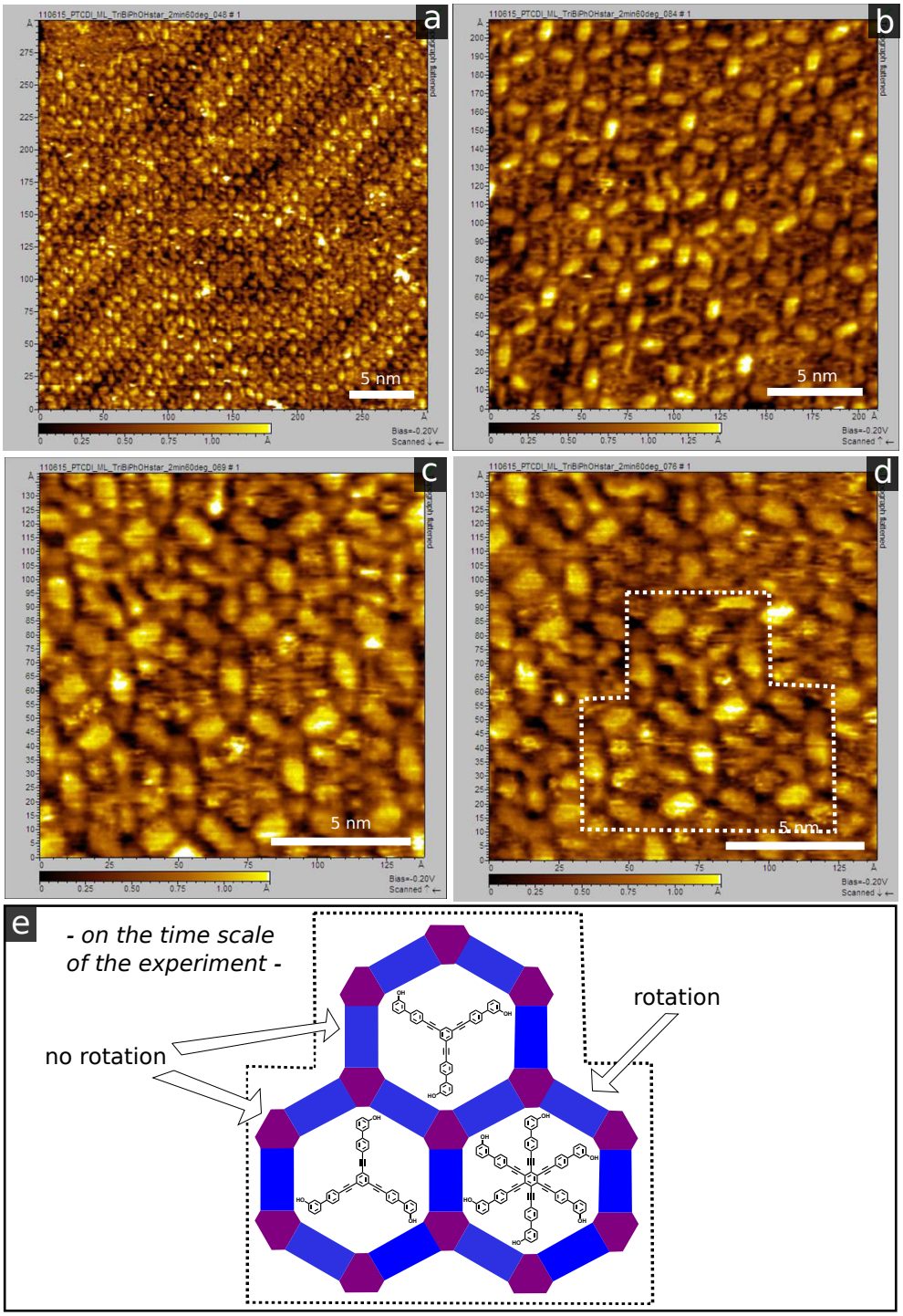

Figure 5.5: **a-d:** Room temperature STM pictures of the biphenyl star **8** on a Au(111) surface previously functionalized with the PTCDI-melamine network. **e:** Schematic representation of three network cavities containing the star. In two of the cavities, the three arms of the star are visible showing no rotation on the time scale of the experiement. The third cavity shows six protrusions indicating a rotation of the molecule on the time scale of the experiment.

high yields.

To obtain the desired 1,2,3,5-tetraethynylbenzene both the 1,2,3,5-tetraiodobenzene **53** and 1,3,5-tribromo-2-iodobenzene **55** were coupled with protected acetylenes. The choice of the appropriate protecting group appeared to be of great importance. The most common protected acetylenes, namely the bulky triisopropylsilyl acetylene (TIPSA), its more labile analog the trimethylsilyl acetylene (TMSA) and the polar 2-methy1-3-butyn-2-ol acetylene (HOPA). The attempt to couple TIPSA to 1,2,3,5-tetraiodobenzene **53** failed probably due to the steric hindrance of two neighboring TIPS protected acetylenes on a aromatic ring. The reaction was performed in the MW at high temperature (110 ° C) during 40 min with a large excess of TIPSA (3 equivalents per iodine), a Pd(II)(5%)/CuI(5%) catalytic system and controlling the evolution of the reaction by TLC every 10 min. The tetrasubstituted product was never isolated but only the protected 1,2,4-triethynylbenzene (dehalogenated product) was obtained in 23% yield. Example of neigh-

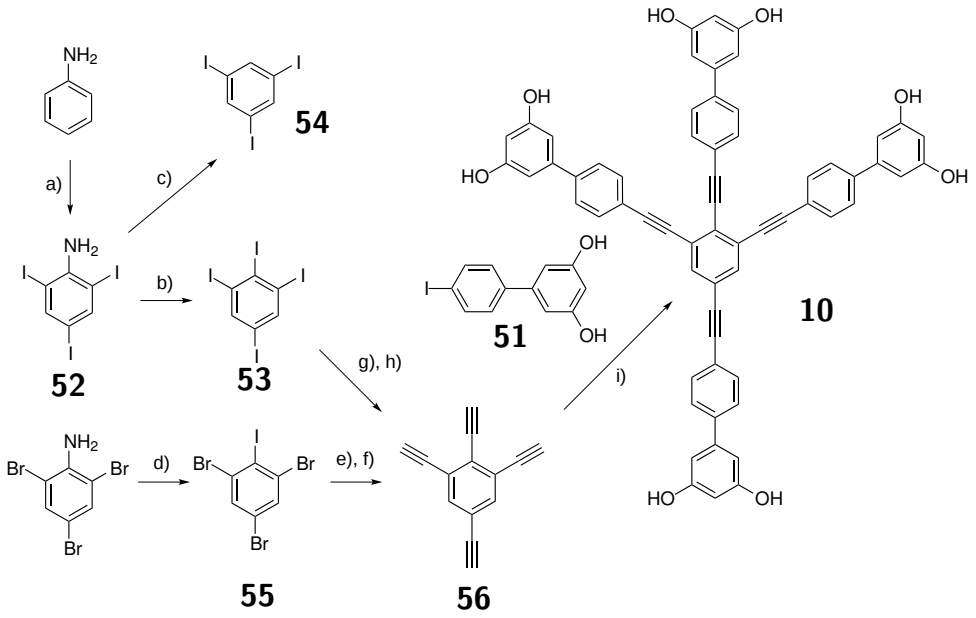

Scheme 5.9: Reagents and conditions: a) ICl, AcOH, 120 ° C, 2h, 22%; b) pTsOH·H_2O, $NaNO_2$, KI, CH_3CN, H_2O, 15 ° C, 10 min.; 2. 20 ° C, 2h, 39%; c) $NaNO_2$, Cu_2O, H_2SO_4, EtOH, AcOH, 100 ° C, 2h, 87%; d) pTsOH·H_2O, $NaNO_2$, KI, CH_3CN, H_2O, 15 ° C, 10 min.; 2. 20 ° C, 2h, 68%; e) 2-methy1-3-butyn-2-ol, $Pd(PPh_3)_2Cl_2$, CuI, DMF, Et_2NH, 80 ° C, 24h, 49%; f) NaH, toluene, 120 ° C, 3h, 49%; g) 2-methy1-3-butyn-2-ol, $Pd(PPh_3)_2Cl_2$, CuI, DMF, Et_2NH, MW 120 ° C, 20 min, 60%; h) NaH, toluene, 120 ° C, 3h, 49%; i) $Pd(PPh_3)_4$, CuI, THF, $^iPr_2NH$, 45 ° C, 16h, 45%.

boring acetylene on an aryl are known in the literature. These examples usually use smaller protected acetylenes such as TMSA or HOPA.[129] Therefore the coupling of TMSA with 1,2,3,5-tetraiodobenzene **53** was attempted. Several reaction conditions were tested going from a traditional oil bath heating to MW heating, varying the temperature from 60 to 110 °C or changing the solvents/base system (THF/$^{i}Pr_2NH$, DMF/Et_2NH). The catalytic system remained the same for all the attempts ($Pd(PPh_3)_2Cl_2$/CuI, 5 mol% each). All these attempts failed in giving the product in reasonable yields and HOPA was then chosen as protected acetylene. The latter has an advantage, its polarity facilitates the purification steps. The protected acetylene HOPA was either coupled with 1,2,3,5-tetraiodobenzene **53** or with 1,3,5-tribromo-2-iodobenzene **55** affording the desired HOP protected 1,2,3,5-tetraethynylbenzene in 60% and 49% yield, respectively. These yields are acceptable taking into consideration that the reaction involves four couplings. The deprotection of this product with TBAF gave 1,2,3,5-tetraethynylbenzene **56** in 49% yield. The final star **10** was then obtained by a Sonogashira reaction between 1,2,3,5-tetraethynylbenzene and compound **51** in fair yields (45%). As described for the previous stars bearing hydroxy groups, the purification was only possible by repeated reverse phase chromatographies, using a mixture of MeOH and water as eluent.

The way imagined to obtain the tetraethynylbenzene (through 1,3,5-tribromo-2-iodobenzene) enables the synthesis of different unsymmetrical four-arms stars bearing three arms with a certain type of functionalization and the fourth arm with a different one. It allows again the fine control of the star rotation in the cavities. This strategy takes advantage of the chemoselectivity of the Sonogashira reaction since the iodine could be coupled with the first type of branch and in a second stage the three bromines could be coupled with a different type of branch. Two orthogonal acetylene protecting groups might be needed in this strategy.

The STM investigations of the four-arms dihydroxy biphenyl star **10** on a Au(111) naked surface are depicted in figure 5.6. The four-arms structure of the star is clearly visible. Scheme 5.6 **c** shows a magnification of the random alignment of the stars on the surface and its schematic representation.

The four-arms star **10** was then deposit on a Au(111) surface previously functionalized with the PTCDI-melamine supramolecular network. STM pictures are shown in figure 5.7. Pictures **a** and **b** are exactly the same portion of surface recorded with an interval of 75 seconds. The cavities with molecules that retained their position are shown in green and the ones that rotated are shown in red. Cavity *A* contains no star and cavity *B* contains a star that rotates 60 ° counterclockwise within 75 secondes. Figure 5.7 *c* show a magnification and schematic representation of cavity *B*. For the previous

three-arm stars, the rotation of the molecules was faster than the time scale of the STM experiment and the three arms were equally distributed in all the six positions of the hexagon. In contrast to what was observed for the other stars, here the STM pictures represent only one position for each star. Here no cavity containing two positions is seen. Either the cavities are empty, or filled with one star of which the four-arms are distinguished. Although the rotation on the time scale of the experiment is not observed, some stars still rotate but with a slower motion. Due to the asymmetry brought by the fourth arm of the star, the direction of the rotation can be observed. In all the cases were the rotation can unambiguously be established, the stars rotate with an angle of 60 ° counterclockwise. The stars posses no chirality

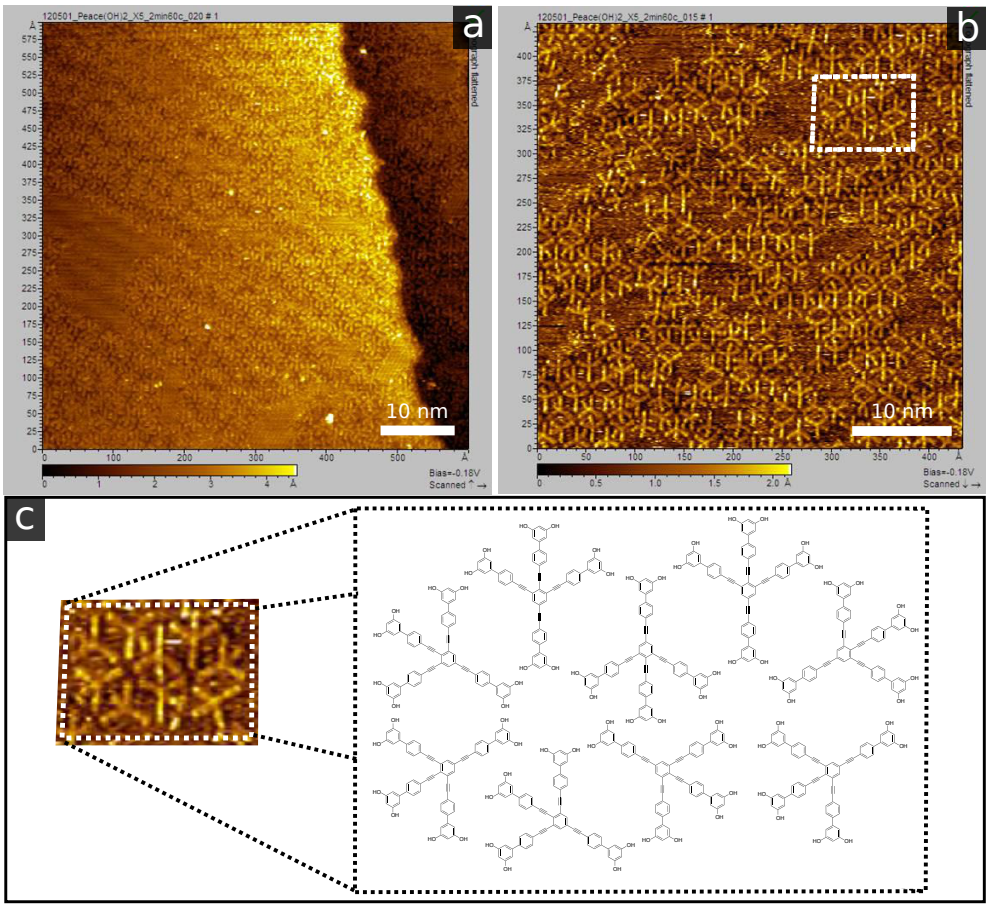

Figure 5.6: **a,b:** Room temperature STM picture of the four-arms dihydroxy biphenyl star **10** on the naked Au(111) surface. **c:** Magnification of a region of the surface with the schematic representation of the star arrangement on it.

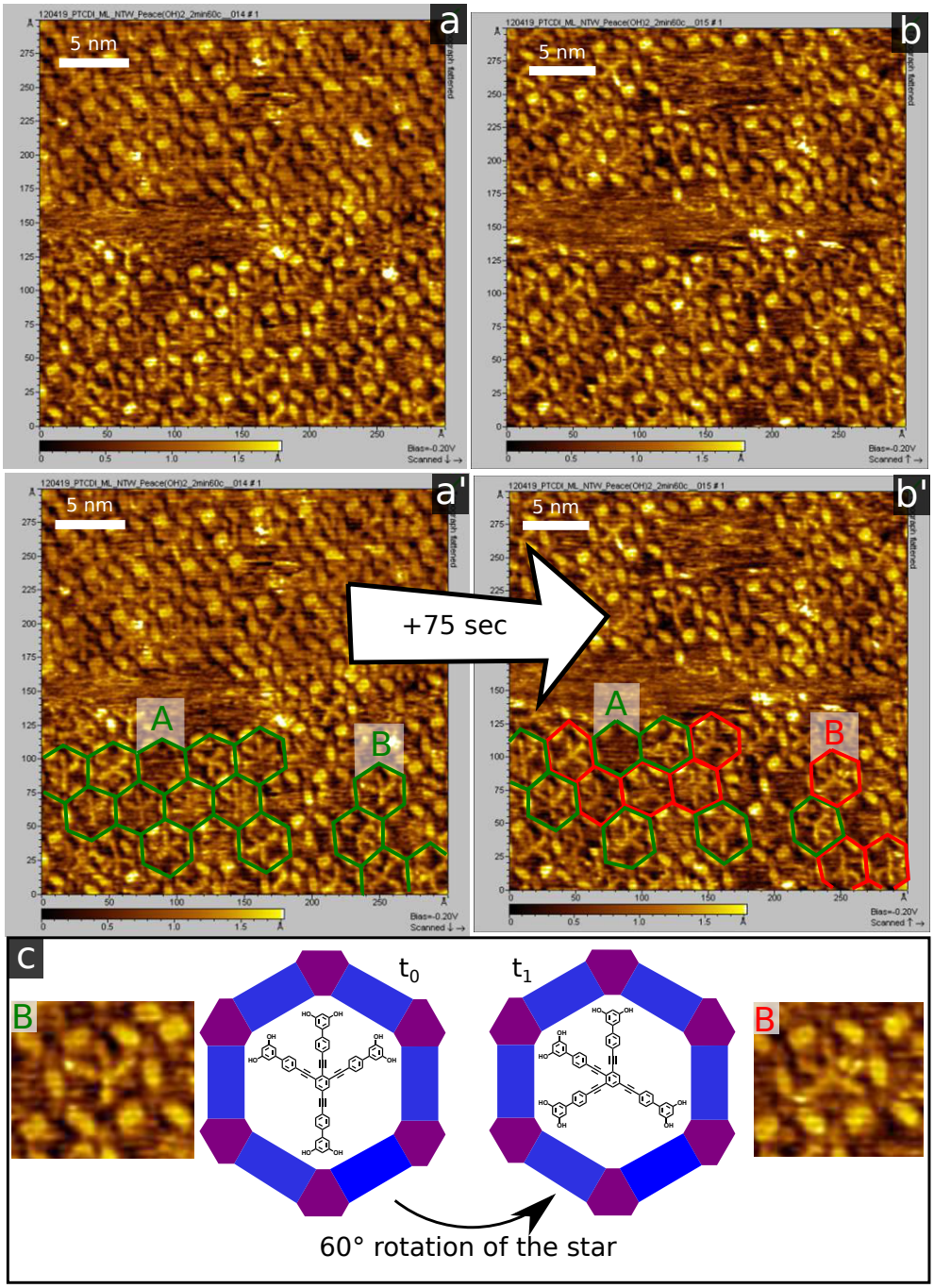

Figure 5.7: **a,b:** Room temperature STM picture of the four-arms dihydroxy biphenyl star **10** on a Au(111) functionalized with the PTCDI-melamine network. Picture **b** was recorded 75 sec after picture **a**. **a',b':** STM pictures **a** and **b** with additional schematic representation of the hexagonal cavities with (green) or without (red) change in the position of the star. Cavity *A* contains no star and cavity *B* contains a star that rotates 60 degrees counterclockwise. **c:** Magnification and schematic representation of the rotation.

that might favor the rotation in one direction and further experiments have to be performed to explain these observations. One possible cause might be the way the surface is scanned by the STM tip which could induce a rotation of the star.

5.4 Conclusion and Outlooks

A series of six star-shaped molecules **5-10** shown in scheme 5.10 was synthesized and deposited on a surface covered with a perylene tetracarboxylic diimide (PTCDI) and melamine supramolecular network. The construction of the stars was supported at every stage by the feedback coming from the STM measurements of the host-guest system. The insertion of the stars in the network cavities was controlled by finely tuning their structure. In a first stage, their size was optimized to allow the star to fit in the cavities. In a second stage, the behavior of the star on the surface was controlled by functionalizing it with hydroxy groups. Indeed the newly formed hydrogen bonds between the hydroxy groups of the stars and the PTCDI-melamine network act as anchors and slow down the rotation of the molecules in the cavities as shown by the STM images. The number of hydrogen bonds was precisely tuned to control the rotation of the star in the network cavities. Finally, a four-arms star was built and deposit on the surface network which

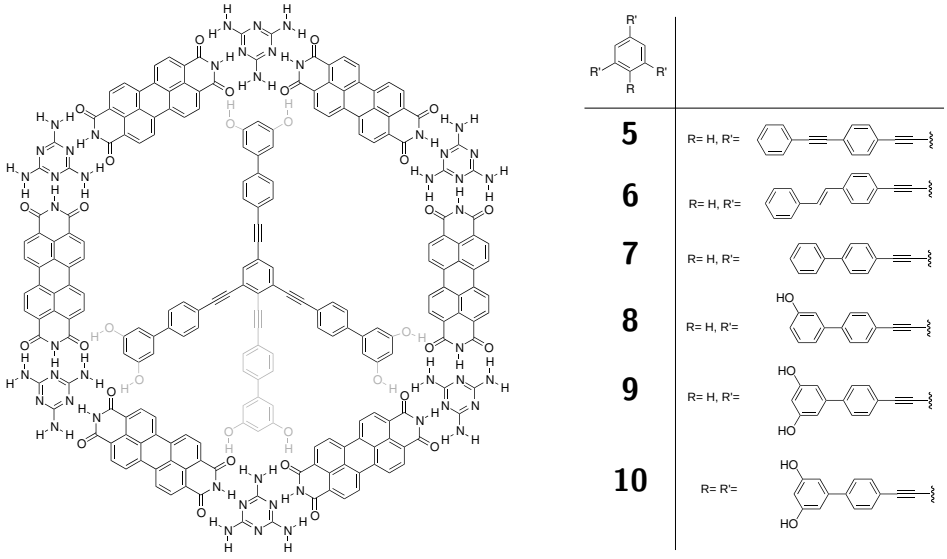

Scheme 5.10: Left: Hexagonal supramolecular cavity containing the four suited targets with respectively 0, 3, 6 or 8 hydroxy groups. Right: Star-shaped molecules synthesized.

allowed the observation of the rotation direction of the star.

The PTCDI-melamine-star system has not delivered all its secrets yet and many experiments can be imagined to exploit the potential of this host-guest system. In the first stage, the cause of the rotation of the stars in the cavities has to be investigated. Is the rotation induced by the STM tip or by anyother factor? The next stage of investigations could bring us to fix the molecule on the surface. To achieve this goal the molecule has to be functionalized with sulfur groups (scheme 5.11). Having the star immobilized on the surface, one could imagine the removal of the PTCDI-melamine network revealing a new organized network formed by the stars (scheme 5.12).

The biphenyl stars proved to have the suited structure to integrate the pores of the network and many other similar structures can be imagined. An example is the hexa-peri-hexabenzocoronene (HBC) depicted in scheme (scheme 5.11) which has a similar size to the biphenyl star but has a larger flat aromatic core that might adsorb better on the surface by increasing the interactions with the substrate. Indeed, the star-shaped molecules have a biphenyl subunit that might be twisted and not lie always flat on the surface. The comparison between HBC structures and the biphenyl stars might be of great interest.

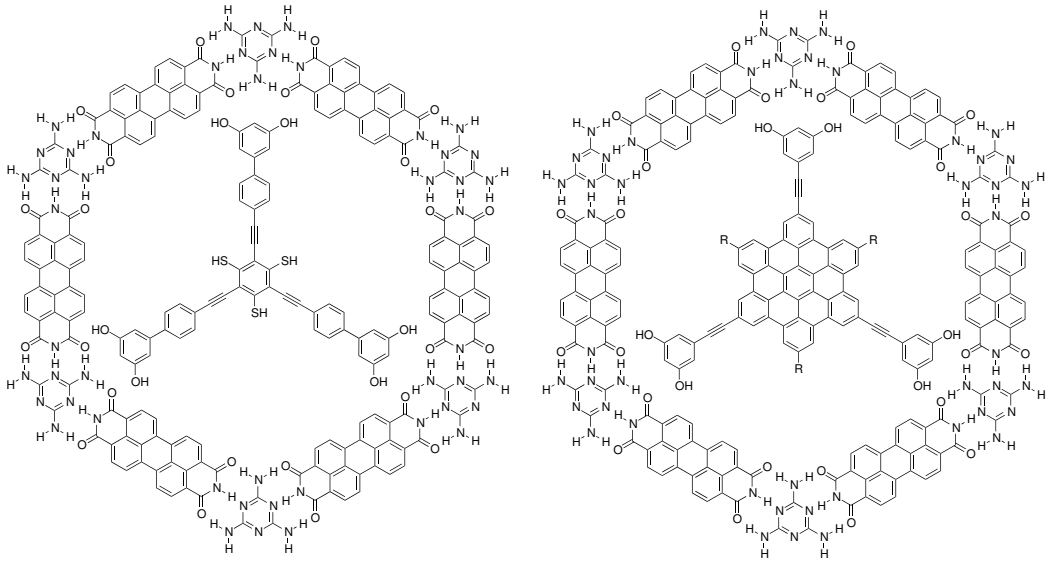

Scheme 5.11: Two examples of structures (sulfur functionalized star, hexa-peri-hexabenzocoronene) as possible candidates to integrate the pores of the supramolecular network.

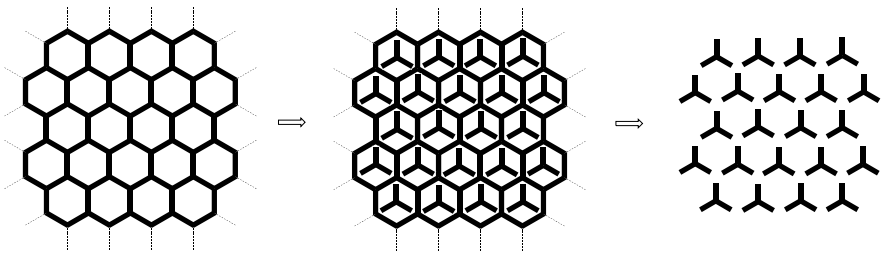

Scheme 5.12: Left: PTCDI-melamine supramolecular network forming a honeycomb porous structure. Middle: PTCDI-melamine supramolecular network after the adsorption of a sulfur functionalized guest structure. Right: Secondary network made of organized guest molecules remaining after the removal of the primary PTCDI-melamine network. Due to sulfur bonds between the guest and the surface the secondary network is not washed off.

Chapter 6

Molecular Rectifiers

6.1 Introduction

The quest of electronic component miniaturization brings scientists to imagine nanoobjects having similar functions with that of the macroscopic electronic components used nowadays. In electronic circuits rectifiers, the term "diode" is also used convert alternating current (AC) into direct current (DC), due to their ability to let the current circulate in only one direction from the anode to the cathode. In our miniaturization approach the quest of a molecule that has the same property is still a challenge. In such a target molecule the current would circulate in one direction better than the other. The concept of molecular rectifier was first introduced by Aviram and Ratner.[130] They proposed a similar system to p-n semiconductor diodes where a molecule is made of a donor unit (electron rich), a sigma linker (breaking the conjugation) and an acceptor unit (electron poor). Their DσA molecule would favor the current flow from the electron rich to the electron poor unit and disfavor the flow in the other direction by a difference of several eV.

Rectification signals were first measured with Langmuir-Blodgett films (LG-films) using block copolymers[131] or with self-assembled monolayers using non-symmetric diblock dipyrimidinyldiphenyl molecules[132] as part of many other DσA systems.[133] Single molecule rectification was first recorded by Elbing *et al.*[134] The investigated molecule was made of two weakly coupled π conjugated systems (one fluorinated and the other one not) bound by a sulfur atom to the gold electrodes of a mechanically controllable break junction (MCBJ) (compound **57** in scheme 6.1). The current-voltage signal showed a dependence on the sign of the applied bias demonstrating a rectification behavior. The same experiment was performed with model compounds (com-

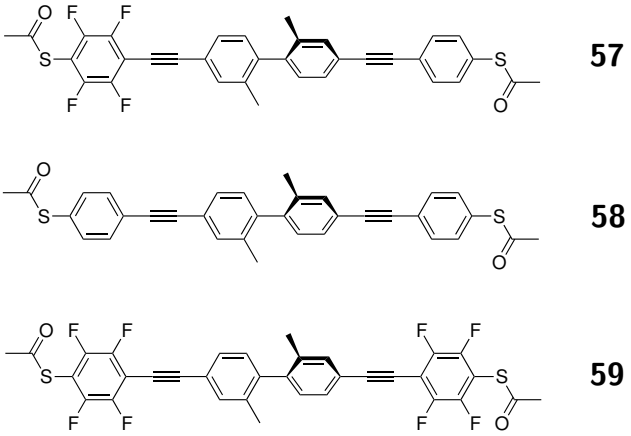

Scheme 6.1: Rectifier **57** and model compounds **58** and **59** for rectification experiments in molecular break junctions

pound **58** and **59** in scheme 6.1) showing no asymmetry in current-voltage characteristics. Recently a diblock dipyrimidinyl diphenyl was reported to have a single molecule rectification behavior.[135]

6.2 Project Description

This project was made in collaboration with Prof. Latha Venkataraman (Columbia University, New York City, United States of Amercia) and based on the work done by Mark Elbing (Mayor group, Karlsruhe Institute of Technology, Germany). They investigated the rectifying properties of compound **57** comparing them with model non-rectifying compounds **58** and **59**[134] (scheme 6.1). This project consists of the synthesis of similar rectifiers and model compounds with methyl thiol instead of thiol anchor group.

6.3 Molecular Design and Synthetic Strategy

As mentioned in the previous section, a molecular rectifier is made of an acceptor (A), a donor (D) and a linker (σ) that breaks the conjugation between the acceptor and the donor. The proposed AσD molecular rectifier is formed by two ethynylbenzenes bearing sulfur anchor groups (conjugated π-system) connected by a biphenyl that is twisted due to steric repulsion. The electronic density asymmetry is brought by a fluorinated ethynylbenzene (EWG) in combination with a π-system bearing hydrogens. Three different routes (depicted in scheme scheme 6.2) lead to the desired targets

(compounds **11**, **12** and **13** in scheme 6.3). The first possible disconnection gives a reaction between a diacetylene and two different aryl halides via a Sonogashira cross-coupling. By experience this way was dismissed since it generally gives many side products (e.g. homocouplings). The second disconnection means also a Sonogashira reaction but where the free acetylene is reacted with a diiodo or dibromobiphenyl. This option was followed by Mark Elbing.[134] Since the central biphenyl was directly availably from Elbing's work it was the strategy chosen to build the first type of target compounds. The third disconnection would mean a Suzuki cross-coupling reaction between acceptor and donor parts.

For the second type of rectifier (compounds **14** in scheme 6.3), the structure was modified to have the fluorinated part more distant to the sulfur-gold bond and it was introduced in the biphenyl central unit. To obtain this compound the second and third strategies were envisaged but the third disconnection was preferred for being a more direct route. Synthetic strategies to the first and second set of molecular rectifiers are depicted in scheme 6.4.

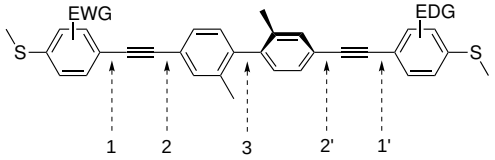

Scheme 6.2: Options of disconnections in the route of the molecular rectifier

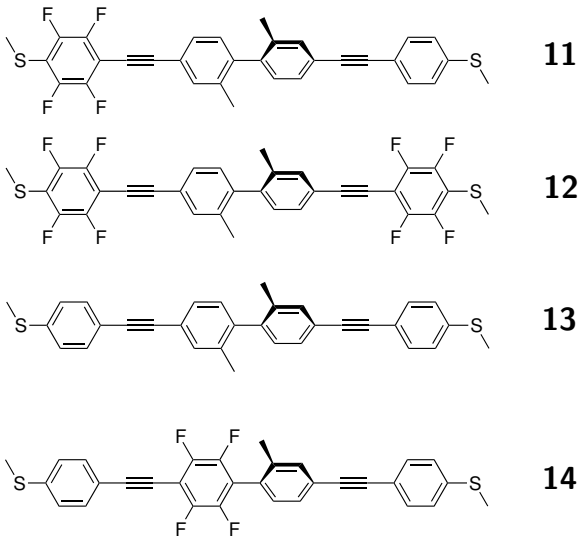

Scheme 6.3: Model compounds **12** and **13** and rectifiers **11** and **14**

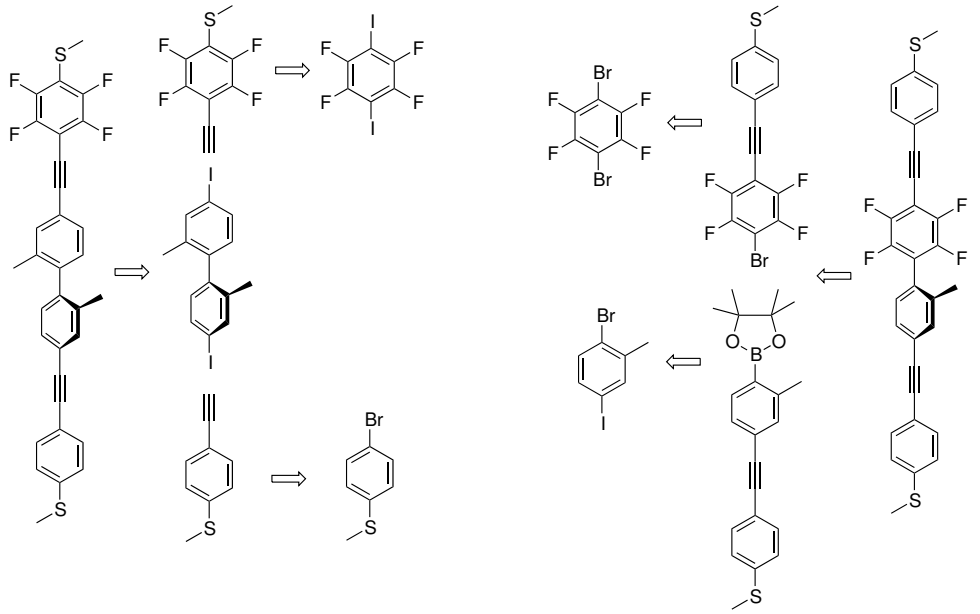

Scheme 6.4: Synthetic approaches for two types of rectifiers

6.4 Synthesis and Characterization

First Targets: Fluorine in the Rod Edges

The reactions discussed in this section follow an adapted version of Elbing's procedures for the synthesis of similar compounds.[134] The first set of targets **11**, **12** and **13** were built via Sonogashira cross coupling reactions between diiodobiphenyl **66**, fluorinated phenyl acetylene **62** and phenyl acetylene **65** (scheme 6.5). Compound **60** was obtained in moderate yields by lithiation of the commercially available 1,4-diiodotetrafluorobenzene with tert-butyl lithium, followed by the quenching with sulfur and the nucleophilic substitution with iodomethane. The free acetylene **62** was formed by a Sonogashira cross-coupling reaction with TIPSA and followed by the cleavage of the protecting group with TBAF. The non-fluorinated phenyl acetylene **65** was obtained from commercially available 4-bromothioanisole by Sonogashira reactions, either with TMSA (low yield) or with TIPSA (higher yield) followed by acetylene deprotection. The central unit **66** was synthesized by Marc Elbing following Wenner's procedure[136] where 3-nitrotoluene reacts with zinc, sodium hydroxide and ethanol forming the benzidine that rearranges in an acidic media giving a diaminobiphenyl. In a second step this compound was transformed into the desired diiodobiphenyl by a Sandmeyer reaction. The symmetric model compounds **12** and **13** were obtained by

Sonogashira reactions with **62** and **65**, respectively. The yield of both reactions were surprisingly low but the side products could not be analyzed to determine the reasons of the low yields. It is assumed that some homocoupled product was formed but it cannot be the single reason. The asymmetric compound **11** was obtained via the statistical reaction of 4,4'-diiodo-2,2'-dimethyl-1,1'-biphenyl **66** (5 equivalents) with the less valuable compound **65** giving compound **67** in fair yields. The yield of this reaction is surprisingly high compared to the formation of the doubly reacted compound

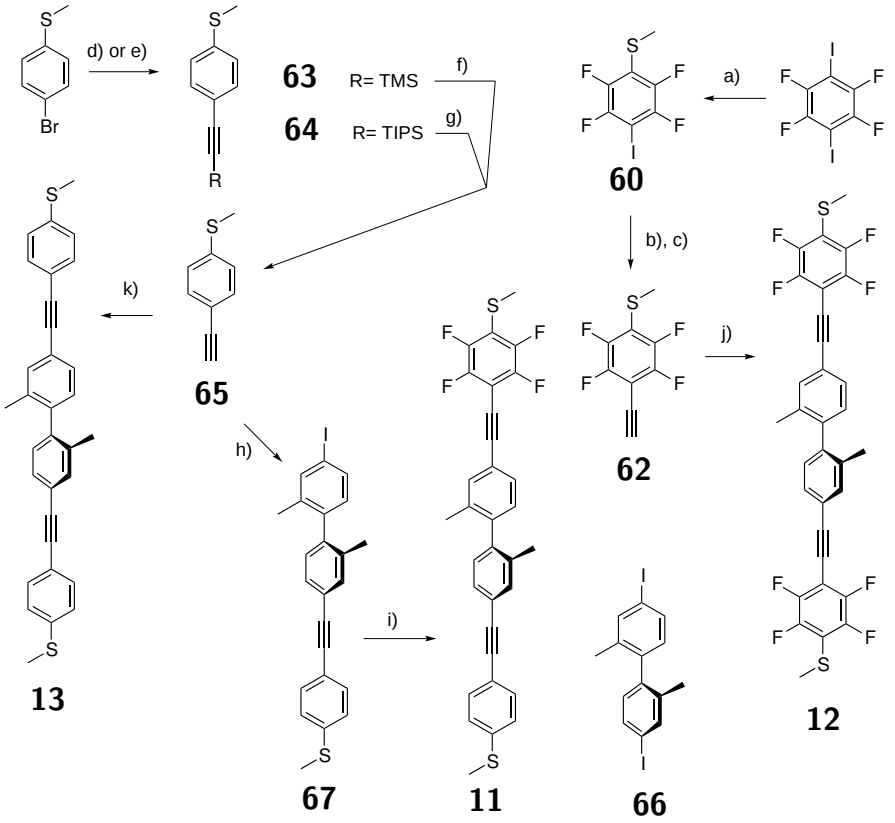

Scheme 6.5: Reagents and conditions: a) 1. tert-BuLi, THF, -78 ° C; 2. S_8, THF, -78 ° C to r.t.; 3. MeI, THF, -78 ° C, 62%; b) TIPSA, $Pd(PPh_3)_2Cl_2$, CuI, THF, $^iPr_2NH$, 60 ° C, 16h., 51%; c) TBAF, THF, 0 ° C, 60 min, quant.; d) TMSA, $Pd(PPh_3)_2Cl_2$, CuI, $^iPr_2NH$, DMF, 10 min., 110 ° C, 29%; e) TIPSA, $Pd(PPh_3)_2Cl_2$, CuI, DMF, $^iPr_2NH$, MW 110 ° C, 10 min., 86%; f) K_2CO_3, MeOH, THF, 24h, r.t., quant.; g) TBAF, THF, 0 ° C, 45 min, 83%; h) **66**, $Pd(PPh_3)_4$, CuI, THF,$^iPr_2NH$, 40 ° C, 8h, 67%; i) **60**, $Pd(PPh_3)_4$, CuI, THF, $^iPr_2NH$, r.t., 16h, 34%; j) **66**, $Pd(PPh_3)_4$, CuI, THF, $^iPr_2NH$, 60 ° C, 16h, 27% k) **66**, $Pd(PPh_3)_4$, CuI, THF, $^iPr_2NH$, r.t., 16h, 26%.

13 obtained in a separate reaction. Moreover the doubly reacted product was not observed in the synthesis of **67**, probably due to the large excess of compound **67** used and also due to the dropwise addition of the acetylene during four hours which might reduce the homocoupling of the acetylenes. This reaction was followed by a Sonogashira cross-coupling with compound **62** giving the desired product in low yield (33%). The molecular rectifier **11** as well as model compounds **12** and **13** were obtained in low yield but the reaction conditions were not further optimized.

Second Target: Fluorine in the Rod Center

A new synthetic strategy afforded the new target which has the fluorine subunit in its center (scheme 6.6). The latter was built by a Sonogashira reaction of the free acetylene **65** previously synthesized with the commercially available dibromotetrafluorobenzene. The product **68** was obtained in a low yield which might be explained by the formation of the doubly coupled product as well as the homocoupled product, although none of them was isolated. Compound **68** was then transformed into dioxaborolane **70** in a low yield reaction. The first microwave assisted attempt afforded the product in 2% yield (DMF, $Pd(dppf)Cl_2$, KOAc). The reaction was repeated in a similar manner but with a traditional oil bath heating, giving the prod-

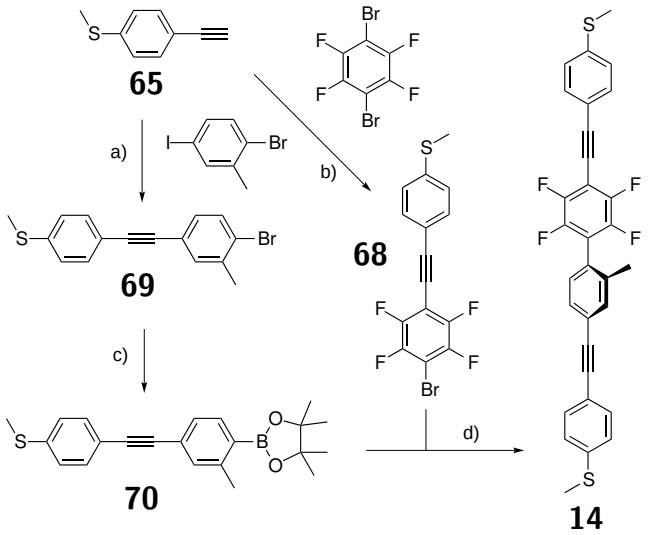

Scheme 6.6: Reagents and conditions: a) $Pd(PPh_3)_4$, CuI, THF, $^iPr_2NH$, 45 °C, 2h, 40%; b) $Pd(PPh_3)_4$, CuI, THF, $^iPr_2NH$, 80 °C, 6h, 22%; c) $Pd(dppf)Cl_2$, KOAc, $(Bpin)_2$, DMF, 100 °C, 4h, 19%; d) DME, THF, NaOH, PPh_3, $Pd(PPh_3)_2Cl_2$, 0 °C to 130 °C in MW, 30 min, 48%.

uct in 17% yield after 3h at 100 °C. In both reactions, similar side products were observed on the TLC. The reaction was repeated a third time leaving the reaction longer at 100 °C giving similar results. There are ways to improve this reaction, starting from the formation of the boronic acid instead of the dioxaborolane (trimethylborate, n–BuLi, THF), although dioxaborolanes are easier to purify by column chromatography. Since the product was obtained in a sufficient amount to accomplish the next step, this reaction was not further optimized. The parallel synthesis of the non-fluorinated subunit was performed in a similar manner reacting compound **65** with 2-bromo-5-iodotoluene at 45 °C. At this temperature the free acetylene reacts only at the iodine position forming the desired mono-subtituted product **69** in moderate yields. Both subunits, the fluorinated **68** and the non-fluorinated **70**, were connected together in the final step by a microwave assisted Suzuki cross-coupling reaction giving the target **14**. A fair yield was obtained after purification by preparative thin layer chromatography.

6.5 Conductance Measurements

Conductance experiments were performed by Brian Capozzi, a collaborator of Prof. Latha Venkataraman (Columbia University, New York City, United States of Amercia) on a AFM molecular junction. The four compounds depicted in scheme 6.3, namely model compounds **12** and **13** and rectifiers **11** and **14** were measured in the molecular junction. Only the conductance of compounds **13** and **14** was observed. Both compound **11** and

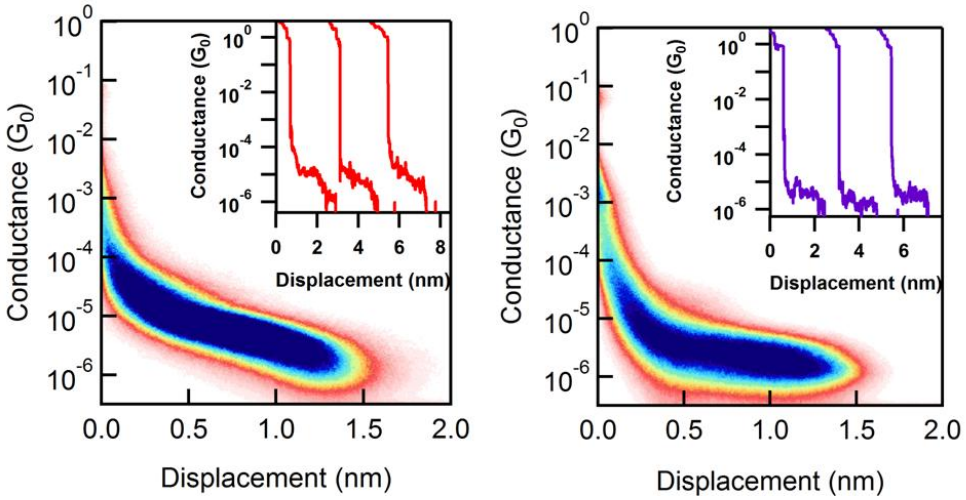

Figure 6.1: 2D histograms for compounds **13** (top) and **14** (down)

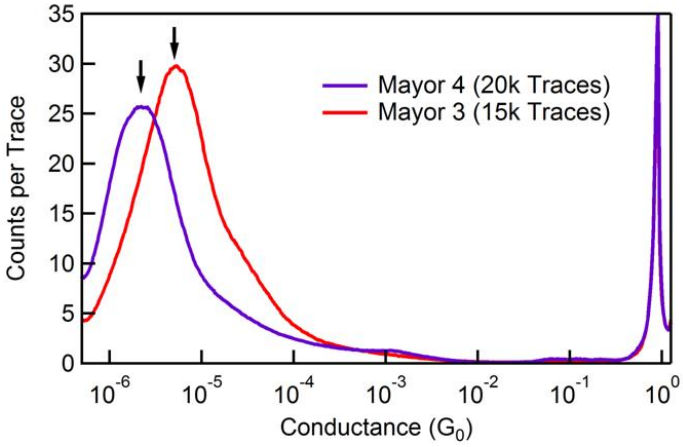

Figure 6.2: Log-binned histogram for compounds **13** (Mayor 3, red) and **14** (Mayor 4, blue)

12 did not show any conductance signatures. The strong electronegativity of the fluorine substituents is probably pulling electron density from the SCH_3 linker and therefore either greatly weakened a possible Au-S donor-acceptor bond, or completely prevented it from forming.

The 2D histograms in figure 6.1 constructed by basically overlaying all of the traces on top of one another. This preserves displacement information, and we get an idea for how long the molecule spends in the junction. In the inset a few sample traces of each molecule are shown. In figure 6.2, the log-binned histogram of compounds **13** (Mayor 3, red) and **14** (Mayor 4, blue) are depicted. To make the 1D histogram, the conductance axis is divided into bins (in the case of log-binning, there are 100 bins per order of magnitude), and the individual traces are then collapsed onto that axis to build up a histogram. Where there are steps in the traces, peaks appear in the histograms. Further conductance experiments are still under investigation in New-York.

6.6 Conclusion and Outlooks

Two types of molecular rectifiers (AσD) were synthesized and investigated in a molecular junction. The first series investigated was composed of three molecules, one of which was a molecular rectifier bearing fluorinated phenyl acetylene as acceptor part and a simple phenylacetylene as donor part. The two others were symmetric model compounds bearing either two fluorinated phenyl acetylenes or two simple phenyl acetylenes. These com-

pounds were targeted to prove their non-rectifying behavior as well as the rectifying behavior of the asymmetric target. The rectification experiments were not conclusive and the structure of the rectifier was modified to have the fluorinated part on the central biphenyl unit. This modification was meant to overcome the possible weakening of the sulfur-gold bond of the molecular junction by the fluorinated unit. A conductance was measured for the second type of rectifier and its electronic properties are still under investigations.

To continue further these studies, other AσD molecular rectifiers might be envisaged. The choice of acceptors or donors could be altered such to have a similar structure than the molecular diode recently published by Lörtscher et al in ACS nano. They studied the charge transport through single diblock dipyrimidinyl diphenyl molecules performed in a mechanically controllable break-junction.[135]

Chapter 7

Conclusion

Three projects geared towards the design of physical properties on a single molecule level were reported.

The synthesis of tailor-made molecules to function in a unique new type of molecular junction measuring optical signals from single molecules was reported. Indeed a series of four naphthalene diimide rods differing from their chromophore or from their oligo(phenylene ethynylene) linkers were synthesized by a convergent strategy through Sonogashira cross-coupling reaction sequences. An asymmetric rod has also been successfully synthesized and is still under investigation in the molecular junction. The deposition of these molecular rods in a carbon nanotube junction and their electroluminescence was investigated.

A series of six star-shaped molecules was synthesized and deposited onto a surface covered with a perylene tetracarboxylic diimide (PTCDI) and melamine supramolecular network. The insertion of the stars in the network cavities was controlled by finely tuning their structure. In a first stage their size was optimized in order to match the pore size. In a second step the behavior of the star on the surface was controlled by functionalizing the molecule with hydroxy groups. Indeed the newly formed hydrogen bonds act as anchor and slow down the rotation of the molecules in the cavities. The number of hydrogen bonds was precisely added to obtain the desired behavior between the host and the guest. The construction of the star was supported at every stage by STM measurements of the host-guest system.

Two types of molecular rectifiers (AσD) were synthesized and investigated in a molecular junction. The first series investigated was composed of three molecules, one of which was a molecular rectifier bearing fluorinated phenyl acetylene as acceptor part and a simple phenylacetylene as donor part. The two others were symmetric model compounds bearing either two fluorinated phenyl acetylenes or two simple phenyl acetylenes. These com-

pounds were targeted to prove their non-rectifying behavior as well as the rectifiying behavior of the asymmetric target. The rectification experiments were not conclusive and the structure of the rectifier was modified to have the fluorinated part on the central biphenyl unit. This modification was meant to overcome the possible weakening of the sulfur-gold bond of the molecular junction by the fluorinated unit. A conductance was measured for the second type of rectifier and its electronic properties are still under investigations.

Part III

Experimental Part

Chapter 8

General Considerations

8.1 Analytical Instruments

Nuclear magnetic resonance (NMR)

Proton NMR (^{1}H NMR) were measured on a Bruker DPX-NMR (400 MHz) or a Bruker DRX-500 (500 MHz) spectrometer at room temperature. For difficult structures the spectra were recorded by Dr. Daniel Häussinger. The peaks were described as follows: ^{1}H NMR (solvent, resonance frequency) chemical shift δ_H: (multiplicity, coupling constant J , number of protons, type of protons). The chemical shifts are given in parts per million (ppm) relative to the internal standard trimethylsilane (TMS, 0.00 ppm). Multiplicities are: s=singlet, d=doublet, t=triplet, q=quartet, m=multiplet and br=broad. Coupling constants ${}^X J_{YY}$ are given in Hertz (Hz) with value X for the number of bonds between the coupling atoms and YY the sort of nucleus coupling (HH, PH, ...). The number of protons is given after integration of the peak. The types of protons are: quaternary (Cq), primary (CH), secondary (CH_2) or tertiary (CH_3).

Carbon NMR (^{13}C NMR) were measured on a Bruker DPX-NMR (100 MHz) or a Bruker DRX-500 (125 MHz) spectrometer at room temperature. For difficult structures the spectra were recorded by Dr. Daniel Häussinger. The peaks were described as follows: ^{13}C NMR (solvent, resonance frequency) chemical shift δ_H: (number of carbons, type carbon). The chemical shifts are given in parts per million (ppm) relative the solvent ($CHCl_3$, 77.16 ppm). The types of carbons are: quaternary (Cq), primary (CH), secondary (CH_2) or tertiary (CH_3). The number of carbons is determined according to the peak heights and their type by resolving the structure using 2D NMR, ^{13}C NMR dept135 or cpd.

Mass spectrometry (MS)
Matrix-assisted laser desorption/ionisation mass spectra in conjunction with time of flight mass analysis (MALDI-TOF-MS) were recorded on a Voyager-De Pro. For MALDI-TOF-MS 1,8,9-anthracenetriol or 2,5-dihydroxybenzoic were used as as matrices . The MS spectra are described as percent intensity (%int.) of the mass per charge (m/z). The molecular peaks are noted as $[M^{+\bullet}]$. Peaks with intensity less than 10% were not considered. Electron impact (EI-MS) mass spectra and fast atom bombardment mass spectra (FAB-MS) were recorded by Dr. H. Nadig on a finnigan MAT 95Q for EI-MS and on a Finnigan MAT 8400 for FAB-MS.

Gas chromatography (GC-MS)
Performed on a Hewlett Packard 5890 series II using a 25 m 5 % phenyl-methylsilicone column coupled with a Hewlett Packard 5970 A (EI) series mass selective detector. Starting with a temperature of 100 °C followed by a gradient of 10 °C/min until 270 °C.

Melting Point (m.p.)
Determined using a Stuart SMP3 apparatus. The reported values (in °C) were averaged over three measurements recorded within an hour.

Elemental Analysis (EA)
Measured by W. Kirsch on a Perkin-Elmer Analyser 240. The values are given in mass percent.

Microwave Reactions (MW)
All the reactions were performed in a microwave using a Biotage Initiator 8.0

Gel Permeation Chromatography (GPC)
The recycling gel permeation chromatography (rec-GPC) were performed with a Shimadzu LC-8A using $CHCl_3$ as elution solvent.

UV-Vis spectroscopy
UV-Vis spectroscopy was measured in CH_2Cl_2 with an Agilent 8453 spectrophotometer.

Fluorescence spectroscopy
Measured on a Shimadzu RF-5301 PC spectrofluorophotometer under normal conditions.

8.2 Synthesis

Solvents and Reagents

All chemicals were directly used for the synthesis without further purification as received from Fluka, Acros, Merck and Aldrich. Dry solvents were purchase directly from Fluka AG, Acros AG, Merck and Aldrich. The following solvent grades were used: technical solvents for chromatography, HPLC grade for recrystallizations, dry and under inert gas solvents for air or moisture sensitive reactions. Silica gel for column chromatography as well as thin layer chromatography plates (precoated on aluminum sheets 20x20 cm) were obtained from Fluka, Acros, Merck and Aldrich. Detection was observed with UV lamp at 254 nm or 366 nm. For normal phase column chromatography silica gel 60 from Fluka (0.043-0.06 mm) or basic aluminium oxide from Fluka (Brockmann activity I, 0.05-0.15 mm) were used. For reversed phase column chromatography silica gel 100 C18 (fully endcapped) from Fluka (0.015-0.035 mm) was used. Argon 4.8 from PanGas AG (Dagmersellen, Switzerland) was used.

Contributions

All the molecules appearing in this work were synthesized by the author except those listed below:

Thomas Eaton†: **6**, **7**, **8**, **9**, **47**, **51**, **71**
Sergio Grunder†: **38**, **25**, **3**, **2**, **4**,
Mark Elbing‡: **66**
Matthias Fischer‡: **29**

† Mayor group, University of Basel, Switzerland
‡ Mayor group, Karlsruhe Institute of Technology, Germany

General Procedures

General procedure used for the following syntheses are described here.

Method A: Typical Sonogashira Reaction

A two necked flask under argon was charged with the aryl halide, dry THF and $^{i}PrNH_2$. The reaction mixture was bubbled with argon for 10 min and then the acetylene was added. The reaction mixture was again bubbled for 5

min and then palladium catalyst and copper iodide were added. The reaction mixture was evaporated to dryness and then adsorbed on SiO_2.

Method B: Typical Sonogashira Reaction in the Microwave

A microwave vessel was charged with the aryl halide, DMF and $^{i}PrNH_2$. The reaction mixture was bubble with argon for 10 min. Then the acetylene, palladium catalyst and copper iodide were successively added and the reaction mixture was irradiated in the microwave (Biotage Initiator 8.0). The reaction mixture was evaporated to dryness and then adsorbed on SiO_2.

Method C: Typical TIPS Deprotection of an Acetylene

The protected acetylene was charged in a two necked flask under argon and dissolved in dry THF. This solution was cooled to 0 °C and degassed with argon for 10 min. TBAF (1.0 M in THF) was added dropwise and the reaction mixture was stirred at this temperature. The evolution of the reaction was followed by TLC. The reaction mixture was then poured on a silica gel plug and eluted with cyclohexane or CH_2Cl_2 depending on the polarity of the product. The filtrate was finally evaporated to dryness.

Method D: Typical TMS Deprotection of an Acetylene

The protected acetylene was dissolved in a dry and degassed mixture of THF/MeOH (1:1). This solution was bubbled for 15 min with argon, it was cooled in an ice bath and K_2CO_3 and stirred at 0 °C. The reaction mixture was quenched with water and extracted with CH_2Cl_2 (3x). The organic phase was washed with water, dried over anhydrous Na_2SO_4 and evaporated.

Method E: Typical Suzuki Reaction

A two necked flask under argon with condenser and septum was charged with the aryl halide, K_2CO_3 and dissolved in THF. The reaction mixture was then heated to 80 °C.

Method F: Typical Suzuki Reaction in the microwave

A microwave vials under argon was charged with the aryl halide, the boronic acid, K_2CO_3, toluene and EtOH. The reaction mixture was bubbled with argon and then the palladium catalyst was added. The bubbling was continued for 2 min more and then the vessel was sealed and heated at 110 $^{\circ}$C in the microwave.

Chapter 9

Synthetic Procedures

9.1 Electroluminescence in a Carbon Nanotube Junction

Compound 31[137]

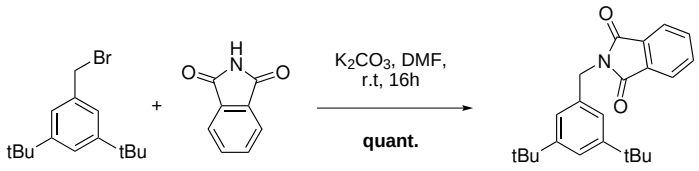

72 **73** **31**

A suspension of 3,5-di-tert-butylbenzyl bromide **72** (1.0 g, 3.53 mmol), phthalimide **73** (0.675 g, 4.59 mmol) and potassium carbonate (0.739 g, 5.3 mmol) in DMF (15 mL) was stirred at room temperature for 24h. The reaction mixture was then extracted with Et_2O (3x) and the combined organic layers were washed with water and brine, dried over Na_2SO_4, filtered and evaporated affording white solid. Purification of the residue by column chromatography (silica gel, EtOAc/hex 25%) afforded the desired product **31** as a white solid (1.24 g, 3.53 mmol, 100 %).

TLC (SiO_2, EtOAc/Hexane 25%): R_f=0.38 **m.p.** =137 ° C ^{1}**H NMR** ($CDCl_3$, 400 MHz) δ_H: 7.83 (*m*, 2H, CH), 7.68 (*m*, 2H, CH), 7.34 (*s*, 3H, CH), 4.83 (*s*, 2H, CH_2), 1.31 (*s*, 18H, CH_3). ^{13}**C NMR** ($CDCl_3$, 100 MHz) δ_C: 168.5 (Cq, 2C), 151.6 (Cq, 2C), 136.0 (Cq, 1C), 134.3 (CH, 2C), 132.7 (Cq, 2C), 123.8 (CH, 2C), 123.7 (CH, 2C), 122.3 (CH, 1C), 42.6 (CH_2, 1C), 35.2 (Cq, 2C),31.8 (CH_3, 6C). **EI-MS** m/z (%int.): found: 349.2 ([$M^{+\bullet}$], 22%), 334.2 (100%), 292.1 (14%), 187.2 (10%), 160.0 (40%), 57.1 (8%); calc. for $C_{23}H_{27}NO_2$: 349.2. **EA** (%) for $C_{23}H_{27}NO_2$: found: C=76.91, H=7.77, N=4.11; calc.: C=79.05, H=7.79, N=4.01

Compound 32[137]

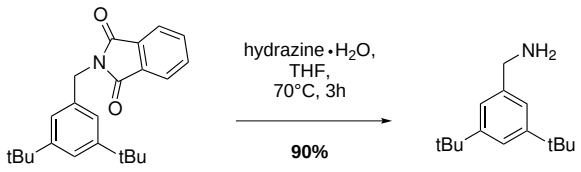

31 **32**

Hydrazine monohydrate (1 mL, 21.3 mmol) was added dropwise to a solution of **31** (1.24 g, 3.55 mmol) in THF (20 mL) at room temperature. The reaction mixture was refluxed for 3h. It was cooled to room temperature and the residue was dissolved in water, extracted with TBME (2x). The combined organic layers were washed with brine, dried over Na_2SO_4, filtered and evaporated affording the desired product **32** a colorless oil that solidifies as a white solid at room temperature (701 mg, 3.2 mmol, 90%).

TLC (SiO_2, EtOAc/Hexane 25%): R_f =0.15 ^{1}**H NMR** ($CDCl_3$, 400 MHz) δ_H: 7.36 (*t*, $^4J_{HH}$ =1.7 Hz, 1H, CH), 7.20 (*d*, $^4J_{HH}$ =1.7 Hz, 2H, CH), 3.89 (*s*, 2H, CH_2), 1.37 (*br s*, 18H, CH_3). ^{13}**C NMR** ($CDCl_3$, 100 MHz) δ_C: 151.4 (Cq, 2C), 142.9 (Cq,1C), 121.7 (CH, 2C), 121.3 (CH, 1C), 47.6 (CH_2, 1C), 35.3 (Cq, 2C), 32.0 (CH_3, 6C). **EI-MS** m/z (%int.): found: 219.2 ([$M^{+\bullet}$], 5%), 218.2 (9%), 204.2 (41%), 187.2 (11%), 162.1 (100%), 131.1 (7%), 57.1 (9%); calc. for $C_{15}H_{25}N$: 219.2. **EA** (%) for $C_{15}H_{25}N$: found: C=77.2, H=10.3, N=5.75; calc.: C=82.13, H=11.49, N=6.39.

Compound 33

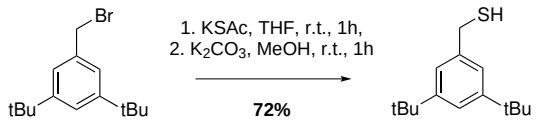

72 **33**

A flask under argon was charged with 3,5-di-tert-butylbenzyl bromide **72** (1.018 g, 3.59 mmol), KSAc (598 mg, 5.24 mmol) and dry THF (20 ml). The white reaction mixture was stirred at room temperature for 1h20. Then, MeOH (20 mL) and K_2CO_3 (750 mg, 5.43 mmol) were added and the reaction mixture was again stirred for 1h20. Water (40 ml) was added to the reaction mixture and it was extracted with Et_2O (3x). The combined organic layers were washed with brine, dried with Na_2SO_4, filtered and evaporated affording a slightly brown oil which was chromatographed (silica gel, hexane/CH_2Cl_2 93:7) affording a slightly yellow oil (582 mg, 2.46 mmol, 70 %).

TLC (SiO_2, CH_2Cl_2/Hexane 1:9): R_f =0.42 ^{1}**H NMR** ($CDCl_3$, 400 MHz) δ_H: 7.31 (*t*, $^4J_{HH}$ =1.8 Hz, 1H, CH), 7.17 (*s*, $^4J_{HH}$ =1.8 Hz, 2H, CH), 3.74 (*d*, $^3J_{HH}$ =7.5 Hz, 2H, CH_2), 1.76 (*t*, $^3J_{HH}$ =7.5 Hz, 1H, SH), 1.33 (*s*, 18H, CH_3). ^{13}**C NMR** ($CDCl_3$, 100 MHz) δ_C: 151.5 (Cq, 2C), 140.6 (Cq), 1C, 122.7 (CH, 2C), 121.6 (CH, 1C), 35.3 (Cq, 2C), 31.9 (CH_3, 6C), 30.0 (CH_2, 1C). **EI-MS** m/z (%int.): found: 236.1 ([$M^{+\bullet}$], 32%), 221.1 (78%), 203.1 (100%), 131.1 (6.43%), 57.1 (21%); calc. for $C_{15}H_{24}S$: 236.16 **EA** (%) for $C_{15}H_{24}S$: found: C=76.19, H=10.28; calc.: C=76.20, H=10.23

Compound 28[124]

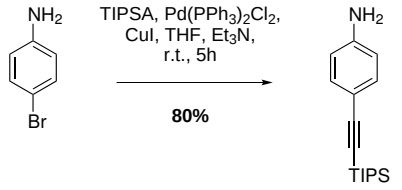

28

Compounds 4-bromoaniline (4.0 g, 18 mmol), $Pd(PPh_3)_2Cl_2$ (128 mg, 0.18 mmol) and CuI (95 mg, 0.36 mmol) were charged in a Schlenk tube which was put under argon atmosphere. Then dry THF (40 mL), Et_3N (40 mL) and TIPSA (4.0 g, 22 mmol) were successively added. The reaction mixture was then stirred at room temperature for 5h. Addition of hexane, filtration over Celite and evaporation of the filtrate afforded a black oil which was chromatographed (silica gel, hexane/CH_2Cl_2 1:1) giving **28** as a slighly yellow oil (4.02 g, 14.7 mmol, 80 %).

^{1}**H NMR** ($CDCl_3$, 400 MHz) δ_H: 7.28 (*td*, $^4J_{HH}$=2.3 Hz, $^3J_{HH}$=9 Hz, 2H, CH), 6.58 (*td*, $^4J_{HH}$=2.3 Hz, $^3J_{HH}$=9 Hz,4H, CH_2), 3.78 (*br s*, 2H, NH_2), 1.11 (*m*, 21H, CH_3. ^{13}**C NMR** ($CDCl_3$, 100 MHz) δ_C: 147.0 (Cq), 133.8 (CH), 114.9 (CH), 113.5 (Cq), 108.3, 87.9 (Cq), 19.1 (CH_3), 11.8 (CH).

Compound 30

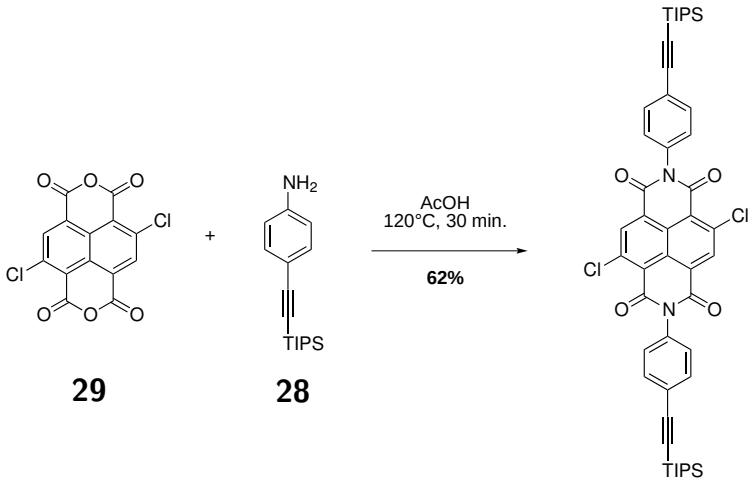

29 **28** **30**

A suspension of 2,6-dichloronaphtalene-1,4,5,6-tetracarboxylic acid bisanhydride **29** (300 mg, 0.89 mmol) in acetic acid (15 mL) was heated at 120 ° C for 30 minutes. To this mixture **28** (1.46 g, 5.34 mmol) was added and instantaneously the color changed from yellow to red. The reaction mixture was kept at reflux for another 30 min and then let to recover room temperature. Filtration over a sintered glass funnel afforded a rosa-pink solid which was adsorbed on silica gel and chromatographed (silica gel, hexane/CH_2Cl_2 1:2) affording **30** (468 mg, 0.55 mmol, 62 %) as a yellow solid.

^{1}**H NMR** ($CDCl_3$, 400 MHz) δ_H: 8.86 (*s*, 2H, CH), 7.68 (*d*, $^3J_{HH}$=8.2 Hz, 4H, CH), 7.27 (*d*, $^3J_{HH}$=8.2 Hz, 4H, CH), 1.15 (*m*, 42H, CH_3). ^{13}**C NMR** ($CDCl_3$, 100 MHz) δ_C: 161.3, 160.9, 141.3, 136.9, 134.2, 133.7, 128.8, 128.0, 126.7, 125.4, 123.1, 106.4, 93.0, 19.1, 11.7.

Compound 75

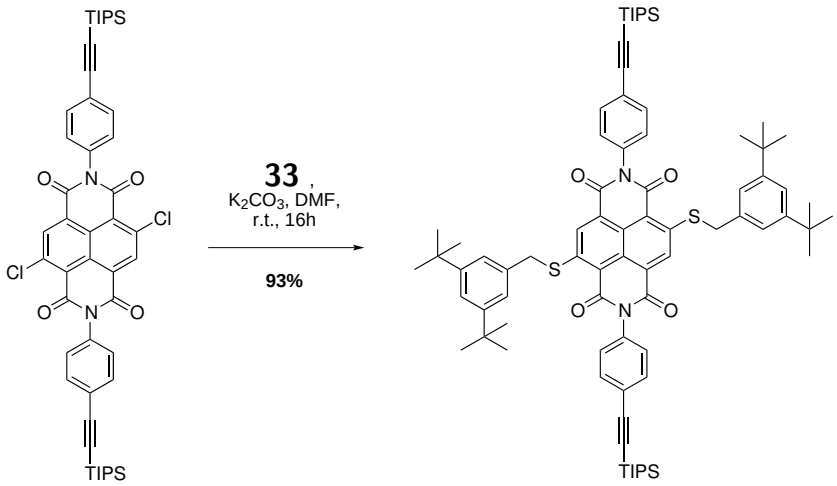

30 **75**

In a flask containing **30** (50 mg, 0.06 mmol), **33** (56 mg, 0.24 mmol), K_2CO_3 (25 mg, 0.18 mmol), dry and degased DMF (3 mL) were added and the reaction mixture was stirred at room temperature overnight. The reaction mixture was evaporated to dryness and the dark red residue was dissolved in CH_2Cl_2 (20 mL), washed with water (4 ml). The aqueous phase was extracted 3x with CH_2Cl_2 and the red combined organic layer were evaporated to dryness. The violet solid obtained was chromatographed (silica gel, CH_2Cl_2/hex 1:3) affording a violet solid (**75**, 68.4 mg, 0.055 mmol, 93 %).

TLC (SiO_2, CH_2Cl_2/Hexane 2:1): R_f =0.49 ^{1}**H NMR** ($CDCl_3$, 400 MHz) δ_H: 8.86 (*s*, 2H, CH), 7.63 (*d*, $^3J_{HH}$ =8.4 Hz, 4H, CH), 7.31 (*d*, $^3J_{HH}$ =8.4 Hz, 4H, CH), 7.31 (*t*, $^4J_{HH}$ =1.8 Hz, 2H, CH), 7.27 (*d*, $^4J_{HH}$ =1.8 Hz, 4H, CH), 4.43 (*s*, 4H, CH_2), 1.25 (*s*, 36H, CH_3), 1.14 (*s*, 42H, CH_3). ^{13}**C NMR** ($CDCl_3$, 100 MHz) δ_C: 163.1 (Cq), 162.0 (Cq), 151.3 (Cq), 149.7 (Cq), 134.2 (Cq), 133.1 (CH), 128.6 (CH), 125.0 (Cq), 124.5 (Cq), 124.2 (CH), 123.8 (CH), 123.6 (Cq), 122.1 (Cq), 118.5 (Cq), 106.3 (Cq), 92.0 (Cq), 38.2 (CH_2, 34.8 (Cq), 31.4 (CH_3), 18.7 (CH_3), 11.3 (CH). **MALDI-MS** m/z (%int.): found: 1246.77; calc. for $C_{78}H_{98}N_2O_4S_2Si_2$: 1246.65. **EA** (%) for $C_{78}H_{98}N_2O_4S_2Si_2$: found: C=71.83, H=7.86, N=2.35; calc.: C=75.07, H=7.92, N=2.24

Compound 76

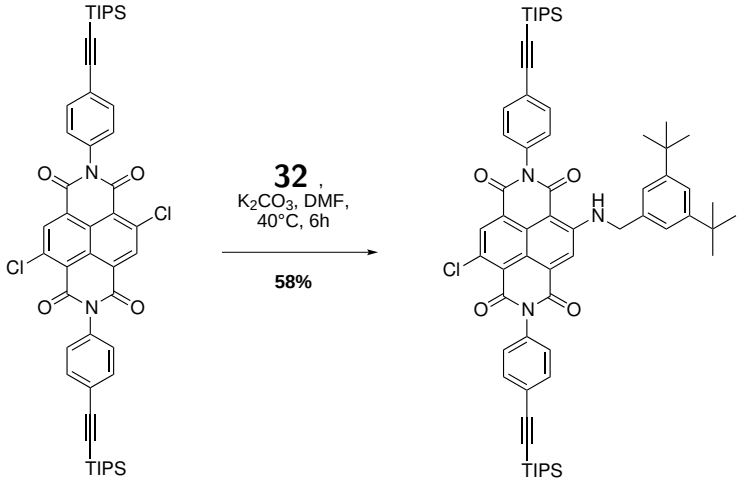

30 **76**

A flask under argon containing **30** (250 mg, 0.295 mmol), **32** (129 mg, 0.590 mmol) and K_2CO_3 (82 mg, 0.590 mmol) in dry DMF (10 mL) was heated at 40 ˚ C for 6h30. The reaction mixture was evaporated, dissolved in CH_2Cl_2 and washed with water. The combined organic layers were evaporated and chromatographed (silica gel, hexane/dcm 1:2) affording red solid (**76**, 177 mg, 0.172 mmol, 58%).

TLC (SiO_2, CH_2Cl_2/Hexane): R_f =0.27 ^{1}**H NMR** ($CDCl_3$, 400 MHz) δ_H: 10.14 (*t*, $^3J_{HH}$ =5.3 Hz, 1H, NH), 8.67 (*s*, 1H, CH), 8.46 (*s*, 1H, CH), 7.66 (*d*, $^3J_{HH}$ =8.5 Hz, 4H, CH), 7.37 (*t*, $^4J_{HH}$ =1.6 Hz, 1H, CH), 7.27 (*d*, $^3J_{HH}$ =8.5 Hz, 4H, CH), 7.20 (*d*, $^4J_{HH}$ =1.6 Hz, 2H, CH), 4.68 (*d*, $^4J_{HH}$ =5.3 Hz, 2H, CH), 1.29 (*m*, 18H, CH_3), 1.16 (*br s*, 21H, CH_3), 1.14 (*br s*, 21H, CH_3). ^{13}**C NMR** ($CDCl_3$, 100 MHz) δ_C: 166.3 (Cq), 162.3 (Cq), 162.2 (Cq), 161.6 (Cq), 152.1 (Cq), 135.8 (CH), 135.3 (Cq), 134.9 (Cq), 134.8 (Cq), 134.3 (Cq), 133.6 (CH), 133.6 (CH), 129.1 (Cq), 128.9 (CH), 128.2 (Cq), 125.1 (Cq), 125.2 (Cq), 124.6 (Cq), 123.0 (CH), 122.8 (CH), 122.7 (Cq), 122.1 (Cq), 121.8 (CH), 106.6 (Cq), 100.7 (Cq), 92.7 (Cq), 48.9 (CH_2), 35.3 (Cq), 31.8 (CH), 30.1 (CH_2), 27.3 (CH_2), 19.1 (CH_3), 19.1 (CH_3), 11.7 (CH_3), 11.7 (CH_3). **MALDI-MS** m/z: found: 1030.22; calc. for $C_{63}H_{76}ClN_3O_4Si_2$: 1029.51.

Compound 77

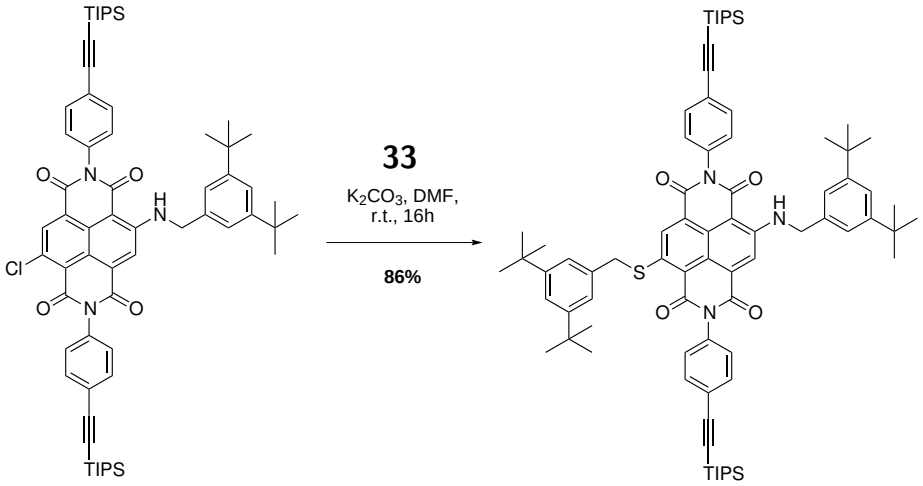

76 **77**

A flask charged with **76** (32 mg, 0.031 mmol), **33** (15 mg, 0.062 mmol) and K_2CO_3 (9 mg, 0.062 mmol) in dry DMF (2 mL) was stirred at room temperature overnight. The violet reaction mixture was evaporated to dryness and chromatographed (silica gel, hexane/CH_2Cl_2 1:2) affording a violet solid (**77**, 33 mg, 0.027 mmol, 86 %).

^{1}**H NMR** ($CDCl_3$, 400 MHz) δ_H: 9.90 (*t*, $^3J_{HH}$ =5.3 Hz, 14H, NH), 8.79 (*s*, 1H, CH), 8.38 (*s*, 1H, CH), 7.66 (*d*, $^3J_{HH}$ =8.4 Hz, 4H, CH), 7.62 (*d*, $^3J_{HH}$ =8.4 Hz, 4H, CH), 7.35 (*s*, 1H, CH), 7.31 (*s*, 1H, CH), 7.28Ð7.26 (*m*, 4H, CH), 4.65 (*d*, $^3J_{HH}$ =5.3 Hz, 2H, CH_2), 4.36 (*s*, 2H, CH_2), 1.28 (*s*, 18H, CH_3), 1.27 (*s*, 18H, CH_3), 1.15 (*s*, 42H, CH_3, CH). ^{13}**C NMR** ($CDCl_3$, 100 MHz) δ_C: 166.4, 163.9, 163.1, 162.6, 152.0, 151.6, 151.3, 145.0, 135.6, 135.2, 134.8, 134.0, 133.6, 133.5, 129.0, 127.5, 126.9, 124.9, 124.6, 124.2, 123.6, 122.8, 122.3, 122.3, 121.8, 120.7, 119.9, 110.0, 101.0, 92.4, 48.8, 35.3, 35.2, 31.8, 31.8, 31.7, 19.1, 11.7, 0.4. **MALDI-MS** m/z (%int.): found: 1229.93; calc. for $C_{78}H_{99}N_3O_4SSi_2$: 1229.69.

Compound 78

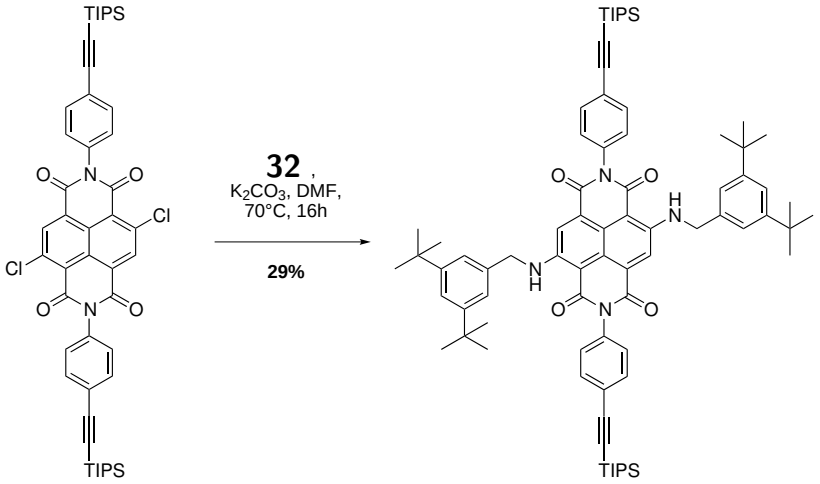

A flask under argon was charged with compound **30** (504 mg, 0.594 mmol) in DMF (20 mL). The suspension was heated at 70 ° C and compound **32** (782 mg, 3.57 mmol) was added by portions for 1h. After the first drops of the amine the reaction mixture turned dark red. It was then heated at this temperature overnight. The dark violet reaction mixture was evaporated to dryness and chromatographed (silica gel, cyclohexane/CH_2Cl_2 1:1 to 1:2) affording the desired product **78** (206 mg, 0.17 mmol, 29 %) and the mono-substituted product (327 mg, 0.317 mmol, 53%).

^{1}H NMR ($CDCl_3$, 400 MHz) δ_H: 9.45 (*t*, $^3J_{HH}$ =5.1 Hz, 2H, NH), 8.26 (*s*, 2H, CH), 7.66 (*d*, $^3J_{HH}$ =8.7 Hz, 4H, CH), 7.30-7.37 (*m*, 6H, CH), 7.21 (*d*, $^4J_{HH}$ =1.8 Hz, 4H, CH), 4.57 (*d*, $^3J_{HH}$ =5.1 Hz, 4H, CH_2), 1.29 (*s*, 36H, CH_3), 1.17 (*s*, 42H, CH_3, CH). **^{13}C NMR** ($CDCl_3$, 100 MHz) δ_C: 166.2, 162.8, 151.5, 149.2, 135.9, 135.1, 133.3, 128.8, 126.1, 124.5, 122.6, 122.3, 121.6, 119.0, 106.5, 102.0, 92.0, 48.5, 34.9, 31.5, 18.8, 11.4. **EI-MS** m/z (%int.): found: 1213.08; calc. for $C_{78}H_{100}N_4O_4Si_2$: 1212.73

Compound 37

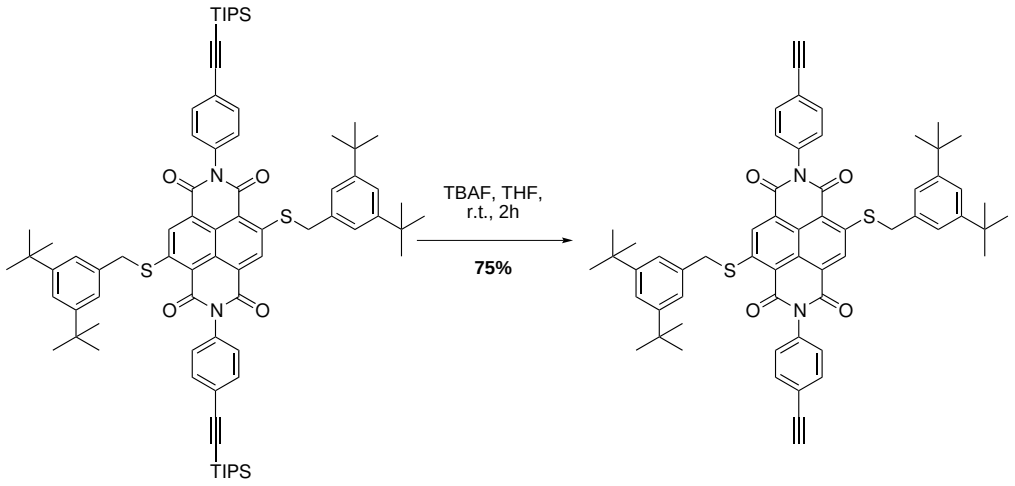

75 **37**

A flask under argon was charged with the violet solid **75** (64 mg, 0.0513 mmol) and dry and degassed THF (13 mL). Then TBAF (1M in THF with 5% water, 21 microL, 0.021 mmol, 0.4 eq) was added and the reaction mixture was stirred at room temperature. Some TBAF was again added after 30 min (15 microL) and after 1h (20 microL). After 2.5h the reaction mixture was filtered over a plug of silica gel (with CH_2Cl_2) and the red filtrate was evaporated affording a red solid which was chromatographed (silica gel, CH_2Cl_2) giving **37** as a red-orange solid (36 mg, 0.038 mmol, 74%).

TLC (SiO_2, CH_2Cl_2): R_f =0.44 ^{1}**H NMR** ($CDCl_3$, 400 MHz) δ_H: 8.91 (*s*, 2H, CH), 7.66 (*d*, $^3J_{HH}$ =8.4 Hz, 4H, CH), 7.33-7.26 (*m*, 12H, CH), 4.39 (*s*, 4H, CH_2), 1.28 (*s*, 36H, CH_3). **MALDI-MS** m/z (%int.): found: 934.82 ; calc. for $C_{60}H_{58}N_2O_4S_2$: 934.38

Compound 35

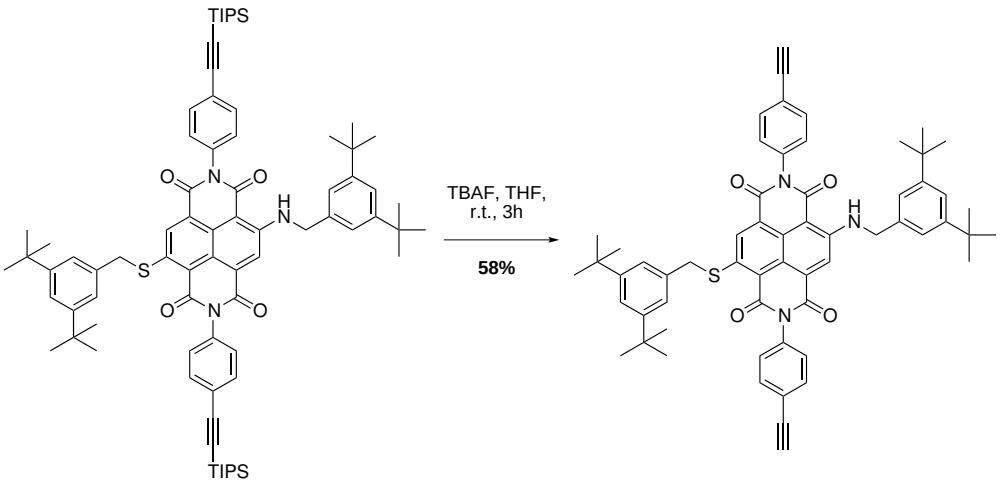

77 **35**

A flask under argon was charged with the violet solid **77** (78.5 mg, 0.064 mmol) and dry and degassed THF (16 mL). TBAF (1M in THF with 5% water, 25 microL, 0.025 mmol) was added and the violet reaction mixture was stirred at room temperature. TBAF was again added after 1h (15 microL), after 2h (20 microL) and after 2.5h (10 microL). After 3h the reaction mixture was filtered over a plug of silica gel with CH_2Cl_2 and the filtrate was evaporated affording a violet solid which was chromatographed (silica gel, hexane/CH_2Cl_2 1:2) giving **35** as a violet solid (34 mg, 0.037 mmol, 58 %).

^{1}H NMR ($CDCl_3$, 400 MHz) δ_H: 9.93 (*t*, $^3J_{HH}$ =5.3 Hz, 1H, NH), 8.83 (*s*, 1H, CH), 8.42 (*s*, 1H, CH), 7.69 (*d*, $^3J_{HH}$ =8.4 Hz, 4H, CH), 7.64 (*d*, $^3J_{HH}$ =8.4 Hz, 4H, CH), 7.36 (*s*, 1H, CH), 7.31 (*s*, 1H, CH), 7.26 (*m*, 6H, CH), 4.65 (*d*, $^3J_{HH}$ =5.3 Hz, 2H, CH_2), 4.36 (*s*, 2H, CH_2), 1.28 (*s*, 18H, CH_3), 1.27 (*s*, 18H, CH_3). **MALDI-MS** m/z (%int.): found: 917.88; calc. for $C_{60}H_{59}N_3O_4S$: 917.42

Compound 34

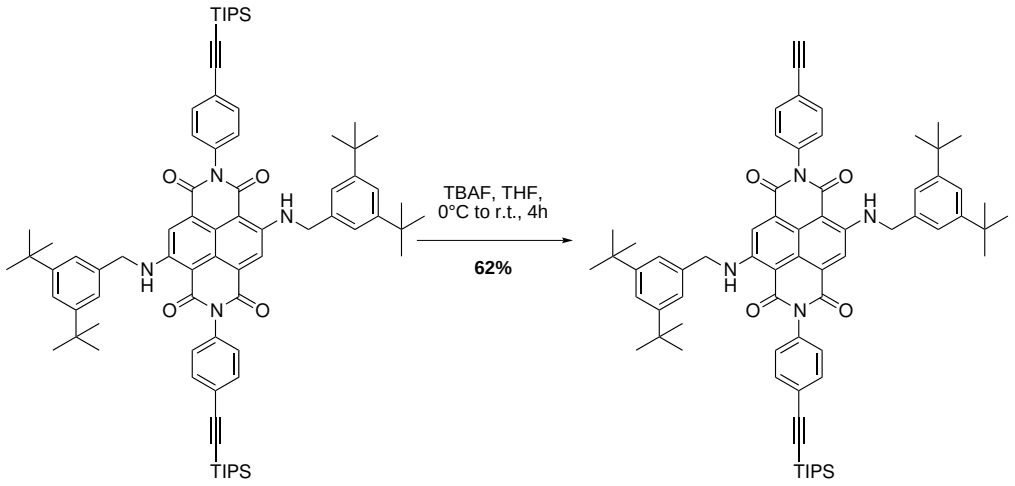

78 **34**

Compound **78** (161 mg, 0.133 mmol) was dissolved in THF and cooled at 0 ° C. This blue solution was degassed for 15 min and then TBAF (1M with 5% water in THF, 24 microL, 0.024 mmol) was added in portions. The evolution of the reaction was controlled by TLC. The reaction mixture was filtered over a plug of silica gel and evaporated. This crude was purified by a flash chromatography (silica gel, cyclohexane/CH_2Cl_2 1:2) affording the monodeprotected product (**34**, 87 mg, 0.082 mmol, 62%), the starting compound (**78**) and the 2x deprotected product **36**.

^{1}**H NMR** ($CDCl_3$, 400 MHz) δ_H: 9.47 (*m*, 2H, NH), 8.30 (*d*, $^4J_{HH}$ =3.5 Hz, 2H, CH), 7.66 (*t*, $^3J_{HH}$ =8.3 Hz, 4H, CH), 7.30 (*m*, 6H, CH), 7.20 (*s*, 4H, CH), 4.60 (*m*, 4H, CH), 3.14 (*s*, 1H, CH), 1.28 (*s*, 36H, CH), 1.15 (*s*, 21H, CH). ^{13}**C NMR** ($CDCl_3$, 100 MHz) δ_C: 166.6, 163.3, 151.8, 149.6, 136.2, 136.0, 135.4, 133.7, 133.6, 129.2, 129.0, 126.6, 124.8, 123.4, 122.8, 122.6, 122.2, 119.5, 106.7, 102.6, 92.4, 83.3, 78.6, 48.7, 35.3, 31.8, 19.1, 14.6, 11.7.

Compound 36

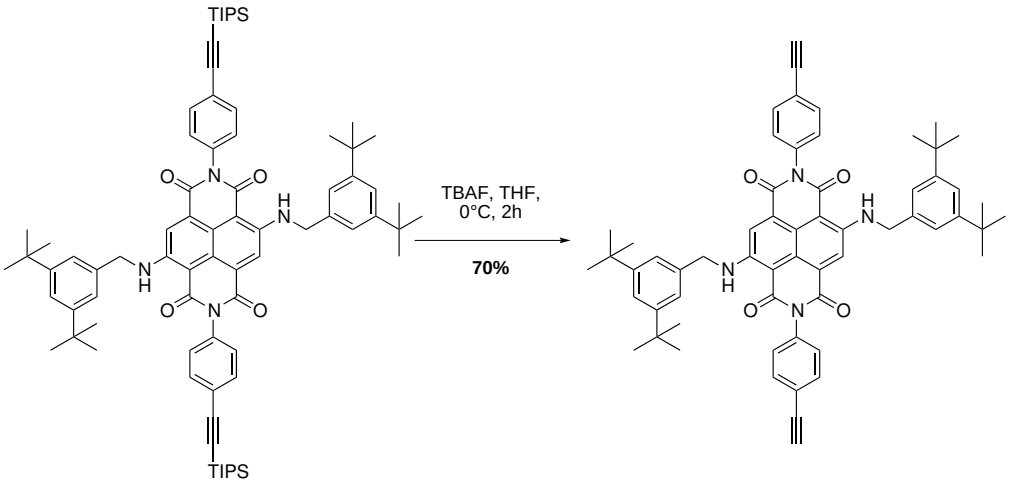

78 **36**

To a flask under argon charged with compound **78** (173 mg, 0.143 mmol), dry and degassed THF (40 mL) was added and the blue solution was degassed another 10 min. Then the reaction mixture was cooled to 0 ° C and TBAF (1M in THF wiht 5% water, 87 microL, 0.09 mmol) was added. The evolution of the reaction was controlled by TLC. The reaction mixture was filtered over a plug of silica gel with CH_2Cl_2 and evaporated. The blue solid obtained was purified by column chromatograhy (CH_2Cl_2/hexane, silica gel) affording **36** violet desired product **36** (90 mg, 0.1 mmol, 70%).

TLC (SiO_2, CH_2Cl_2): R_f =0.55 ^{1}**H NMR** ($CDCl_3$, 400 MHz) δ_H: 9.48 (*m*, 2H, NH), 8.34 (*s*, 2H, CH), 7.67 (*d*, $^3J_{HH}$ =8.5 Hz, 4H, CH), 7.34 (*t*, $^4J_{HH}$ =1.7 Hz, 2H, CH), 7.28 (*d*, $^3J_{HH}$ =8.5 Hz, 4H, CH), 7.19 (*d*, $^4J_{HH}$ =1.8 Hz, 4H, CH), 4.61 (*d*, $^3J_{HH}$ =5.1 Hz, 4H, CH), 3.14 (*s*, 2H, CH), 1.29 (*s*, 36H, CH). ^{13}**C NMR** ($CDCl_3$, 100 MHz) δ_C: 166.6, 163.3, 151.9, 149.8, 136.3, 136.0, 133.7, 129.2, 126.7, 124.6, 123.4, 122.7, 122.5, 122.4, 119.7, 102.7, 90.7, 48.7, 35.3, 31.8. **FAB-MS** m/z (%int.): found: 900.4 (26) ([$M^{+\bullet}$], 203.2 (100); calc. for $C_{60}H_{60}N_4O_4$: 900.46

Compound 79[138]

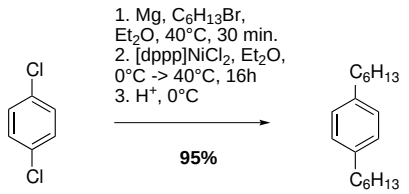

80 **79**

To a suspension of magnesium turnings (2.5 g, 102 mmol) in dry diethyl ether (20 mL) under argon was added dropwise a solution of $C_6H_{13}Br$ (14 g, 85 mmol) in dry diethyl ether (100 mL). The reaction mixture was maintained at slight reflux for the addition. After complete addition the solution was refluxed for 30 minutes in a oil bath. To a flask under argon **80** (5.0 g, 34 mmol), [dppp]$NiCl_2$ (19.6 mg, 0.1 mol%) and dry diethyl ether (40 mL) were successively added. This solution was cooled to 0 ° C in a ice/water bath and then the Grignard reagent was added to it by small portions. The reaction mixture changed immediately from red-orange to yellow and then to green. When the addition was completed the ice/water bath was removed and the reaction mixture refluxed in a oil bath for 16h. The reaction mixture containing a precipitate was cooled to 0 ° C in a ice/water bath and then quenched successively with water (10 mL) and HCl (2M, 50 mL). The organic phase was then separated and the aqueous phase was extracted (3x) with diethyl ether. The combined organic phases were then washed with water, dried with Na_2SO_4, filtered and evaporated. The slighly yellow oil obtained was purified by Kugelrohr distillation affording **79** (7.963 g, 32.3 mmol, 95 %) as a colorless oil.

^{1}**H NMR** ($CDCl_3$, 400 MHz) δ_H: 7.09 (*s*, 4H, CH), 2.57 (*m*, 4H, CH_2), 1.59 (*m*, 4H, CH_2), 1.31 (*m*, 12H, CH_2), 0.88 (*m*, 6H, CH_3). ^{13}**C NMR** ($CDCl_3$, 100 MHz) δ_C: 140.5 (Cq, 2C), 128.6 (CH, 2C), 36.0 (CH_2, 2C), 32.2 (CH_2, 2C), 32.0 (CH_2, 2C), 29.5 (CH_2, 2C), 23.0 (CH_2, 2C), 14.5 (CH_3, 2C). **EI-MS** m/z (%int.): found: 246 ([$M^{+\bullet}$], 25%), 175 (100), 117, 104, 91, 43; calc. for $C_{18}H_{30}$: 246.23

Compound 23[122]

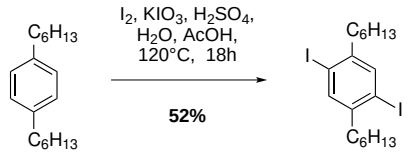

79 **23**

A two necked flask with a condenser containing **79** (4.5 g, 18.3 mmol), KIO_3 (1.95 g, 9.1 mmol), I_2 (5.1 g, 20 mmol), acetic acid (60 mL), conc. H_2SO_4 (4 ml) and H_2O (0.6 mL) was refluxed for 18h. The reaction mixture was then concentrated to 50% of its initial volume (oil bath 100 °C, 1 bar) and the residue was filtered at room temperature while washed with methanol. This dark brown solid was passed through a small column (silica gel, hexane). Two recrystalizations in ethanol afforded **23** (4.74 g, 9.12 mmol, 52 %) as white needles.

^{1}H NMR ($CDCl_3$, 400 MHz) δ_H: 7.59 (*s*, 2H, CH), 2.59 (*m*, 4H, CH_2), 1.54 (*m*, 4H, CH_2), 1.33 (*m*, 12H, CH_2), 0.90 (*t*, $^3J_{HH}$=6.9 Hz, 6H, CH_3). **^{13}C NMR** ($CDCl_3$, 100 MHz) δ_C: 145.2 (Cq, 2C), 139.7 (CH, 2C), 100.8 (Cq, 2C), 40.2 (CH_2, 2C), 32.0 (CH_2, 2C), 30.6 (CH_2, 2C), 29.4 (CH_2, 2C), 23.0 (CH_2, 2C), 14.5 (CH_3, 2C).

Compound 24[20]

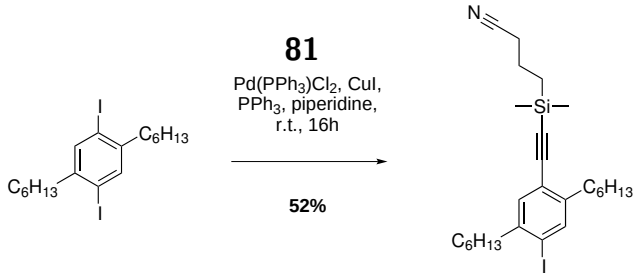

23 **24**

A Schlenk tube under argon was charged with **23** (10.7 g, 21.5 mmol), CuI (13 mg, 0.07 mmol, 2 mol%), $Pd(PPh_3)_2Cl_2$ (23 mg, 0.036 mmol, 1 mol%) and PPh_3 (26 mg, 0.036 mmol). It was degassed and put under argon. The piperidine (15 mL) and 4-(ethynyldimethylsilyl)butanenitrile **81** (0.532 g, 3.52 mmol) were successively added. The reaction mixture was stirred at room temperature overnight, evaporated and chromatographed (silica gel, hexane/CH_2Cl_2 2:1) giving the desired product **24** as a yellow oil (1.22 g, 2.28 mmol, 68%).

^{1}**H NMR** ($CDCl_3$, 400 MHz) δ_H: 7.63 (*s*, 1H, CH), 7.22 (*s*, 1H, CH), 2.63 (*m*, 4H, CH_2), 2.42 (*m*, 2H, CH_2), 1.82 (*m*, 2H, CH_2), 1.56 (*m*, 4H, CH_2), 1.31 (*m*, 12H, CH_2), 0.89 (*m*, 6H, CH_3), 0.85 (*m*, 2H, CH_2), 0.25 (*m*, 6H, CH_3). ^{13}**C NMR** ($CDCl_3$, 100 MHz) δ_C: 144.9 (Cq, 1C), 143.2 (Cq, 1C), 139.9 (CH, 1C), 132.9 (CH, 1C), 122.6 (Cq, 1C), 120.0 (Cq, 1C), 105.1 (Cq, 1C), 101.9 (Cq, 1C), 96.7 (Cq, 1C), 40.6 (CH_2, 1C), 34.3 (CH_2, 1C), 32.1 (CH_2, 1C), 32.0 (CH_2, 1C), 31.0 (CH_2, 1C), 30.6 (CH_2, 1C), 29.7 (CH_2, 1C), 29.5 (CH_2, 1C), 23.0 (CH_2, 1C), 23.0 (CH_2, 1C), 21.1 (CH_2, 1C), 20.9 (CH_2, 1C), 16.2 (CH_2, 1C), 14.5 (CH_3, 1C), 14.5 (CH_3, 1C), -1.4 (CH_3, 2C). **EI-MS** m/z (%int.): found: 521.2 ([$M^{+\bullet}$], 47.38%), 506.2 (15.09%), 453.2 (25.37%), 126.0 (100%), 98.0 (34.31%); calc. for $C_{26}H_{40}INSi$: 521.2 **EA** (%) for $C_{26}H_{40}INSi$: found: C=60.36, H=7.9, N=3.00; calc.: C=59.87, H=7.73, N=2.69

Compound 26

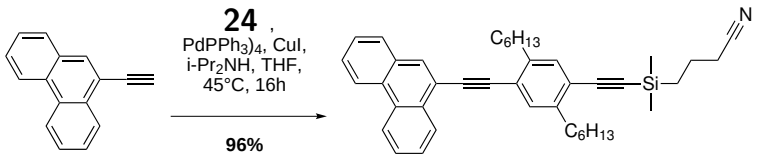

25 **26**

A flask charged with **25** (791 mg, 3.91 mmol) and **24** (1.7 g, 3.6 mmol) was put under argon. Dry THF (60 mL) and diisopropylamine (10 mL) were added and the reaction mixture was bubble with argon for 10 minutes. $Pd(PPh_3)_4$ (190 mg, 0.163 mmol) and CuI (31 mg, 0.163 mmol) were added and the heated at 45 ° C for 16h. The reaction mixture was evaporated and the residue chromatographed (silica gel, hexane/CH_2Cl_2 2:1) affording the desired product **26** as a yellow oil (1.86 g, 3.12 mmol, 96%).

TLC (SiO_2, CH_2Cl_2/Hexane 1:2): R_f =0.19 ^{1}**H NMR** ($CDCl_3$, 400 MHz) δ_H: 8.72 (*m*, 1H, CH), 8.67 (*d*, $^3J_{HH}$=8.2 Hz, 1H, CH), 8.54 (*m*, 1H, CH), 8.08 (*s*, 1H, CH), 7.88 (*d*, $^3J_{HH}$=7.0 Hz, 1H, CH), 7.58-7.75 (*m*, 4H, CH), 7.48 (*s*, 1H, CH), 7.36 (*s*, 1H, CH). 2.93 (*m*, 2H, CH_2), 2.77 (*m*, 2H, CH_2), 2.45 (*t*, $^3J_{HH}$=7.0 Hz, 2H, CH_2), 1.87 (*m*, 2H, CH_2), 1.78 (*m*, 2H, CH_2), 1.69 (*m*, 2H, CH_2), 1.26-1.53 (*m*, 12H, CH_2), 0.82-0.98 (*m*, 8H, CH_3, CH_2), 0.30 (*s*, 6H, CH_3). ^{13}**C NMR** ($CDCl_3$, 100 MHz) δ_C: 143.3 (Cq, 1C), 142.7 (Cq, 1C), 133.2 (CH, 1C), 133.0 (CH, 1C), 132.4 (CH, 1C), 131.7 (Cq, 1C), 131.5 (Cq, 1C), 130.7 (Cq, 1C), 130.6 (Cq, 1C), 129.0 (CH, 1C), 127.9 (CH, 1C), 127.5 (CH, 1C), 127.4 (CH, 1C), 127.4 (CH, 1C), 127.4 (CH, 1C), 123.6 (Cq, 1C), 123.3 (CH, 1C), 123.1 (CH, 1C), 122.6 (Cq, 1C), 120.3 (Cq, 1C), 120.1 (Cq, 1C), 105.8 (Cq, 1C), 97.2 (Cq, 1C), 93.2 (Cq, 1C), 92.9 (Cq, 1C), 34.9 (CH_2, 1C), 34.7 (CH_2, 1C), 32.2 (CH_2, 2C), 31.3 (CH_2, 1C), 31.1 (CH_2, 1C), 29.8 (CH_2, 1C), 29.8 (CH_2, 1C), 23.1 (CH_2, 2C), 21.1 (CH_2, 1C), 21.0 (CH_2, 1C), 16.2 (CH_2, 1C), 14.6 (CH_3, 1C), 14.5 (CH_3, 1C), -1.4 (CH_3, 2C).

Compound 82

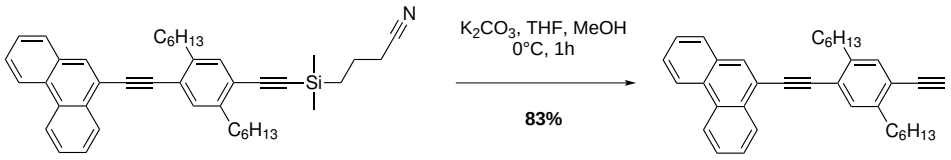

26 **82**

Compound **26** (1.7 g, 2.85 mmol) was dissolved in dry and degassed THF (60 mL) and MeOH (60mL). This solution was bubbled for 15 min with argon, it was cooled in an ice bath and K_2CO_3 (797 mg, 5.71 mmol) and stirred at 0 ° C for 1h. The reaction mixture was quenched with water and extracted 3x with CH_2Cl_2. The organic phase was washed with water, dried over Na_2SO_4 and evaporated affording a yellow oil that was chromatographed (silica gel, cyclohexane/CH_2Cl_2 9:1) affording the product **82** as a yellow oil (1.1 g, 2.34 mmol, 83%).

^{1}**H NMR** ($CDCl_3$, 400 MHz) δ_H: 8.72 (*m*, 1H, CH), 8.67 (*d*, $^3J_{HH}$=8.2 Hz, 1H, CH), 8.57 (*m*, 1H, CH), 8.10 (*s*, 1H, CH), 7.89 (*d*, $^3J_{HH}$=7.8 Hz, 1H, CH), 7.73 (*m*, 2H, CH), 7.64 (*m*, 2H, CH), 7.52 (*s*, 1H, CH), 7.42 (*s*, 1H, CH). 3.36 (*s*, 1H, CH), 2.96 (*m*, 2H, CH_2), 2.83 (*m*, 2H, CH_2), 1.81 (*m*, 2H, CH_2), 1.72 (*m*, 2H, CH_2), 1.32-1.54 (*m*, 12H, CH_2), 0.95 (*m*, 3H, CH_3), 0.90 (*m*, 3H, CH_3). ^{13}**C NMR** ($CDCl_3$, 100 MHz) δ_C: 143.4 (Cq, 1C), 142.6 (Cq, 1C), 133.6 (CH, 1C), 133.0 (CH, 1C), 132.4 (CH, 1C), 131.7 (Cq, 1C), 131.5 (Cq, 1C), 130.7 (Cq, 1C), 130.6 (Cq, 1C), 129.0 (CH, 1C), 127.9 (CH, 1C), 127.5 (CH, 1C), 127.5 (CH, 1C), 127.4 (CH, 1C), 127.4 (CH, 1C), 123.6 (Cq, 1C), 123.3 (CH, 1C), 123.1 (CH, 1C), 122.0 (Cq, 1C), 120.3 (Cq, 1C), 93.2 (Cq, 1C), 92.8 (Cq, 1C), 83.0 (Cq, 1C), 82.0 (Cq, 1C), 34.9 (CH_2, 1C), 34.4 (CH_2, 1C), 32.2 (CH_2, 1C), 32.1 (CH_2, 1C), 31.3 (CH_2, 1C), 31.0 (CH_2, 1C), 29.8 (CH_2, 1C), 29.6 (CH_2, 1C), 23.1 (CH_2, 1C), 23.1 (CH_2, 1C), 14.6 (CH_3, 1C), 14.6 (CH_3, 1C).

Compound 83

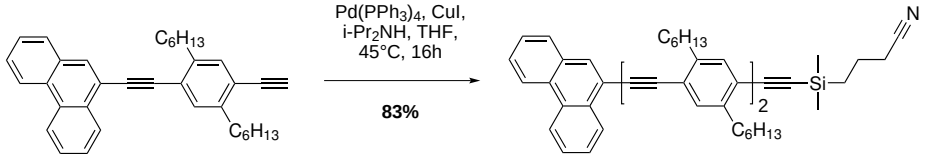

82 **83**

Compound **24** (1.034 g, 1.98 mmol) was dissolved in dry and degassed THF (20 mL) and was added to a Schlenk tube under argon charged with $Pd(PPh_3)_4$ (116 mg, 0.099 mmol) and CuI (19 mg, 0.099 mmol). Diisopropylamine was added (10 mL) and the reaction mixture was bubbled for 10 min. Then **82** (933 mg, 1.98 mmol) in dry and degassed THF (20 mL) was added and the reaction mixture was bubble for 10 min. It was then heated at 45 ° C overnight. The reaction mixture was filtered over a plug of silica gel with CH_2Cl_2 and the yellow filtrate was evaporated affording a dark yellow oil. The crude was chromatographed (silica gel, cyclohexane/CH_2Cl_2 9:1 to 8:2) yielding to a yellow oil (**83**, 1.47 g, 1.64 mmol, 83%).

TLC (SiO_2, CH_2Cl_2/Hexane 1:5): R_f =0.08 ^{1}**H NMR** ($CDCl_3$, 400 MHz) δ_H: 8.72 (*m*, 1H, CH), 8.69 (*d*, $^3J_{HH}$=8.1 Hz, 1H, CH), 8.57 (*m*, 1H, CH), 8.10 (*s*, 1H, CH), 7.89 (*d*, $^3J_{HH}$=7.8 Hz, 1H, CH), 7.59-7.88 (*m*, 4H, CH), 7.54 (*s*, 1H, CH), 7.43 (*s*, 1H, CH), 7.36 (*s*, 1H, CH). 7.33 (*s*, 1H, CH), 2.97 (*m*, 2H, CH_2), 2.84 (*m*, 4H, CH_2), 2.75 (*m*, 2H, CH_2), 2.45 (*t*, $^3J_{HH}$=7.0 Hz, 2H, CH_2), 1.62-1.89 (*m*, 10H, CH_2), 1.27-1.56 (*m*, 24H, CH_2), 0.90 (*m*, 14H, CH_3, CH_2), 0.29 (*s*, 6H, CH_3). ^{13}**C NMR** ($CDCl_3$, 100 MHz) δ_C: 143.2 (Cq, 1C), 142.8 (Cq, 1C), 142.5 (Cq, 1C), 142.3 (Cq, 1C), 133.1 (CH, 1C), 133.0 (CH, 1C), 132.9 (CH, 1C), 132.3 (CH, 1C), 131.7 (Cq, 1C), 131.5 (Cq, 1C), 130.7 (Cq, 1C), 130.6 (Cq, 1C), 129.0 (CH, 1C), 127.9 (CH, 1C), 127.5 (CH, 1C), 127.5 (CH, 1C), 127.5 (CH, 1C), 127.4 (CH, 1C), 123.7 (Cq, 1C), 123.3 (CH, 1C), 123.3 (CH, 1C), 123.1 (Cq, 1C), 123.1 (CH, 1C), 122.4 (Cq, 1C), 120.3 (Cq, 1C), 120.1 (Cq, 1C), 105.8 (Cq, 1C), 97.1 (Cq, 1C), 93.6 (Cq, 1C), 93.4 (Cq, 1C), 93.4 (Cq, 1C), 92.8 (Cq, 1C), 35.0 (CH_2, 1C), 34.7 (CH_2, 2C), 34.6 (CH_2, 1C), 32.3 (CH_2, 1C), 32.3 (CH_2, 1C), 32.2 (CH_2, 1C), 32.3 (CH_2, 1C), 31.4 (CH_2, 1C), 31.2 (CH_2, 1C), 31.1 (CH_2, 1C), 31.1 (CH_2, 1C), 29.9 (CH_2, 1C), 29.7 (CH_2, 3C), 23.1 (CH_2, 4C), 21.1 (CH_2, 1C), 21.0 (CH_2, 1C), 16.2 (CH_2, 1C), 14.6 (CH_3, 4C), -1.3 (CH_3, 2C).

Compound 84

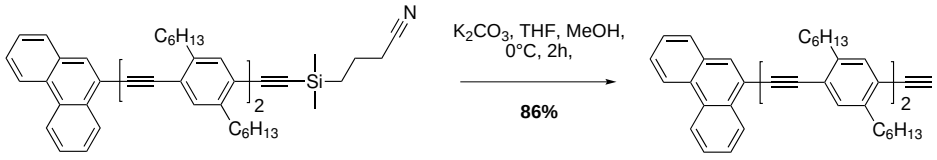

83 **84**

Compound **83** (0.658 g, 0.735 mmol) was dissovled in dry and degassed THF (20 mL) and MeOH (20 mL). This solution was cooled in a ice bath and K_2CO_3 (205 mg, 147 mmol) was added. The reaction mixture was stirred at 0 ° C for 2h and then quenched with water and extracted 3x with CH_2Cl_2. The organic phase was washed with water, dried over Na_2SO_4 and evaporated affording a very viscous yellow oil that was chromatographed (silica gel, cyclohexane/CH_2Cl_2 9:1) affording a yellow oil (**84**, 0.465 g, 0.629 mmol, 86 %).

^{1}H NMR ($CDCl_3$, 400 MHz) δ_H: 8.72 (*m*, 1H, CH), 8.68 (*d*, $^3J_{HH}$=8.1 Hz, 1H, CH), 8.59 (*m*, 1H, CH), 8.11 (*s*, 1H, CH), 7.90 (*d*, $^3J_{HH}$=7.8 Hz, 1H, CH), 7.70-7.75 (*m*, 2H, CH), 7.60-7.70 (*m*, 2H, CH), 7.55 (*s*, 1H, CH), 7.45 (*s*, 1H, CH), 7.39 (*s*, 1H, CH), 7.38 (*s*, 1H, CH), 3.34 (*m*, 2H, CH_2), 2.97 (*m*, 2H, CH_2), 2.87 (*m*, 4H, CH_2), 2.79 (*m*, 2H, CH_2), 1.65-1.88 (*m*, 8H, CH_2), 1.29-1.57 (*m*, 24H, CH_2), 0.93 (*m*, 12H, CH_3). **^{13}C NMR** ($CDCl_3$, 100 MHz) δ_C: 143.3 (Cq, 1C), 142.7 (Cq, 1C), 142.5 (Cq, 1C), 142.3 (Cq, 1C), 133.5 (CH, 1C), 133.0 (CH, 1C), 132.8 (CH, 1C), 132.3 (CH, 1C), 131.8 (Cq, 1C), 131.5 (Cq, 1C), 130.7 (Cq, 1C), 130.6 (Cq, 1C), 129.0 (CH, 1C), 127.9 (CH, 1C), 127.5 (CH, 1C), 127.5 (CH, 1C), 127.4 (CH, 1C), 127.4 (CH, 1C), 123.8 (Cq, 1C), 123.3 (CH, 1C), 123.3 (CH, 1C), 123.2 (Cq, 1C), 123.1 (CH, 1C), 121.8 (Cq, 1C), 120.4 (Cq, 1C), 93.5 (Cq, 1C), 93.4 (Cq, 1C), 93.3 (Cq, 1C), 92.8 (Cq, 1C), 83.0 (Cq, 1C), 81.9 (Cq, 1C), 35.0 (CH_2, 1C), 34.7 (CH_2, 1C), 34.6 (CH_2, 1C), 34.4 (CH_2, 1C), 32.3 (CH_2, 1C), 32.3 (CH_2, 1C), 32.3 (CH_2, 1C), 32.1 (CH_2, 1C), 31.4 (CH_2, 1C), 31.2 (CH_2, 1C), 31.1 (CH_2, 1C), 31.0 (CH_2, 1C), 29.9 (CH_2, 1C), 29.8 (CH_2, 1C), 29.7 (CH_2, 1C), 29.6 (CH_2, 1C), 23.1 (CH_2, 2C), 23.1 (CH_2, 1C), 23.1 (CH_2, 1C), 14.6 (CH_3, 4C).

Compound 27

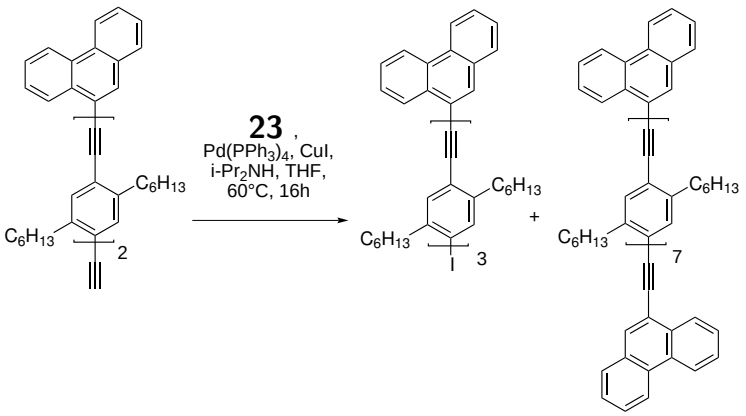

84 **27** (37%) **85** (28%)

A two necked flask was charged with compound **84** (465 mg, 0.626 mmol) and **23** (4.5 g, 9.06 mmol). Dry and degassed THF (60 mL) and $^{i}Pr_2NH$ (10 mL) were added and the reaction mixture was degassed for 10 min. Then $Pd(PPh_3)_4$ (73 mg) and CuI (6 mg) were added the reaction mixture was heated at 60 ° C overnight. After recovering room temperature it was filtered over a plug of silica gel and evaporated affording a orange oil that solidifies at room temperature. The crude was then chromatographed (silica gel, cyclohexane/CH_2Cl_2 9:1) giving the desired product (257 mg, 0.232 mmol, 37 %), the two times coupled product **85** (150 mg, 0.087 mmol, 28 %).

For compound **27**: **^{1}H NMR** ($CDCl_3$, 400 MHz) δ_H: 8.73 (*m*, 1H, CH), 8.69 (*d*, $^3J_{HH}$=8.1 Hz, 1H, CH), 8.59 (*m*, 1H, CH), 8.11 (*s*, 1H, CH), 7.91 (*d*, $^3J_{HH}$=7.8 Hz, 1H, CH), 7.60-7.77 (*m*, 5H, CH), 7.56 (*s*, 1H, CH), 7.46 (*s*, 1H, CH), 7.42 (*s*, 1H, CH). 7.40 (*s*, 1H, CH). 7.34 (*s*, 1H, CH), 2.99 (*m*, 2H, CH_2), 2.89 (*m*, 6H, CH_2), 2.80 (*m*, 2H, CH_2), 2.69 (*m*, 2H, CH_2), 1.66-1.88 (*m*, 10H, CH_2), 1.62 (*m*, 2H, CH_2), 1.26-1.56 (*m*, 36H, CH_2), 0.93 (*m*, 18H, CH_3). **^{13}C NMR** ($CDCl_3$, 100 MHz) δ_C: 144.2 (Cq, 1C), 143.2 (Cq, 1C), 142.7 (Cq, 1C), 142.5 (Cq, 1C), 142.4 (Cq, 1C), 142.4 (Cq, 1C), 139.9 (CH, 1C), 133.0 (CH, 1C), 133.0 (CH, 1C), 132.9 (CH, 1C), 132.8 (CH, 1C), 132.8 (CH, 1C), 132.3 (CH, 1C), 131.8 (Cq, 1C), 131.5 (Cq, 1C), 130.7 (Cq, 1C), 130.6 (Cq, 1C), 129.0 (CH, 1C), 127.9 (CH, 1C), 127.5 (CH, 1C), 127.5 (CH, 1C), 127.4 (CH, 1C), 127.4 (CH, 1C), 126.0 (Cq, 1C), 123.4 (Cq, 1C), 123.3 (CH, 1C), 123.1 (Cq, 1C), 123.1 (CH, 1C), 120.4 (Cq, 1C), 101.3 (Cq, 1C), 93.6 (Cq, 1C), 93.5 (Cq, 1C), 93.4 (Cq, 1C), 93.0 (Cq, 1C), 92.8 (Cq, 2C),

40.7 (CH_2, 1C), 35.0 (CH_2, 1C), 34.7 (CH_2, 1C), 34.7 (CH_2, 2C), 34.3 (CH_2, 1C), 32.3 (CH_2, 1C), 32.3 (CH_2, 1C), 32.3 (CH_2, 1C), 32.3 (CH_2, 1C), 32.2 (CH_2, 1C), 32.1 (CH_2, 1C), 31.4 (CH_2, 1C), 31.2 (CH_2, 1C), 31.2 (CH_2, 1C), 31.1 (CH_2, 1C), 31.1 (CH_2, 1C), 30.7 (CH_2, 1C), 29.9 (CH_2, 1C), 29.8 (CH_2, 1C), 29.8 (CH_2, 1C), 29.8 (CH_2, 1C), 29.7 (CH_2, 1C), 29.5 (CH_2, 1C), 23.1 (CH_2, 3C), 23.1 (CH_2, 1C), 23.1 (CH_2, 1C), 23.1 (CH_2, 1C), 14.6 (CH_3, 3C), 14.6 (CH_3, 3C). **MALDI-MS** m/z (%int.): found: 1108.95 ([$M^{+\bullet}$], 32%), 983.02 (100%); calc. for $C_{74}H_{93}I$: 1108.63

For compound **85**: ^{1}**H NMR** ($CDCl_3$, 500 MHz) δ_H: 8.73 (*m*, 2H, CH), 8.68 (*d*, $^3J_{HH}$=7.9 Hz, 2H, CH), 8.57 (*m*, 2H, CH), 8.10 (*s*, 2H, CH), 7.89 (*d*, $^3J_{HH}$=7.9 Hz, 2H, CH), 7.72 (*m*, 4H, CH), 7.68 (*m*, 2H, CH), 7.62 (*m*, 2H, CH), 7.53 (*s*, 2H, CH), 7.44 (*s*, 2H, CH), 7.40 (*s*, 2H, CH), 7.40 (*s*, 2H, CH), 7.39 (*s*, 2H, CH), 2.97 (*m*, 4H, CH_2), 2.86 (*m*, 16H, CH_2), 1.82 (*m*, 4H, CH_2), 1.73 (*m*, 16H, CH_2), 1.29-1.54 (*m*, 60H, CH_2), 0.83-0.94 (*m*, 30H, CH_3). ^{13}**C NMR** ($CDCl_3$, 125 MHz) δ_C: 142.3, 142.1, 142.0, 132.6, 132.6, 132.5, 131.9, 131.4, 131.1, 130.3, 130.2, 128.6, 127.2, 127.0, 127.1, 127.0, 123.0, 122.9, 122.8, 122.8, 122.7, 122.7, 120.0, 93.2, 93.1, 93.0, 92.3, 34.6, 34.3, 34.3, 31.9, 31.8, 31.0, 30.8, 30.8, 29.5, 29.4, 22.7, 14.2. **MALDI-MS** m/z (%int.): found: 1719.98 ([$M^{+\bullet}$]; calc. for $C_{130}H_{158}$: 1719.24

Compound 86

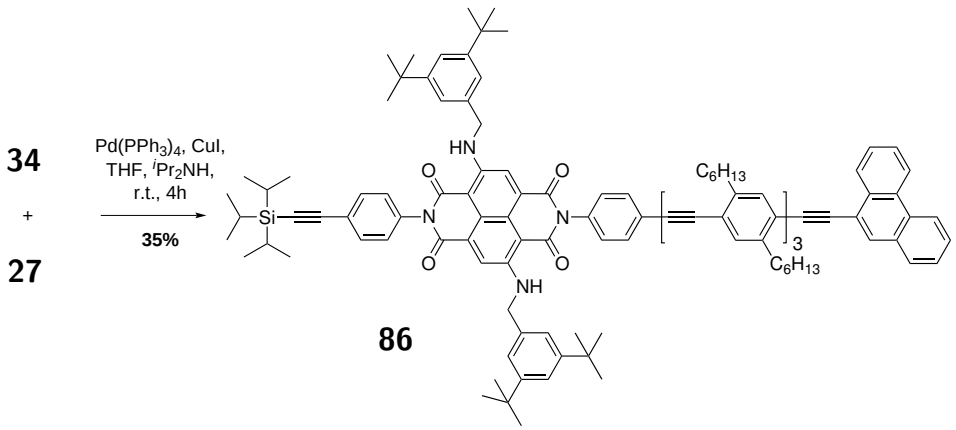

Compound **34** (45.5 mg, 0.043 mmol) in dry THF (20 ml) and compound **27** (66 mg, 0.054 mmol) in dry THF (20 ml) were added in a two necked flask followed by dry $^{i}Pr_2NH$ (10 mL). The reaction mixture was degassed for 15 min. and $Pd(PPh_3)_4$ (5 mg, 0.004) and CuI (0.7 mg, 0.004 mmol) were added, and it was stirred at room temperature for 4h. The reaction mixture was evaporated to dryness and the residue was chromatographed (silica gel, cyclohexane/CH_2Cl_2 1:1 to CH_2Cl_2) affording the desired product **86** (31 mg, 0.015 mmol, 35%) and also the homocoupled product (35 mg, 0.015 mmol, 35%).

TLC (SiO_2, CH_2Cl_2/cyclohexane 1:1): R_f =0.15 **TLC** (SiO_2, CH_2Cl_2/cyclohexane 2:1): R_f =0.58 ^{1}**H NMR** ($CDCl_3$, 400 MHz) δ_H: 9.5 (*m*, 2H, NH), 8.69 (*m*, 2H, CH), 8.56 (*m*, 1H, CH), 8.34 (*s*, 2H, CH), 8.09 (*s*, 1H, CH), 7.89 (*m*, 1H, CH), 7.60-7.75 (*m*, 8H, CH), 7.54 (*s*, 1H, CH), 7.45 (*s*, 1H, CH), 7.38 (*m*, 8H, CH), 7.29 (*m*, 2H, CH), 7.22 (*m*, 4H, CH), 4.61 (*m*, 4H, CH_2), 2.98 (*m*, 2H, CH_2), 2.86 (*m*, 10H, CH_2), 1.74 (*m*, 12H, CH_2), 1.18-1.59 (*m*, 72H, CH_2, CH_3), 1.15 (*m*, 21H, CH_3, CH), 0.91 (*m*, 18H, CH_3). ^{13}**C NMR** ($CDCl_3$, 100 MHz) δ_C: 166.7, 166.6, 163.4, 163.3, 151.8, 149.7, 149.7, 142.8, 142.7, 142.5, 142.5, 136.3, 136.3, 135.4, 135.4, 133.6, 133.0, 133.0, 132.9, 132.9, 132.9, 132.8, 132.3, 132.0, 131.7, 131.5, 130.7, 130.6, 129.2, 129.0, 129.0, 127.9, 127.5, 127.4, 126.7, 126.7, 126.0, 125.5, 124.9, 123.4, 123.2, 123.1, 122.8, 122.6, 122.2, 120.4, 119.6, 119.6, 102.6, 93.6, 93.5, 93.5, 92.7, 48.7, 35.3, 34.7, 32.3, 32.2, 31.9, 31.4, 31.4, 31.2, 31.2, 30.1, 29.9, 29.8, 23.1, 19.1, 14.6, 11.7, 0.4. **MALDI-MS** m/z (%int.): found: 2037.46 ([$M^{+\bullet}$], 100%); calc. for $C_{143}H_{172}N_4O_4Si$: 2037.31

Compound 87

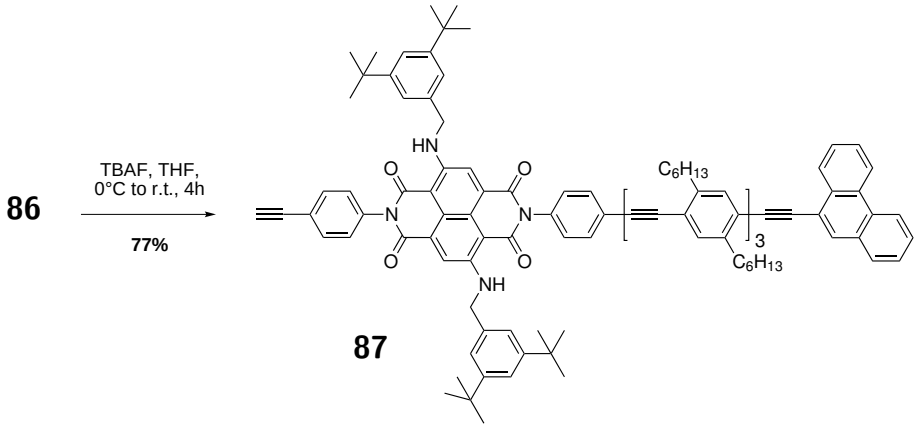

Compound **86** (48 mg, 0.024 mmol) was dissolved in dry THF (40 mL) and the solution was bubbled for 10 min with argon. Then the reaction mixture was cooled to 0 ° C and TBAF (1M in THF, 0.5 eq.) was added. After 30 min the ice bath was removed and the reaction mixture was stirred at RT. More TBAF was added (0.5 eq) until everthing was deprotected. The reaction mixture was then filtered over a plug of silica gel with CH_2Cl_2 and the filtrate was evaporated. The crude was then chromatographed (silica gel, cyclohexane/CH_2Cl_2 1:2) affording the desired product **87** (34 mg, 0.018 mmol, 77%).

TLC (SiO_2, cyclohexane/CH_2Cl_2 1:2): R_f =0.33

Compound 1

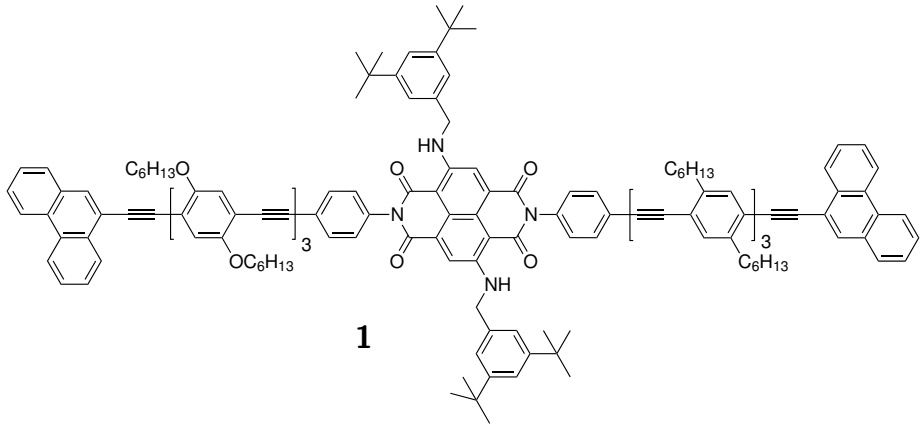

1

A Schlenk tube was charged with **88** (21 mg, 0.017 mmol) and **87** (30 mg, 0.016 mmol) in dry THF. Diisopropylamine (2 mL) was added and the reaction mixture was degassed by freeze-pump-thaw with nitrogen (3 cycles). Then $Pd(PPh_3)_4$ (2 mg, 0.0016 mmol) and CuI (0.3 mg, 0.0016 mmol) were added and the 3rd cycle was done. Then the reaction mixture was stirred at 45 ° for 2h and at 60 ° C for 2h. The crude was first purified by column chromatography (silica gel, cyclohexane/CH_2Cl_2 1:1 to 1:5) to remove the starting compouinds and then by preparative TLC (silica gel, 2 mm thick, hexane/CH_2Cl_2 1:2) affording 21 mg of the green desired product **1** (21 mg, 0.007 mmol, 45%).

^{1}H NMR ($CDCl_3$, 500 MHz) δ_H: 9.52 (*m*, 2H, NH), 8.70 (*m*, 5H, CH), 8.56 (*m*, 1H, CH), 8.36 (*s*, 2H, CH), 8.09 (*d*, $^3J_{HH}$=2.7 Hz, 2H, CH), 7.88 (*t*, $^3J_{HH}$=7.0 Hz, 2H, CH), 7.72 (*m*, 10H, CH), 7.62 (*m*, 2H, CH), 7.53 (*s*, 1H, CH), 7.44 (*s*, 1H, CH), 7.40 (*m*, 4H, CH), 7.33 (*m*, 6H, CH), 7.22 (*s*, 4H, CH), 7.15 (*s*, 1H, CH), 7.08 (*s*, 1H, CH), 7.04 (*s*, 1H, CH), 4.63 (*m*, 4H, CH_2), 4.09 (*m*, 12H, CH_2), 2.97 (*m*, 2H, CH_2), 2.85 (*m*, 10H, CH_2), 2.00 (*m*, 2H, CH_2), 1.88 (*m*, 10H, CH_2), 1.73 (*m*, 12H, CH_2), 1.56 (*m*, 24H, CH_2), 1.35 (*m*, 84H, CH_2, CH_3), 0.90 (*m*, 36H, CH_3). **^{13}C NMR** ($CDCl_3$, 125 MHz) δ_C: 175.7, 174.9, 163.0, 153.5, 151.4, 142.0, 132.6, 128.8, 127.1, 127.0, 127.0, 122.7, 122.3, 122.3, 122.1, 69.7, 48.3, 34.9, 34.2, 31.9, 31.8, 31.7, 31.6, 31.4, 30.7, 29.7, 29.6, 29.5, 29.3, 25.8, 25.8, 25.7, 22.7, 14.1, 14.1, 14.0. **MALDI-MS** m/z (%int.): found: 2958.94 ([$M^{+\bullet}$], 22%); calc. for $C_{208}H_{244}N_4O_{10}$: 2957.87

9.2 Host-Guest in a Surface Network

Compound 39

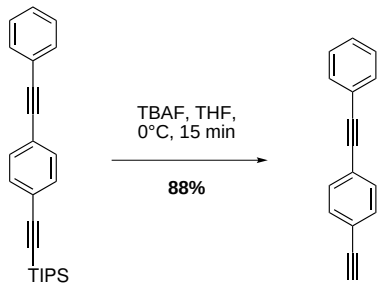

89 **39**

A flask charge with **89** (1.05 g, 2.93 mmol) in dry THF (60 mL) under argon was cooled to 0 ° C and TBAF was added dropwise (6 mL, 1M in THF, 6 mmol) for 15 min. The reaction mixture was then filtered over a plug of silica gel, eluted with CH_2Cl_2 and the yellow-orange filtrate was evaporated affording a yellow solid. The crude was chromatographed (silica gel, cyclohexane) affording to the desired product **39** as a white solid (523 mg, 2.59 mmol, 88%).

^{1}H NMR ($CDCl_3$, 400 MHz) δ_H: 7.56 (*m*, 2H, CH), 7.50 (*m*, 4H, CH), 7.37 (*m*, 3H, CH), 3.19 (*s*, 3H, CH). **^{13}C NMR** ($CDCl_3$, 100 MHz) δ_C: 132.5 (CH, 2C), 132.1 (CH, 2C), 131.9 (CH, 2C), 129.0 (CH, 1C), 128.8 (CH, 2C), 124.2 (Cq, 1C), 123.4 (Cq, 1C), 122.3 (Cq, 1C), 91.8 (CH, 1C), 89.3 (CH, 1C), 83.7 (CH, 1C), 79.4 (CH, 1C). **EI-MS** m/z (%int.): found: 202.1 ([$M^{+\bullet}$], 100%), 200.1 (18%), 101.0 (5%); calc. for $C_{16}H_{10}$: 202.1 **EA** (%) for $C_{16}H_{10}$: found: C=94.16, H=5.34; calc.: C=95.02, H=4.98.

Compound 5

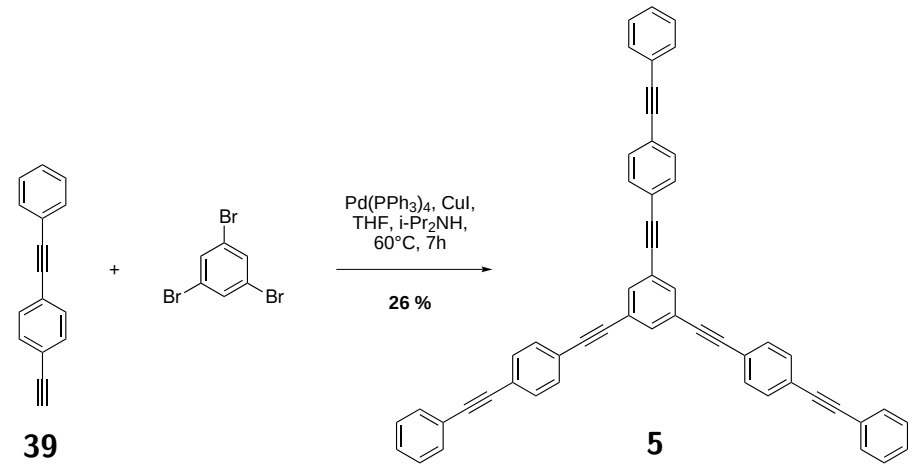

Compound **5** was obtained following **method A**: Compound **39** (110 mg, 0.545 mmol), 1,3,5-tribromobenzene (50 mg, 0.156 mmol), $Pd(PPh_3)_4$ (18 mg, 0.016 mmol) and CuI (0.8 mg, 0.016 mmol), dry THF (40 mL) and $^{i}Pr_2NH$ (4 mL). The reaction mixture was stirred at 60 °C for 8h. The crude was chromatographed (silica gel, cyclohexane/CH_2Cl_2 9:1 to 4:1) giving the desired product and a side product. This mixture was purified by recycling GPC (CH_3Cl) giving desired product **5** (27.6 mg, 0.04 mmol, 26%).

TLC (SiO_2, Cyclohexane/CH_2Cl_2 4:1): R_f=0.23 **m.p.**=241.1 °C ^{1}**H NMR** ($CDCl_3$, 400 MHz) δ_H: 7.67 (*s*, 3H, CH), 7.53 (*m*, 18H, CH), 7.36 (*m*, 9H, CH). ^{13}**C NMR** ($CDCl_3$, 100 MHz) δ_C: 134.2 (CH, 3C), 131.7 (CH, 6C), 131.7 (CH, 6C), 131.6 (CH, 6C), 128.6 (CH, 3C), 128.4 (CH, 6C), 124.0 (Cq, 3C), 123.6 (Cq, 3C), 123.0 (Cq, 3C), 122.6 (Cq, 3C), 91.5 (Cq, 3C), 90.4 (Cq, 3C), 89.5 (Cq, 3C), 89.0 (Cq, 3C). **MALDI** m/z: found: 679.31; calc. for $C_{54}H_{30}$: 678.23

Compound 43[139]

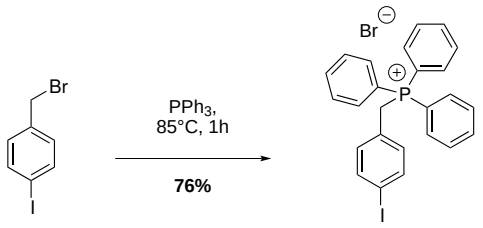

42 **43**

A two necked flask charged with **42** (1.024 g, 3.45 mmol) in dry DMF (30 mL) was heated at 85 ° C. Compound **90** (905 mg, 3.45 mmol) was added and the reaction mixture was stirred at this temperature for 1h and then let to recover room temperature. Toluene (20 mL) was added, and it was cooled in an ice bath. The white precipitate was washed with toluene and centrifuged (2x). The desired product **43** was obtained (1.46 g, 2.61 mmol, 76 %).

^{1}**H NMR** ($CDCl_3$, 400 MHz) δ_H: 7.75 (*m*, 9H, CH), 7.60 (*m*, 6H, CH), 7.37 (*d*, $^3J_{HH}$=8.2 Hz, $^4J_{HH}$=2.5 Hz, 2H, CH), 6.91 (*dd*, $^3J_{HH}$=8.2 Hz, $^4J_{PH}$=2.5 Hz, 2H, CH), 5.52 (*d*, $^2J_{PH}$=14.8 Hz, 2H, CH).

Compound 44[139]

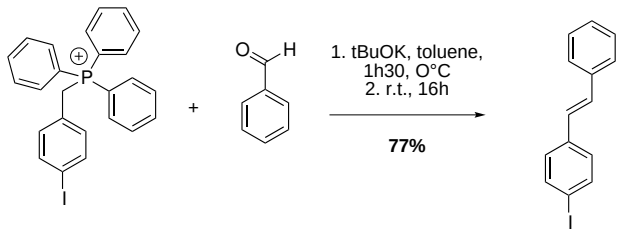

43 **44**

A two necked flask under argon was charged with **43** (517 mg, 0.924 mmol) in dry toluene (15 mL). This suspension was cooled to 0 ° C and potassium tert-butoxide (120 mg, 0.924 mmol) was added. The orange reaction mixture was stirred at this temperature for 1h30 min. and then benzaldehyde (120 mg, 1.13 mmol) was injected all at once. The reaction mixture was stirred at room temperature overnight and then evaporated. The obtained oil was dissolved in CH_2Cl_2 and washed with water. The organic layer was dried over Na_2SO_4, filtered and evaporated giving a yellow solid that was chromatographed (silica gel, CH_2Cl_2/cyclohexane 2:1) giving the product as a mixture of isomers which was refluxed in toluene (10 mL) with catalytic amount of iodine to isomerize the Z-conformation to the E-conformation. The pink solution was evaporated giving compound **44** as a yellow solid (217 mg, 0.709 mmol, 77%).

^{1}H NMR ($CDCl_3$, 500 MHz) δ_H: 7.66 (*d*, $^3J_{HH}$=8.3 Hz, 2H, CH), 7.49 (*d*, $^3J_{HH}$=7.7 Hz, 2H, CH), 7.35 (*dd*, $^3J_{HH}$=7.6 Hz, 2H, CH), 7.26 (*t*, $^3J_{HH}$=7.3 Hz, 1H, CH), 7.22 (*d*, $^3J_{HH}$=8.3 Hz, 2H, CH), 7.09 (*d*, $^3J_{HH}$=16.3 Hz, 1H, CH), 6.99 (*d*, $^3J_{HH}$=16.3 Hz, 1H, CH). **^{13}C NMR** ($CDCl_3$, 126 MHz) δ_C: 137.8 (CH, 2C), 137.0 (Cq, 1C), 136.9 (Cq, 1C), 129.6 (CH, 1C), 128.8 (CH, 2C), 128.3 (CH, 2C), 128.0 (CH, 1C), 127.6 (CH, 1C), 126.7 (CH, 2C), 92.9 (Cq, 1C).**EI-MS** m/z (%int.): found: 306 ([$M^{+\bullet}$], 100%), 178.1 (57%), 152 (8%), 89 (10%); calc. for $C_{23}H_{27}NO_2$: 305.99 **EA** (%) for $C_{23}H_{27}NO_2$: found: C=54.82, H=3.76; calc.: C=54.93, H=3.62.

Compound 92

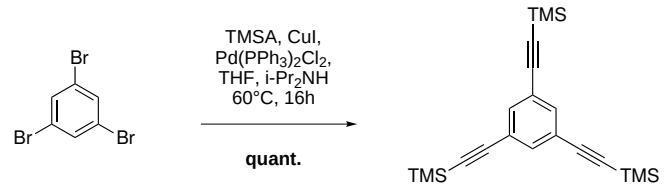

92

Compound **92** was obtained following **method A**: 1,3,5-tribromobenzene (5 g, 15.6 mmol), THF (80 mL) $^{i}PrNH_2$ (10 mL), acetylene (5.31 g, 54 mmol), $Pd(PPh_3)_2Cl_2$ (547 mg, 0.778 mmol) and CuI (149 mg, 0.778 mmol). The reaction mixture was stirred at 60 ° C overnight. The crude was chromatographed (silica gel, cyclohexane) giving the desired product **92** as a white solid (5.6 g, 15.3 mmol, 99%).

TLC (SiO_2, CH_2Cl_2/cyclohexane): R_f=0.6 ^{1}**H NMR** ($CDCl_3$, 400 MHz) δ_H: 7.51 (*s*, 3H, CH), 0.25 (*s*, 27H, $SiCH_3$). ^{13}**C NMR** ($CDCl_3$, 100 MHz) δ_C: 135.1 (CH, 3C), 123.8 (Cq, 3C), 103.3 (Cq, 3C), 95.8 (Cq, 3C), 0.0 (CH_3, 9C).

Compound 46

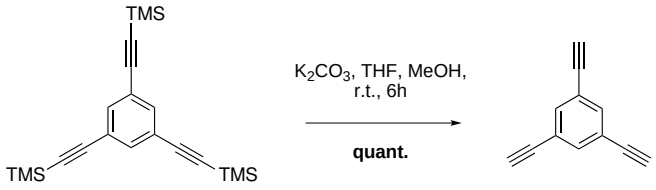

92 **46**

Compound **92** (2 g, 5.45 mmol) was dissolved in a 1:1 mixture of THF/MeOH to make a 80 mL solution. This solution was bubbled with argon for 20 min, K_2CO_3 (3.81 g, 27.3 mmol) was added and the mixture stirred at room temperature. The reaction mixture was poured into water and extracted with CH_2Cl_2 (3x). The combined organic layers were dried over Na_2SO_4, filtered and evaporated giving the desired product **46** as a yellow solid (818 mg, 5.45 mmol, quant.).

TLC (SiO_2, (CH2Cl2)/cyclohexane): R_f=0.37 **TLC** (SiO_2, hexane): R_f=0.18 ^{1}**H NMR** ($CDCl_3$, 400 MHz) δ_H: 7.57 (*s*, 3H, CH), 3.10 (*s*, 3H, CH). ^{13}**C NMR** ($CDCl_3$, 100 MHz) δ_C: 135.7 (CH, 3C). 122.9 (Cq, 3C), 81.6 (Cq, 3C), 78.7 (CH, 3C).

Compound 48[126]

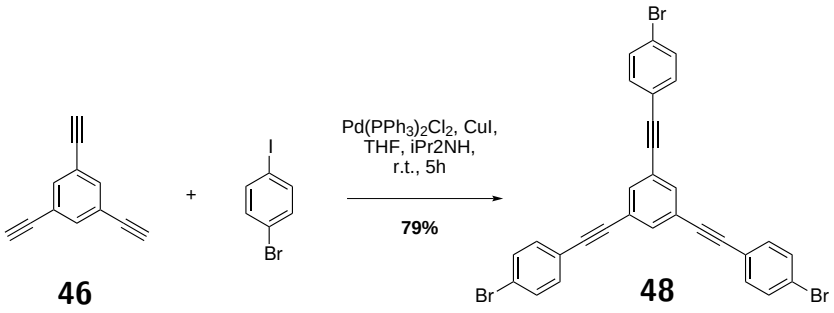

Compound **48** was obtained following **method A**: Compound **46** (500 mg, 3.33 mmol), 1-bromo-4-iodobenzene (3.7 g, 13.3 mmol), THF (80 mL) $^{i}Pr_2NH$ (4 mL), $Pd(PPh_3)_2Cl_2$ (120 mg, 0.166 mmol), CuI (30 mg, 0.166 mmol). The reaction mixture was stirred at r.t. for 5h poored into 1 M HCl and extracted with Ch_2Cl_2(3x). The combined organic layers were washed with water, dried over Na_2SO_4, filtered and evaporated. The crude was chromatographed (silica gel, CH_2Cl_2/cyclohexane 5:95) giving the desired product **48** (1.61 g, 2.62 mmol, 79%).

TLC (SiO_2, hexane): R_f=0.18 ^{1}**H NMR** ($CDCl_3$, 400 MHz) δ_H: 7.63 (*s*, 3H, CH), 7.49 (*dt*, $^{3}J_{HH}$=8.6 Hz, $^{4}J_{HH}$=2.0 Hz, 6H, CH), 7.38 (*dt*, $^{3}J_{HH}$=8.6 Hz, $^{4}J_{HH}$=2.0 Hz, 6H, CH), ^{13}**C NMR** ($CDCl_3$, 100 MHz) δ_C: 134.2 (CH, 3C). 133.1 (CH, 6C). 131.8 (CH, 6C). 123.9 (Cq, 3C), 123.0 (Cq, 3C), 121.7 (Cq, 3C), 89.7 (CH, 3C). 88.7 (CH, 3C).

Compound 94

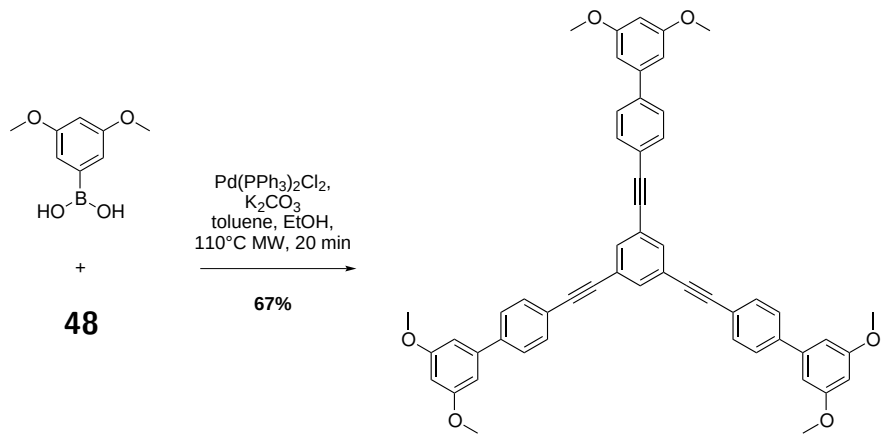

Compound **48** (102 mg, 0.165 mmol), 3,5-dimethoxyphenylboronic acid (120 mg, 0.662 mmol) and K_2CO_3 (140 mg, 0.992 mmol) were mixed with toluene (1.5 mL) and EtOH (1 mL). It was degassed with argon, $Pd(PPh)_2Cl_2$ (6 mg, 0.008 mmol) was added and it was degassed again. The vessel was sealed and heated at 110 ˚ C for 20 min in the microwave. The reaction mixture was washed with water. The aqueous phase was extracted twice with CH_2Cl_2, the combined organic phases were washed with brine, dried over Na_2SO_4, filtered and evaporated. The crude was chromatographed (silica gel, cyclohexane/CH_2Cl_2 1:2 to 1:7) affording **94** as a white solid (87 mg, 0.111 mmol, 67 %).

TLC (SiO_2, (CH_2Cl_2/cyclohexane 2:1): R_f=0.2 ^{1}**H NMR** ($CDCl_3$, 400 MHz) δ_H: 7.71 (*s*, 3H, CH), 7.61 (*s*, 12H, CH), 6.77 (*s*, 6H, CH), 6.51 (*s*, 3H, CH). ^{13}**C NMR** ($CDCl_3$, 100 MHz) δ_C: 161.6 (Cq, 6C), 142.9 (Cq, 3C), 141.7 (Cq, 3C), 134.5 (CH, 3C), 132.5 (CH, 6C), 127.6 (CH, 6C), 124.5 (Cq, 3C), 122.4 (Cq, 3C), 105.8 (CH, 6C), 100.1 (CH, 3C), 91.0 (Cq, 6C), 89.1 (Cq, 6C), 55.9 (OCH_3, 6C). **MALDI** m/z (%int.):found: 788.87; calc. for $C_{54}H_{42}O_6$: 786.30

Compound 96

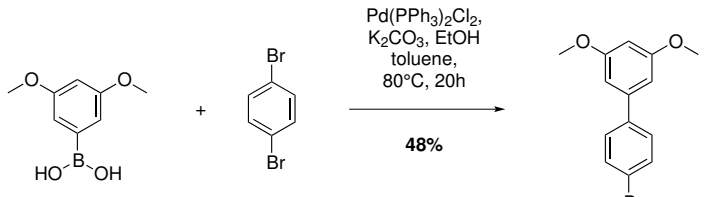

95 **96**

A two necked flask under argon was charged with compound 1,4-dibromobenzene **97** (1.56 g, 6.59 mmol), $Pd(PPh_3)_2Cl_2$ (40 mg, 0.055 mmol) and K_2CO_3 (460 mg, 3.3 mmol). Toluene (15 mL) and ethanol (5 mL) were added and the reaction mixture was bubbled with argon for 10 min and heated to 80 ° C. 3,5-dimethoxyphenylboronic acid **95** (200 mg, 1.1 mmol) in toluene (5 mL) was added dropwise over 4h via a serynge. The reaction mixture was stirred at this temperature overnight, washed with water and extracted with CH_2Cl_2. The aqueuse phase was extracted 3x with CH_2Cl_2. The combined organic phases were washed with brine, dried over Na_2SO_4, filtered and evaporated. The oil was dried in the HV pump giving a brown solid. The crude was chromatographed (silica gel, hexane/CH_2Cl_2 2:1) giving the desired product **96** yellow solid (156 mg, 0.53 mmol, 48%) and the dehalogenated product (72 mg, 0.34 mmol, 31%).

TLC (SiO_2, hexane/CH_2Cl_2 2:1): R_f=0.23 ^{1}**H NMR** ($CDCl_3$, 400 MHz) δ_H: 7.54 (*dt*, $^3J_{HH}$=8.6 Hz, $^4J_{HH}$=2.3 Hz, 2H, CH), 7.43 (*dt*, $^3J_{HH}$=8.6 Hz, $^4J_{HH}$=2.3 Hz, 2H, CH), 6.68 (*d*, $^4J_{HH}$=2.3 Hz, 2H, CH), 6.47 (*t*, $^4J_{HH}$=2.3 Hz, 1H, CH), 3.84 (*s*, 6H, OCH_3). ^{13}**C NMR** ($CDCl_3$, 100 MHz) δ_C: 161.2 (Cq, 2C), 142.2 (Cq, 1C), 140.1 (Cq, 1C), 131.8 (CH, 2C), 128.8 (CH, 2C), 121.8 (Cq, 1C), 105.3 (CH, 2C), 99.5 (CH, 1C), 55.5 (OCH_3, 2C).

Compound 49

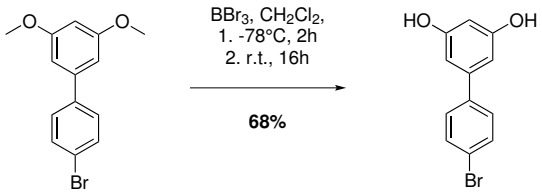

96 **49**

In a flask under argon was dissolved **96** (138 mg, 0.47 mmol) in 20 mL dry and degassed CH_2Cl_2. The solution was degassed with argon for 10 min and BBr_3 (3 eq, 1.4 mL, 1M in DCM) was added dropwise at -78 °C. The reaction mixture was left under stirring at this temperature overnight. Water was added and the reaction mixture was acidified (1M HCl), extracted (3x) with CH_2Cl_2, washed with brine. The combined organic layers were dried over Na_2SO_4, filtered and evaporated. The crude was chromatographed (silica gel, CH_2Cl_2/EtOAc 8:2) giving the monodeprotected product **98** as a grew solid (52 mg) and the desired product **49** as a white solid (86 mg, 0.324 mmol, 69%).

^{1}H NMR ($CDCl_3$, 400 MHz) δ_H: 7.57 (*dt*, $^3J_{HH}$=8.6 Hz, $^4J_{HH}$=2.3 Hz, 2H, CH), 7.49 (*dt*, $^3J_{HH}$=8.6 Hz, $^4J_{HH}$=2.3 Hz, 2H, CH), 7.10 (*br s*, 2H, OH), 6.60 (*d*, $^4J_{HH}$=2.2 Hz, 2H, CH), 6.36 (*t*, $^4J_{HH}$=2.2 Hz, 1H, CH). **^{13}C NMR** ($CDCl_3$, 100 MHz) δ_C: 158.1 (Cq, 2C), 141.6 (Cq, 1C), 139.5 (Cq, 1C), 131.3 (CH, 2C), 128.4 (CH, 2C), 120.8 (Cq, 1C), 105.3 (CH, 2C), 101.6 (CH, 1C).

Compound 52[127]

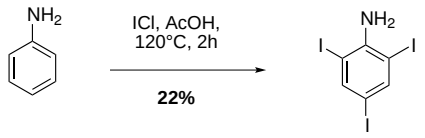

52

Aniline **99** (4 g, 43 mmol) was dissolved in glacial acetic acid (30 mL) and this solution was heated at 60 ° C. To this solution was added a solution of ICl (24.9 g, 150 mmol) in glacial acetic acid (20 mL) that was previously heated at 50 ° C. The reaction mixture was then heated to reflux in an oil bath for 2h. Deionized water was added and the reaction mixture was distilled to remove most of the iodine, the acetic acid and HCl. The rest of the reaction mixture was filtered. The black solid was adsorbed on silica gel and passed through a plug of silica gel with cyclohexane without pressure. The solid obtained was recrystalised (EtOH) giving the desired product **52** (4.45 g, 9.5 mmol, 22%).

^{1}**H NMR** ($CDCl_3$, 400 MHz) δ_H: 7.86 (*s*, 2H, CH), 4.66 (*br s*, 2H, NH_2).

Compound 54

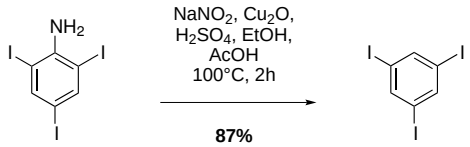

52 **54**

Finely ground $NaNO_2$ (1.46 g, 21.1 mmol) was slowly added to sulfuric acid 95 % (3 mL) under stirring. Then a solution of **52** (2.21 g, 4.69 mmol) in glacial acetic acid (130 mL) was added dropwise to the cooled $NaNO_2$ solution and the yellow reaction mixture was stirred 30 min at room temperature. This solution was added dropwise to a suspension of copper oxide (2 g, 14.1 mmol) in dry EtOH (60 mL). The reaction mixture was heated at 100 °C until no nitrogen was formed (2h). The reaction mixture was let to recover room temperature overnight and then it was poored into ice and extracted with CH_2Cl_2 (3x). The combined org layers were washed with water, dried over Na_2SO_4, filtered and evaporated affording a yellow solid that was recrystallized from EtOH (2x 150 mL) giving a pale yellow solid **54** (1.86 g, mmol, 87%).

TLC (SiO_2, Cyclohexane): R_f=0.47 **m.p.**: 183 °C ^{1}**H NMR** ($CDCl_3$, 400 MHz) δ_H: 8.00 (*s*, 3H, CH). ^{13}**C NMR** ($CDCl_3$, 100 MHz) δ_C: 144.8 (CH, 3C), 95.7 (Cq, 3C).

Compound 53

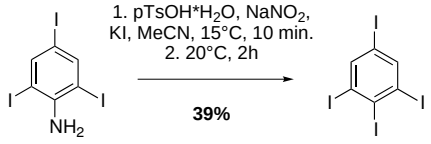

52 **53**

To a solution of *p*-TsOH·H_2O (645 mg, 3.39 mmol) in MeCN (40 mL) was added compound **52** (532 mg, 1.13 mmol). The resulting suspension of amine salt was cooled to 10-15 ˚ C and a solution of $NaNO_2$ (156 mg, 2.26 mmol) and KI (475 mg, 2.82 mmol) in water (2 mL) was gradually added. The reaction mixture was stirred for 10 min. at this temperature and then for 2h at 20 ˚ C. Water, $NaHCO_3$ (1M, until pH=9-10) and $Na_2S_2O_3$ (2 M, mL) were successively added to the reaction mixture. The precipitated aromatic iodide was extracted with TBME, washed with water 2x (until neutral pH), dried over Na_2SO_4, filtered and evaporated giving a brown solid.The crude was adsorbed on silica gel and chromatographed (silical gel, cyclohexane) giving the desired product **53** (256 mg, 0.44 mmol, 39%).

^{1}**H NMR** ($CDCl_3$, 400 MHz) δ_H: 8.1 (*s*, 2H, CH). ^{13}**C NMR** ($CDCl_3$, 100 MHz) δ_C: 146.6 (CH, 2C), 121.1 (Cq, 1C), 108.2 (Cq, 2C), 95.1 (Cq, 1C). **EI-MS** m/z (%int.): found: 581.6 ([$M^{+\bullet}$], 100%), 454.7 (21.66%), 327.8 (7.9%), 200.9 (12.28%), 74.0 (12.70%); calc. for $C_6H_2I_4$: 581.63.

Compound 100

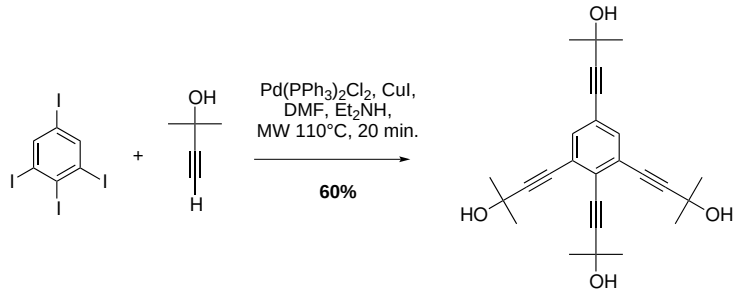

54 **100**

Compound **100** was obtained following **method B**: Compound **54** (50 mg, 0.086 mmol), (2-hydroxypropyl)acetylene (145 g, 1.72 mmol), $Pd(PPh_3)_2Cl_2$ (3 mg, 0.04 mmol), CuI (0.8 mg, 0.04 mmol), THF (4 mL), Et_2NH (2 mL). The crude was chromatographed (silica gel, EtOAc/CH_2Cl_2 6:4 to EtOAc) giving the desired product **100** (21 mg, 0.05 mmol, 60%).

^{1}H NMR ($CDCl_3$, 400 MHz) δ_H: 7.33 (*s*, 2H, CH), 1.65 (*s*, 6H, CH_3). 1.62 (*s*, 12H, CH_3). 1.59 (*s*, 6H, CH_3). **^{13}C NMR** ($CDCl_3$, 100 MHz) δ_C: 133.7 (CH, 2C), 127.5 (Cq, 1C), 125.6 (Cq, 2C), 122.2 (Cq, 1C), 103.6 (Cq, 1C), 98.6 (Cq, 2C), 96.2 (Cq, 1C), 80.4 (Cq, 1C), 79.8 (Cq, 2C), 79.6 (Cq, 1C), 65.7 (Cq, 1C), 65.6 (CH, 2C), 65.5 (Cq, 1C), 31.4 (CH, 2C), 31.4 (CH, 4C), 31.3 (CH, 2C).

Compound 55

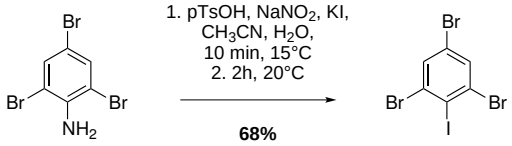

102 **55**

To a solution of pTsOH·H_2O (35 g, 182 mmol) in MeCN (240 mL) in a two necked 1L flask was added compound **102** (20 g, 61 mmol). The resulting suspension of amine salt was cooled to 5-10 ° C and to this was added, gradually via a droping funnel, a solution of $NaNO_2$ (8.37 g, 121 mmol) and KI (25 g, 152 mmol) in water (36 mL). The reaction mixture was stirred for 10 min at this temperature and then allowed to reach 20 ° C and stirred again for 2h. The reaction mixture was then basified with a solution of $NaHCO_3$ (1M, until pH=9-10) and extracted with TBME (3x). The combined organic layers were then washed with a solution of $Na_2S_2O_3$ (20% aq.), washed with water (until neutral pH), dried over Na_2SO_4, filtered and evaporated. The rest of the crude (23.71 g, dark brown solid) was recrystallized in EtOH (200 mL) giving the desired compound **55** as brown needles (18.2 g, 41.3 mmol, 68%).

TLC (SiO_2, hexane): R_f=0.4 ^{1}**H NMR** ($CDCl_3$, 400 MHz) δ_H: 7.70 (*s*, 2H, CH). ^{13}**C NMR** ($CDCl_3$, 100 MHz) δ_C: 133.6 (CH, 2C), 131.8 (Cq, 2C), 123.0 (CH, 1C), 108.1 (CH, 1C).

Compound 103

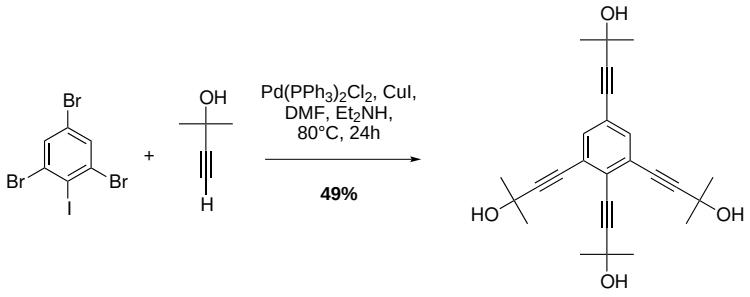

55 **103**

Compound **103** was obtained following **method A**: Compound **55** (4.0 g, 9.08 mmol), DMF (40 mL) $^{i}Pr_2NH$ (4 mL), (2-hydroxypropyl)acetylene (9.16 g, 109 mmol), $Pd(PPh_3)_4$ (319 mg, 0.454 mmol) and CuI (86 mg, 0.454 mmol). The reaction mixture was stirred at 80 ° C for 24h. The crude was chromatographed (silica gel, CH_2Cl_2/EtOAc 6:4) giving the desired product **103** (1.8 g, 4.43 mmol, 49%).

^{1}H NMR ($CDCl_3$, 400 MHz) δ_H: 7.30 (*s*, 2H, CH), 1.64 (*s*, 6H, CH_3). 1.61 (*s*, 12H, CH_3). 1.58 (*s*, 6H, CH_3). **^{13}C NMR** ($CDCl_3$, 100 MHz) δ_C: 133.7 (CH, 2C), 127.3 (Cq, 1C), 125.6 (Cq, 2C), 122.2 (Cq, 1C), 103.6 (Cq, 1C), 98.7 (Cq, 2C), 96.3 (Cq, 1C), 80.3 (Cq, 1C), 79.7 (Cq, 2C), 79.4 (Cq, 1C), 65.6 (Cq, 1C), 65.4 (CH, 2C), 65.3 (Cq, 1C), 31.4 (CH, 2C), 31.4 (CH, 4C), 31.3 (CH, 2C),

Compound 56

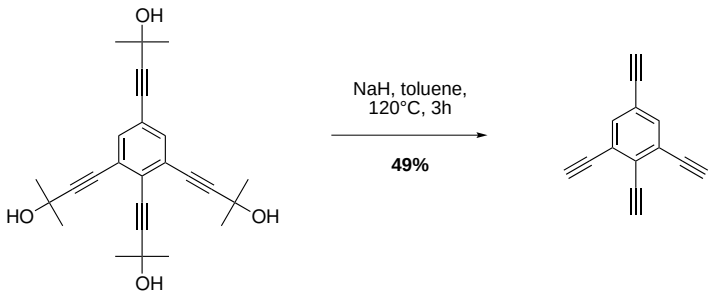

103 **56**

Compound **103** (440 mg, 1.08 mmol) was dissolved in dry toluene and this solution was degassed for 10 min. Sodium hydride (173 mg, 4.33 mmol, 60% dispersion in oil) was added and the reaction mixture was stirred at 120 ˚ C for 3h. The reaction mixture was poured on a silica plug, eluted with CH_2Cl_2 giving the crude mixture which was then chromatographed (silica gel, CH_2Cl_2/cyclohexane 1:2) giving the desired product **56** as a yellow solid (92 mg, 0.528 mmol, 49%).

^{1}H NMR ($CDCl_3$, 400 MHz) δ_H: 7.60 (*s*, 2H, CH), 3.67 (*s*, 1H, CH), 3.36 (*s*, 2H, CH), 3.19 (*s*, 1H, CH).

Compound 10

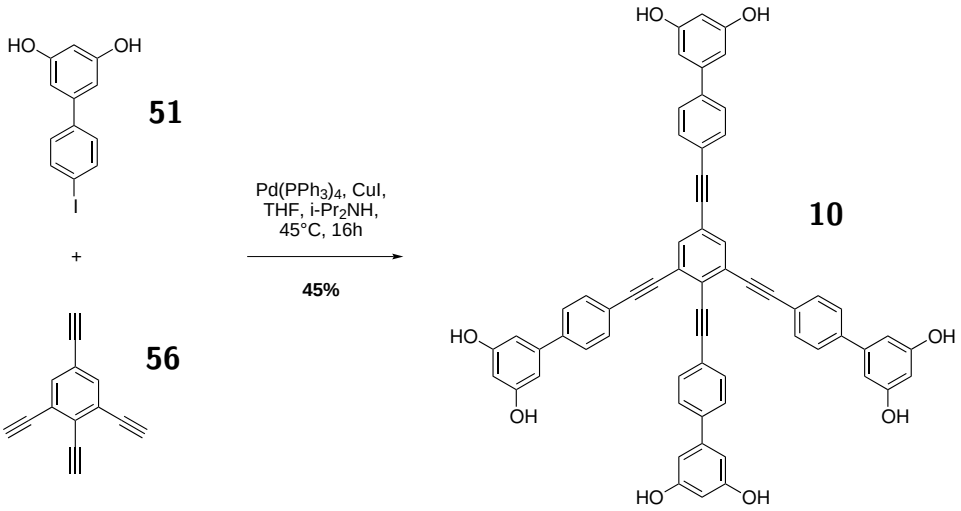

Compound **10** was obtained following **method A**: Compound **51** (264 mg, 0.846 mmol), THF (20 mL) $^{i}Pr_2NH$ (2 mL), **56** (37 mg, 0.211 mmol), $Pd(PPh_3)_4$ (24 mg, 0.021 mmol) and CuI (2.0 mg, 0.0106 mmol). The reaction mixture was stirred at 45 °C overnight. The crude was chromatographed (reverse phase column (C18 40-60 RP-silica), $MeOH/H_2O$ 9:1) giving the desired product **10** (86 mg, 0.094 mmol, 45%).

^{1}**H NMR** (MeOD, 500 MHz) δ_H: 7.49-7.58 (*m*, 14H, CH), 7.44 (*m*, 3H, CH), 7.42 (*m*, 1H, CH), 6.62 (*t*, $^{4}J_{HH}$=2.0 Hz, 8H, CH), 6.35 (*m*, 4H, CH), 5.11 (*br s*, 8H, OH). ^{13}**C NMR** (MeOD, 125 MHz) δ_C: 158.6 (CH, 8C), 142.3 (Cq, 1C), 142.2 (Cq, 3C), 141.4 (Cq, 1C), 141.4 (Cq, 2C), 141.3 (Cq, 1C), 133.4 (CH, 2C), 131.9 (CH, 8C), 127.3 (Cq, 1C), 126.6 (CH, 8C), 126.4 (Cq, 2C), 122.9 (Cq, 1C), 122.1 (Cq, 1C), 121.8 (Cq, 2C), 121.4 (Cq, 1C), 105.4 (CH, 8C), 101.8 (CH, 3C), 99.2 (Cq, 1C), 94.1 (Cq, 2C), 91.7 (Cq, 1C), 88.2 (Cq, 1C), 88.1 (Cq, 1C), 88.0 (Cq, 2C),

9.3 Molecular Rectifiers

Compound 64

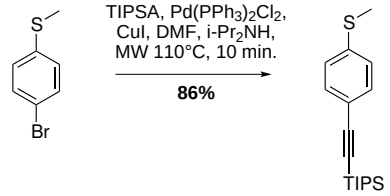

104 **64**

Compound **64** was obtained following **method B**: Compound **104** (3.57 g, 17.6 mmol), TIPSA (3.6 g, 19.3 mmol), $Pd(PPh_3)_2Cl_2$ (247 mg, 0.4 mmol), CuI (67 mg, 0.4 mmol), DMF (12 mL), $^{i}Pr_2NH$ (2 mL). The crude was chromatographed (silica gel, cyclohexane) giving the desired product **64** as a colorless oil (4.6 g, 15.1 mmol, 86%).

^{1}H NMR ($CDCl_3$, 400 MHz) δ_H: 7.38 (*d*, $^{3}J_{HH}$=8.6 Hz, 2H, CH), 7.15 (*d*, $^{3}J_{HH}$=8.6 Hz, 2H, CH), 2.47 (*s*, 2H, CH_3), 1.12 (*br s*, 21H, CH, CH_3). **^{13}C NMR** ($CDCl_3$, 100 MHz) δ_C: 139.3 (Cq, 1C), 132.3 (CH, 2C), 125.8 (CH, 2C), 119.9 (Cq, 1C), 106.8 (Cq, 1C), 90.5 (Cq, 1C), 18.6 (CH_3, 6C), 15.4 (SCH_3, 1C), 11.3 (CH, 3C).

Compound 65

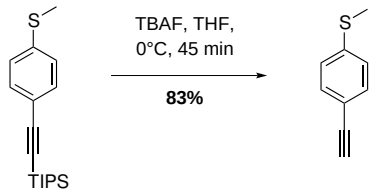

64 **65**

Compound **65** was obtained following **method C**: Compound **64** (1.49 g, 4.88 mmol), TBAF (0.5 mL, 0.5 mmol), THF (40 mL). The reaction mixture was stirred at 0 ° C for 45 min. The crude was chromatographed (silica gel, cyclohexane/CH_2Cl_2 9:1) giving the desired product **65** as a colorless oil (603 mg, 4.07 mmol, 83 %).

^{1}H NMR ($CDCl_3$, 400 MHz) δ_H: 7.39 (*d*, $^3J_{HH}$=8.5 Hz, 2H, CH), 7.18 (*d*, $^3J_{HH}$=8.5 Hz, 2H, CH), 3.07 (*s*, 1H, CH), 2.48 (*s*, 3H, SCH_3). **^{13}C NMR** ($CDCl_3$, 100 MHz) δ_C: 140.1 (Cq, 1C), 132.4 (CH, 2C), 125.7 (CH, 2C), 118.3 (Cq, 1C), 83.5 (Cq, 1C), 15.3 (SCH_3, 1C). **EI-MS** m/z (%int.): 148 ([$M^{+\bullet}$], 100%), 133, 115, 102, 89.

Compound 60[134]

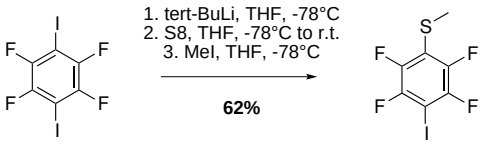

105 **60**

In a two-neck flask equipped with a magnetic stirrer and a septum 1,4-diiodotetrafluorobenzene **105** (500 mg, 1.22 mmol) was dissolved in dry, Ar-saturated THF (10 mL) and the solution was cooled to -78 ˚ C using a dry ice/isopropanol bath. ^{t}BuLi (1.8 mL, 1.7 M in pentane, 3.1 mmol) at -78 ˚ C was slowly dropped in via syringe (reaction mixture turned slightly yellow). After stirring for 20 min sulfur (39 mg, 1.22 mmol) was added and the cooling bath removed. Stirring was continued until all sulfur disappeared (about 30 min). The mixture was then cooled again to -78 ˚ C and CH_3I (433 mg, 3.05 mmol) was added and the cooling bath was removed. The reaction mixture was stirred for 1h and then the solvents were evaporated while adsorbing on silica gel. The crude was chromatographed (silica gel, cyclohexane) giving the desired product **60** (243 mg, 0.755 mmol, 62%).

TLC (SiO_2, cyclohexane/toluene): R_f=0.28 ^{1}**H NMR** ($CDCl_3$, 400 MHz) δ_H: 2.53 (*s*, 3H, SCH_3). ^{13}**C NMR** ($CDCl_3$, 100 MHz) δ_C: 148.5 (Cq, 1C), 147.7 (Cq, 1C), 146.1 (Cq, 1C), 144.8 (Cq, 1C), 117.2 (Cq, 1C), 71.3 (Cq, 1C), 17.6 (SCH_3, 1C). **EI-MS** m/z (%int.): 321.9 ([$M^{+\bullet}$], 100%), 306.9 (23%), 210.0 (46%), 180.0 (17%).

Compound 61

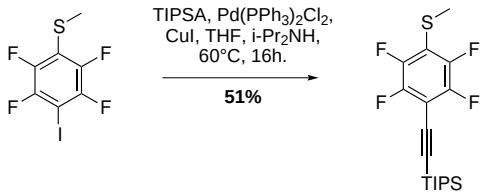

60 **61**

Compound **61** was obtained following **method A**: Compound **60** (493 mg, mmol), TIPSA (432 mg, 2.3 mmol), $Pd(PPh_3)_2Cl_2$ (54 mg, 0.08 mmol), CuI (15 mg, 0.08 mmol), THF (40 mL), $^{i}Pr_2NH$ (5 mL). The reaction mixture was stirred at 60 ° C overnight. The crude was chromatographed (silica gel, cyclohexane) giving the desired product **61** (294 mg, 0.781 mmol, 51%).

TLC (SiO_2, hexane): R_f=0.31 ^{1}**H NMR** ($CDCl_3$, 400 MHz) δ_H: 2.53 (*s*, 3H, SCH_3), 1.14 (*s*, 21H, CH_3, CH). ^{13}**C NMR** ($CDCl_3$, 100 MHz) δ_C: 148.5 (Cq, 1C), 147.5 (Cq, 1C), 146.0 (Cq, 1C), 144.9 (Cq, 1C), 117.1 (Cq, 1C), 106.7 (CH, 1C). 100.0 (Cq, 1C), 90.5 (CH, 1C), 18.5 (CH_3, 6C), 17.6 (SCH_3, 1C), 11.1 (CH, 3C). **EI-MS** m/z (%int.) found: 376.1([$M^{+\bullet}$], 15.73), 334.1 (22.21), 333.0 (100), 305.0 (21.99), 291.0 (10.719), 277.0 (34.04), 263.0 (38.75), 138.5 (26.06); calculated for $C_{18}H_{24}SSi$: 376.13

Compound 62

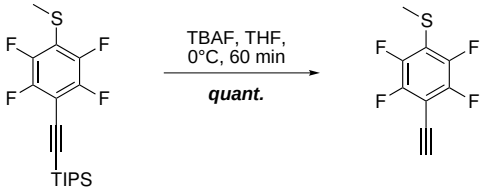

61 **62**

Compound **62** was obtained following **method C**: Compound **61** (131 g, 0.35 mmol), TBAF (0.1 mL, 0.1 mmol), THF (20 mL). The reaction mixture was stirred at 0 ° C for 60 min. The crude was used in the next step without further purification.

TLC (SiO_2, hexane): R_f=0.21

Compound 67

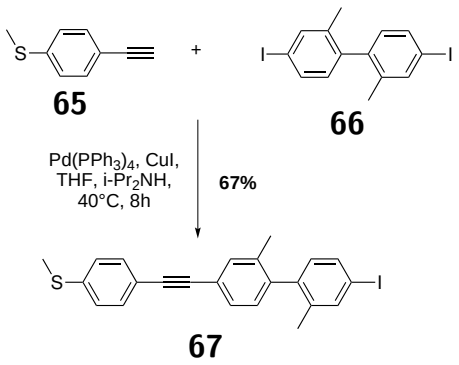

Compound **67** was obtained following **method A**: **66** (1.46 g, 3.37 mmol), THF (30 mL), $^{i}Pr_2NH$ (4 mL), $Pd(PPh_3)_4$ (40 mg, 0.03 mmol) and CuI (6 mg, 0.03 mmol). The reaction mixture was heated at 40 °C and then **65** (100 mg, 0.68 mmol) in dry degassed THF (10 mL) was added to the reaction mixture over a period of 4h via a syringe. The orange-red reaction mixture was cooled to room temperature and then poored into HCl 1M and extracted with CH_2Cl_2 (3x). The combined organic layers were washed with water, dried over Na_2SO_4, filtered and evaporated. The crude was then chromatographed (silica gel, hexane to hexane/CH_2Cl_2 2:1) affording the desired product **67** (204 mg, 0.45 mmol, 67%).

TLC (SiO_2, hexane/CH_2Cl_2 2:1): R_f=0.52 **TLC** (SiO_2, hexane): R_f=0.12 **^{1}H NMR** ($CDCl_3$, 400 MHz) δ_H: 7.64 (*d*, $^4J_{HH}$=0.9 Hz, 1H, CH), 7.56 (*dd*, $^3J_{HH}$=8.0 Hz, $^4J_{HH}$=1.3 Hz, 1H, CH), 7.44 (*m*, 3H, CH), 7.36 (*dd*, $^3J_{HH}$=7.8 Hz, $^4J_{HH}$=1.1 Hz, 1H, CH), 7.21 (*d*, $^3J_{HH}$=8.5 Hz, 2H, CH), 7.03 (*d*, $^3J_{HH}$=7.8 Hz, 1H, CH), 6.82 (*d*, $^3J_{HH}$=8.0 Hz, 1H, CH), 2.5 (*s*, 3H, SCH_3), 2.04 (*s*, 3H, CH_3), 2.0 (*s*, 3H, CH_3). **^{13}C NMR** ($CDCl_3$, 100 MHz) δ_C: 140.6 (Cq, 1C), 140.5 (Cq, 1C), 139.3 (Cq, 1C), 138.7 (CH, 1C), 138.3(Cq, 1C), 135.9 (Cq, 1C), 134.8 (CH, 1C), 133.0 (CH, 1C), 131.9 (CH, 2C), 130.9 (CH, 1C), 129.2 (CH, 1C), 128.9 (CH, 1C), 125.9 (CH, 2C), 122.4 (Cq, 1C), 119.6 (Cq, 1C), 93.0 (Cq, 1C), 89.4 (Cq,1C), 89.2 (Cq, 1C), 19.7 (CH_3, 1C), 19.5 (CH_3, 1C), 15.4 (SCH_3, 1C).

Compound 11

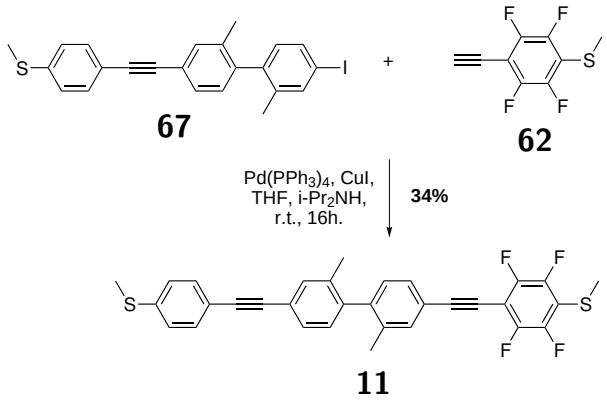

Compound **11** was obtained following **method A**: Compound **67** (128 mg, 0.28 mmol), THF (20 mL) $^{i}Pr_2NH$ (5 mL), **62** (74 mg, 0.34 mmol), CuI (2.7 mg, 0.01 mmol) and $Pd(PPh_3)_2Cl_2$ (16 mg, 0.01 mmol). The reaction mixture was stirred at r.t. overnight. The crude was chromatographed (silica gel, cyclohexane/dmc 8:2) giving the desired product **11** (52 mg, 0.095 mmol, 34%).

^{1}H NMR ($CDCl_3$, 400 MHz) δ_H: 7.51 (*s*, 1H, CH), 7.45 (*m*, 4H, CH), 7.39 (*d*, $^3J_{HH}$=6.8 Hz, 1H, CH_3), 7.21 (*d*, 2H, $^3J_{HH}$=10.5 Hz, CH_3), 7.12 (*d*, 1H, $^3J_{HH}$=7.8 Hz, CH_3), 7.06 (*d*, 1H, $^3J_{HH}$=7.8 Hz, CH_3), 2.56 (*s*, 3H, SCH_3), 2.50 (*s*, 3H, SCH_3), 2.07 (*s*, 3H, CH_3), 2.05 (*s*, 3H, CH_3). **^{13}C NMR** ($CDCl_3$, 100 MHz) δ_C: 147.8 (Cq, 2C), 145.3 (Cq, 2C), 142.6 (Cq, 1C), 140.8 (Cq, 1C), 139.4 (Cq, 1C), 136.4 (Cq, 1C), 135.9 (Cq, 1C), 133.4 (CH, 1C), 133.0 (CH, 1C), 131.9 (CH, 2C), 129.5 (CH, 1C), 129.3 (CH, 1C), 129.1 (CH, 1C), 128.9 (CH, 1C), 125.9 (CH, 2C), 122.5 (Cq, 1C), 120.7 (Cq, 1C), 119.6 (Cq, 1C), 117.0 (Cq, 1C), 103.8 (Cq, 1C), 102.2 (Cq, 1C), 89.4 (Cq, 1C), 89.3 (Cq, 1C), 74.4 (Cq, 1C), 19.6 (CH_3, 2C), 15.4 (SCH_3, 2C). **EI-MS** m/z (%int.): found: 548.1 (15.09), 547.1 (35.56), 546.1 ([$M^{+\bullet}$], 100%), 273.1 (13.22); calculated for $C_{32}H_{22}F_4S_2$: 546.11

Compound 12

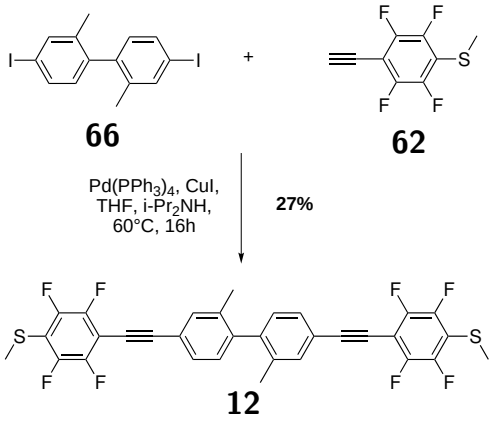

Compound **12** was obtained following **method A**: Compound **66** (81 mg, 0.186 mmol), THF (40 mL) $^{i}Pr_2NH$ (5 mL), **62** (90 mg, 0409 mmol), CuI (2 mg, 0.01 mmol) and $Pd(PPh_3)_4$ (11 mg, 0.01 mmol). The reaction mixture was stirred at 60 °C overnight. The crude was chromatographed (silica gel, cyclohexane/CH_2Cl_2 8:2) giving the desired product **12** (31 mg, 0.05 mmol, 27%).

^{1}H NMR ($CDCl_3$, 400 MHz) δ_H: 7.52 (*s*, 2H, CH), 7.47 (*dd*, 2H, $^3J_{HH}$=7.8 Hz, $^4J_{HH}$=1.0 Hz, CH), 7.12 (*d*, 2H, $^3J_{HH}$=7.8 Hz, CH), 2.57 (*s*, 6H, SCH_3), 2.08 (*s*, 6H, CH_3), **^{13}C NMR** ($CDCl_3$, 100 MHz) δ_C: 147.8 (Cq, 4C), 145.2 (Cq, 4C), 142.3 (Cq, 2C), 136.2 (Cq, 2C), 133.4 (CH, 2C), 129.3 (CH, 2C), 129.3 (CH, 2C), 120.9 (Cq, 2C), 117.0 (Cq, 2C), 103.8 (Cq, 2C), 102.0 (Cq, 2C), 74.4 (Cq, 2C), 19.6 (CH_3, 2C), 17.7 (SCH_3, 2C). **EI-MS** m/z (%int.): found: 618.1 ([$M^{+\bullet}$], 100%), 603.0 (6.58), 309.0 (14.36%), 301.5 (7.12%); calculated for $C_{32}H_{18}F_8S_2$: 618.07

Compound 13

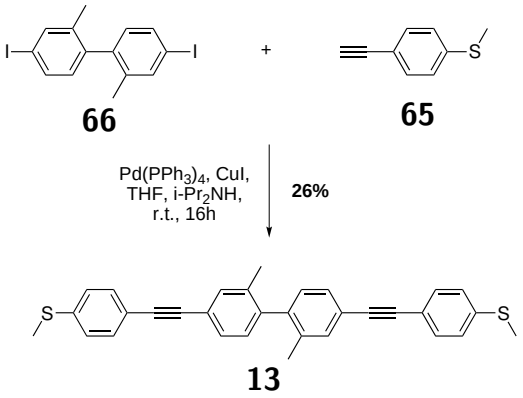

Compound **13** was obtained following **method A**: Compound **66** (175 mg, 0.403 mmol), THF (50 mL) $^{i}Pr_2NH$ (5 mL), **65** (149 mg, 1.01 mmol), CuI (4 mg, 0.02 mmol) and $Pd(PPh_3)_4$ (23 mg, 0.02 mmol). The reaction mixture was stirred at r.t. overnight. The crude was chromatographed (silica gel, cyclohexane/CH_2Cl_2 8:2) giving the desired product **13** (49 mg, 0.103 mmol, 26%).

^{1}H NMR ($CDCl_3$, 400 MHz) δ_H: 7.46 (*m*, 6H, CH), 7.39 (*d*, 2H, $^3J_{HH}$=8.3 Hz, CH), 7.22 (*d*, 4H, $^3J_{HH}$=8.3 Hz, CH), 7.08 (*d*, 2H, $^3J_{HH}$=7.8 Hz, CH), 2.51 (*s*, 6H, SCH_3), 2.06 (*s*, 6H, CH_3). **^{13}C NMR** ($CDCl_3$, 100 MHz) δ_C: 141.2 (Cq, 2C), 139.3 (Cq, 2C), 136.0 (Cq, 2C), 133.0 (CH, 2C), 131.9 (CH, 4C), 129.3 (CH, 2C), 128.8 (CH, 2C), 125.9 (CH, 4C), 122.3 (Cq, 2C), 119.7 (Cq, 2C), 89.5 (Cq, 2C), 89.1 (Cq, 2C), 19.7 (CH_3, 2C), 15.4 (SCH_3, 2C). **EI-MS** m/z (%int.): found: 476.2 (15.28%), 475.1 (36.29%), 474.1 ([$M^{+\bullet}$], 100%), 237.1 (13.72%); calculated for $C_{32}H_{26}S_2$: 474.15

Compound 68

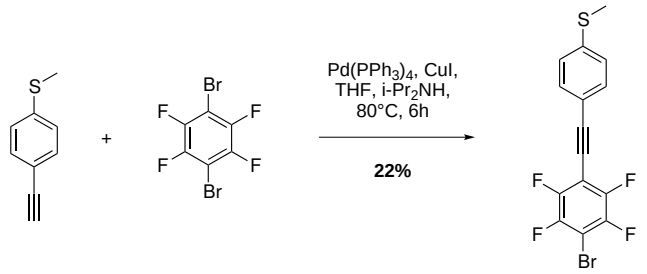

65 **106** **68**

Compound **68** was obtained following **method A**: Compound **106** (1.0 g, 3.26 mmol), THF (15 mL) $^{i}Pr_2NH$ (2 mL), **65** (312 mg, 2.1 mmol), $Pd(PPh_3)_4$ (122 mg, 105 mmol) and CuI (20 mg, 105 mmol). The reaction mixture was stirred at 80 ° C for 6h. The crude was chromatographed (silica gel, cyclohexane/CH_2Cl_2 9:1 to 8:2) giving the desired product **68** as a white solid (174 mg, mmol, 22%).

^{1}**H NMR** ($CDCl_3$, 400 MHz) δ_H: 7.47 (*d*, 2H, $^3J_{HH}$=8.5 Hz, CH), 7.21 (*d*, 2H, $^3J_{HH}$=8.5 Hz, CH), 2.50 (*s*, 3H, SCH_3), ^{13}**C NMR** ($CDCl_3$, 100 MHz) δ_C: 132.1 (CH, 2C), 125.6 (CH, 2C), 15.1 (SCH_3, 2C).

Compound 69

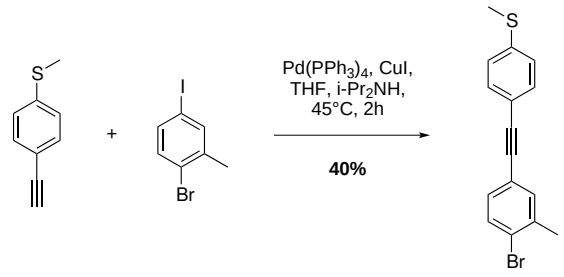

65 **107** **69**

Compound **69** was obtained following **method A**: Compound **107** (1.0 g, 3.37 mmol), THF (15 mL), $^{i}Pr_2NH$ (2 mL), **65** (454 mg, 3.06 mmol), $Pd(PPh_3)_4$ (177 mg, 153 mmol) and CuI (29 mg, 153 mmol). The reaction mixture was stirred at 45 °C overnight. The crude was chromatographed (silica gel, cyclohexane/CH_2Cl_2 9:1 to 8:2) giving the desired product **69** (385 mg, 1.21 mmol, 40 %).

^{1}H NMR ($CDCl_3$, 400 MHz) δ_H: 7.49 (*d*, 1H, $^3J_{HH}$=8.2 Hz, CH), 7.42 (*d*, 2H, $^3J_{HH}$=9.6 Hz, CH), 7.38 (*m*, 1H, CH), 7.19 (*m*, 3H, CH), 2.49 (*s*, 3H, SCH_3), 2.39 (*s*, 3H, CH_3). **^{13}C NMR** ($CDCl_3$, 100 MHz) δ_C: 139.6 (Cq, 1C), 138.8 (Cq, 1C), 133.6 (CH, 1C), 132.4 (CH, 2C), 131.9 (CH, 1C), 130.2 (CH, 1C), 125.9 (CH, 2C), 125.0 (Cq, 1C), 122.5 (Cq, 1C), 119.3 (Cq, 1C), 89.9 (Cq, 1C), 88.6 (Cq, 1C), 22.8 (CH_3, 1C), 15.4 (SCH_3, 1C).

Compound 70

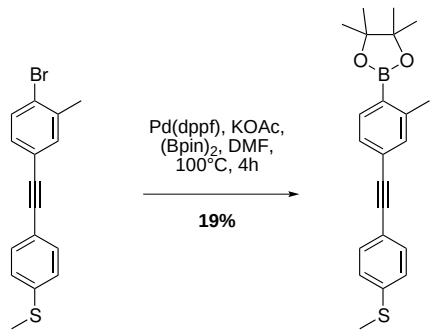

69 **70**

Compound **69** (200 mg, 637 mmol), bis(pinacolato)diboron (180 mg, 0.7 mmol) and KOAc (186 mg, 191 mmol) were dissolved in dry DMF (5 mL). The reaction mixture was degassed with argon for 10 min and the catalyst Pd(dppf) (25 mg, 0.03 mmol) was then added. The reaction mixture was heated for 4h at 100 ° C followed by the evaporation of the solvents. The crude was then chromatographed (silica gel, CH_2Cl_2/cyclohexane 1:2) giving the desired product **70** as a yellow solid (43 mg, 0.118 mmol, 19 %).

^{1}**H NMR** ($CDCl_3$, 400 MHz) δ_H: 7.73 (*d*, 1H, $^3J_{HH}$=7.5 Hz, CH), 7.43 (*d*, 2H, $^3J_{HH}$=8.6 Hz, CH), 7.32 (*s*, 1H, CH), 7.31 (*d*, 1H, $^3J_{HH}$=9.5 Hz, CH), 7.20 (*d*, 2H, $^3J_{HH}$=8.5 Hz, CH), 2.53 (*s*, 3H, CH_3), 2.49 (*s*, 3H, SCH_3), 1.34 (*s*, 12H, CH_3). ^{13}**C NMR** ($CDCl_3$, 100 MHz) δ_C: 144.8 (Cq, 2C), 139.4 (Cq, 1C), 135.8 (CH, 1C), 132.6 (CH, 1C), 131.9 (CH, 2C), 127.7 (CH, 1C), 125.9 (CH, 2C), 125.4 (Cq, 1C), 119.6 (Cq, 1C), 90.1 (Cq, 1C), 89.8 (Cq, 1C), 83.6 (Cq, 2C), 24.9 (CH_3, 4C), 22.0 (CH_3, 1C), 15.4 (SCH_3, 1C).

Compound 14

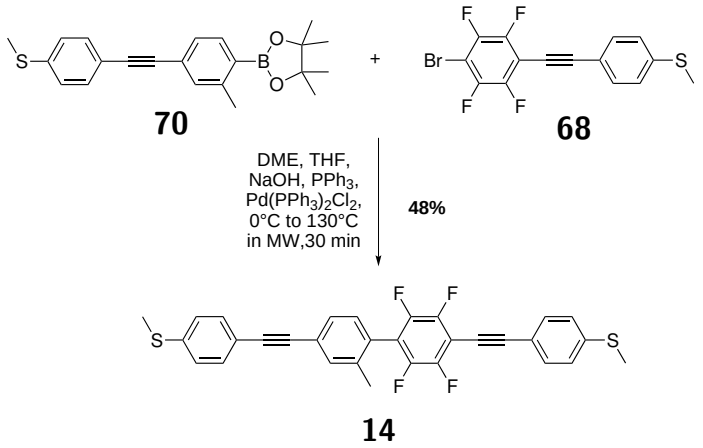

Compound **68** (20.6 mg, 0.055 mmol) was dissolved in dimethoxyethane (0.8 mL) and THF (0.8 mL). This solution was degassed with argon and cooled at 0 ˚C. Compound **70** (20 mg, 0.055 mmol), $Pd(PPh_3)_2Cl_2$ (1.5 mg, 0.002 mmol) and PPh_3 (2.3 g, 0.009 mmol) were added (yellow suspension) followed by NaOH (2M, 0.4 mL) at 0 ˚C. The vial was irradiated at 130 ˚C for 30 min in the microwave. The reaction mixture was extracted with CH_2Cl_2 (3x). The combined organic layers were dried over Na_2SO_4, filtered and evaporated giving a yellow solid. The crude was chromatographed twice with a preparative thin layer chromatography (silica gel, CH_2Cl_2/hexane 1:2) and (silica gel, CH_2Cl_2/hexane 4:6) giving the desired compound **14** (14 mg, 0.026 mmol, 48%).

^{1}H NMR ($CDCl_3$, 400 MHz) δ_H: 7.52 (*m*, 3H, CH), 7.45 (*m*, 3H, CH), 7.21-7.26 (*m*, 5H, CH), 2.52 (*s*, 3H, SCH_3), 2.51 (*s*, 3H, SCH_3), 2.21 (*s*, 12H, CH_3). **^{13}C NMR** ($CDCl_3$, 100 MHz) δ_C: 141.4 (Cq, 2C), 139.7 (Cq, 2C), 137.6 (Cq, 2C), 133.4 (CH, 1C), 132.2 (CH, 2C), 132.0 (CH, 2C), 130.6 (CH, 1C), 129.0 (CH, 1C), 125.9 (CH, 2C), 125.7 (CH, 2C), 124.7 (Cq, 2C), 120.0 (Cq, 1C), 119.3 (Cq, 2C), 117.8 (Cq, 2C), 90.3 (Cq, 2C), 88.9 (Cq, 2C), 19.6 (CH_3, 1C), 15.4 (SCH_3, 1C), 15.2 (SCH_3, 1C). **EI-MS** m/z (%int.): found: 532.1 ([$M^{+\bullet}$], 100%), 517.1 (15.8%), 502.0 (7.87%), 266.0 (11.37%); calculated for $C_{31}H_{20}F_4S_2$: 532.09

Bibliography

[1] de Meijere, A.; Diederich, F. *Metal-Catalyzed Cross-Coupling Reactions*, 2nd ed.; Wiley-VCH Verlag GmbH & Co. KGaA, 2004.

[2] Sonogashira, K.; Tohda, Y.; Hagihara, N. *Tetrahedron Lett.* **1975**, *16*, 4467–4470.

[3] Nicolaou, K. C.; Sorensen, E. J. *Classics in total synthesis : targets, strategies, methods*; VCH: Weinheim; New York, 1996.

[4] Nicolaou, K. C.; Bulger, P. G.; Sarlah, D. *Angew. Chem. Int. Ed.* **2005**, *44*, 4442–4489.

[5] Weibel, N.; Grunder, S.; Mayor, M. *Org. Biomol. Chem.* **2007**, 2343–2353.

[6] (a) Nicolaou, K. C.; Dai, W.-M. *Angew. Chem. Int. Ed.* **1991**, *30*, 1387–1416; (b) Nicolaou, K. C.; Smith, A. L. *Acc. Chem. Res.* **1992**, *25*, 497–503; (c) Nicolaou, K. C.; Smith, A. L.; Yue, E. W. *Proc. Natl. Acad. Sci. U.S.A.* **1993**, *90*, 5881–5888.

[7] Diederich, F.; Stang, P.; Tykwinski, R. *Acetylene chemistry : chemistry, biology and material science*; Wiley-VCH: Weinheim, 2005.

[8] Rucareanu, S.; Schuwey, A.; Gossauer, A. *J. Am. Chem. Soc.* **2006**, *128*, 3396–3413.

[9] Jones, L.; Schumm, J. S.; Tour, J. M. *J. Org. Chem.* **1997**, *62*, 1388–1410.

[10] Jenny, N. M.; Mayor, M.; Eaton, T. R. *Eur. J. Org. Chem.* **2011**, *2011*, 4965–4983.

[11] Stephens, R. D.; Castro, C. E. *J. Org. Chem.* **1963**, *28*, 3313–3315.

[12] Dieck, H.; Heck, F. *J. Organomet. Chem.* **1975**, *93*, 259–263.

[13] Chinchilla, R.; Nájera, C. *Chem. Rev.* **2007**, *107*, 874–922.

[14] Xue, L.; Lin, Z. *Chem. Soc. Rev.* **2010**, *39*, 1692–1705.

[15] Chinchilla, R.; Nájera, C. *Chem. Soc. Rev.* **2011**, *40*, 5084–5121.

[16] Siemsen, P.; Livingston, R. C.; Diederich, F. *Angew. Chem. Int. Ed.* **2000**, *39*, 2632–2657.

[17] Fleckenstein, C. A.; Plenio, H. *Chem. Soc. Rev.* **2010**, *39*, 694–711.

[18] Li, Z.; Fu, Y.; Guo, Q.; Liu, L. *Organometallics* **2008**, *27*, 4043–4049.

[19] Wuts, P. G. M.; Greene, T. W. *Greene's Protective Groups in Organic Synthesis*; John Wiley and Sons, 2006.

[20] Höger, S.; Bonrad, K. *J. Org. Chem.* **2000**, *65*, 2243–2245.

[21] Gaefke, G.; Höger, S. *Synthesis* **2008**, *2008*, 2155–2157.

[22] Mayor, M.; Didschies, C. *Angew. Chem. Int. Ed.* **2003**, *42*, 3176–3179.

[23] Sonoda, M.; Inaba, A.; Itahashi, K.; Tobe, Y. *Org. Lett.* **2001**, *3*, 2419–2421.

[24] Shultz, D. A.; Gwaltney, K. P.; Lee, H. *J. Org. Chem.* **1998**, *63*, 4034–4038.

[25] Haley, M. M.; Brand, S. C.; Pak, J. J. *Angew. Chem. Int. Ed.* **1997**, *36*, 836–838.

[26] Mio, M. J.; Kopel, L. C.; Braun, J. B.; Gadzikwa, T. L.; Hull, K. L.; Brisbois, R. G.; Markworth, C. J.; Grieco, P. A. *Org. Lett.* **2002**, *4*, 3199–3202.

[27] Smith, M.; March, J. *March's advanced organic chemistry : reactions, mechanisms, and structure.*; Wiley-VCH, 2007.

[28] Müller, S.; Liepold, B.; Roth, G. J.; Bestmann, H. J. *Synlett* **1996**, 521–522.

[29] Corey, E.; Fuchs, P. *Tetrahedron Lett.* **1972**, *13*, 3769–3772.

[30] Miyaura, N.; Suzuki, A. *Chem. Commun.* **1979**, 866–867.

[31] Miyaura, N.; Yamada, K.; Suzuki, A. *Tetrahedron Lett.* **1979**, *20*, 3437–3440.

[32] C. Nicolaou, K.; M. Ramanjulu, J.; Natarajan, S.; Bräse, S.; Rübsam, F. *Chem. Commun.* **1997**, 1899–1900.

[33] Nicolaou, K. C.; Koumbis, A. E.; Takayanagi, M.; Natarajan, S.; Jain, N. F.; Bando, T.; Li, H.; Hughes, R. *Chem. Eur. J.* **1999**, *5*, 2622–2647.

[34] Rehahn, M.; Schlüter, A.-D.; Wegner, G.; Feast, W. J. *Polymer* **1989**, *30*, 1054–1059.

[35] Schlüter, A. D. *J. Polym. Sci., Part A: Polym. Chem.* **2001**, *39*, 1533–1556.

[36] Miyaura, N.; Suzuki, A. *Chem. Rev.* **1995**, *95*, 2457–2483.

[37] Suzuki, A. *J. Organomet. Chem.* **1999**, *576*, 147–168.

[38] Suzuki, A. *Angew. Chem. Int. Ed.* **2011**, *50*, 6722–6737.

[39] Ridgway, B. H.; Woerpel, K. A. *J. Org. Chem.* **1998**, *63*, 458–460.

[40] Matos, K.; Soderquist, J. A. *J. Org. Chem.* **1998**, *63*, 461–470.

[41] Kappe, C. O. *Angew. Chem. Int. Ed.* **2004**, *43*, 6250–6284.

[42] Oliver Kappe, C. *Chem. Soc. Rev.* **2008**, *37*, 1127–1139.

[43] Larhed, M., Olofssonq, K., Eds. *Microwave Methods in Organic Synthesis*; Topics in Current Chemistry; Springer Berlin, Heidelberg, 2006; Vol. 266.

[44] Kappe, C. O.; Stadler, A. *Microwaves in organic and medicinal chemistry*; Wiley-VCH: Weinheim, 2005.

[45] Kappe, C. O.; Dallinger, D.; Murphree, S. *Practical microwave synthesis for organic chemists : strategies, instruments, and protocols*; Wiley-VCH: Weinheim, 2009.

[46] Mehta, V. P.; Van der Eycken, E. V. *Chem. Soc. Rev.* **2011**, *40*, 4925–4936.

[47] Erdélyi, M.; Gogoll, A. *J. Org. Chem.* **2001**, *66*, 4165–4169.

[48] Kwan, P. H.; MacLachlan, M. J.; Swager, T. M. *J. Am. Chem. Soc.* **2004**, *126*, 8638–8639.

[49] Khan, A.; Hecht, S. *Chem. Commun.* **2004**, 300–301.

[50] Han, J. W.; Castro, J. C.; Burgess, K. *Tetrahedron Lett.* **2003**, *44*, 9359–9362.

[51] Nehls, B. S.; Asawapirom, U.; Füldner, S.; Preis, E.; Farrell, T.; Scherf, U. *Adv. Funct. Mater.* **2004**, *14*, 352–356.

[52] Cargill, M. R.; Sandford, G.; Tadeusiak, A. J.; Yufit, D. S.; Howard, J. A. K.; Kilickiran, P.; Nelles, G. *J. Org. Chem.* **2010**, *75*, 5860–5866.

[53] Höger, S. *Nachrichten aus der Chemie* **2011**, *59*, 453–455.

[54] Lakowicz, J. R. *Principles of fluorescence spectroscopy*, 3rd ed.; Springer: New York, 2006.

[55] Brouwer, A. M. *Pure Appl. Chem.* **2011**, *83*, 2213–2228.

[56] Würthner, F.; Ahmed, S.; Thalacker, C.; Debaerdemaeker, T. *Chem. Eur. J.* **2002**, *8*, 4742–4750.

[57] Thalacker, C.; Miura, A.; Feyter, S. D.; Schryver, F. C. D.; Würthner, F. *Org. Biomol. Chem.* **2005**, *3*, 414–422.

[58] Karstens, T.; Kobs, K. *J. Phys. Chem.* **1980**, *84*, 1871–1872.

[59] Umberger, J. Q.; LaMer, V. K. *J. Am. Chem. Soc.* **1945**, *67*, 1099–1109.

[60] Melhuish, W. H. *J. Phys. Chem.* **1961**, *65*, 229–235.

[61] Kirby, E. P.; Steiner, R. F. *J. Phys. Chem.* **1970**, *74*, 4480–4490.

[62] Hamai, S.; Hirayama, F. *J. Phys. Chem* **1983**, *87*, 83–89.

[63] Seybold, G.; Wagenblast, G. *Dyes Pigm.* **1989**, *11*, 303–317.

[64] Gvishi, R.; Reisfeld, R.; Burshtein, Z. *Chem. Phys. Lett.* **1993**, *213*, 338–344.

[65] Haick, H.; Cahen, D. *Prog. Surf. Sci.* **2008**, *83*, 217–261.

[66] Prokopuk, N.; Son, K.-A. *J. Phys. Condens. Matter* **2008**, *20*, 374116.

[67] McCreery, R. L.; Bergren, A. J. *Adv. Mater.* **2009**, *21*, 4303–4322.

[68] Bumm, L. A.; Arnold, J. J.; Cygan, M. T.; Dunbar, T. D.; Burgin, T. P.; Jones, L.; Allara, D. L.; Tour, J. M.; Weiss, P. S. *Science* **1996**, *271*, 1705–1707.

[69] Xu, B.; Tao, N. J. *Science* **2003**, *301*, 1221–1223.

[70] Cui, X. D.; Primak, A.; Zarate, X.; Tomfohr, J.; Sankey, O. F.; Moore, A. L.; Moore, T. A.; Gust, D.; Harris, G.; Lindsay, S. M. *Science* **2001**, *294*, 571–574.

[71] Choi, S. H.; Kim, B.; Frisbie, C. D. *Science* **2008**, *320*, 1482–1486.

[72] Frei, M.; Aradhya, S. V.; Hybertsen, M. S.; Venkataraman, L. *J. Am. Chem. Soc.* **2012**, *134*, 4003–4006.

[73] Wu, S.; González, M. T.; Huber, R.; Grunder, S.; Mayor, M.; Schönenberger, C.; Calame, M. *Nat. Nanotechnol.* **2008**, *3*, 569–574.

[74] Reichert, J.; Ochs, R.; Beckmann, D.; Weber, H. B.; Mayor, M.; Löhneysen, H. v. *Phys. Rev. Lett.* **2002**, *88*, 176804.

[75] Huber, R.; González, M. T.; Wu, S.; Langer, M.; Grunder, S.; Horhoiu, V.; Mayor, M.; Bryce, M. R.; Wang, C.; Jitchati, R.; Schönenberger, C.; Calame, M. *J. Am. Chem. Soc.* **2007**, *130*, 1080–1084.

[76] Vonlanthen, D.; Mishchenko, A.; Elbing, M.; Neuburger, M.; Wandlowski, T.; Mayor, M. *Angew. Chem. Int. Ed.* **2009**, *48*, 8886–8890.

[77] Chen, F.; Li, X.; Hihath, J.; Huang, Z.; Tao, N. *J. Am. Chem. Soc.* **2006**, *128*, 15874–15881.

[78] Tour, J. M.; Jones, L.; Pearson, D. L.; Lamba, J. J. S.; Burgin, T. P.; Whitesides, G. M.; Allara, D. L.; Parikh, A. N.; Atre, S. *J. Am. Chem. Soc.* **1995**, *117*, 9529–9534.

[79] Park, Y. S.; Whalley, A. C.; Kamenetska, M.; Steigerwald, M. L.; Hybertsen, M. S.; Nuckolls, C.; Venkataraman, L. *J. Am. Chem. Soc.* **2007**, *129*, 15768–15769.

[80] Meisner, J. S.; Kamenetska, M.; Krikorian, M.; Steigerwald, M. L.; Venkataraman, L. *Nano Lett.* **2011**, *11*, 1575–1579.

[81] Mishchenko, A.; Zotti, L. A.; Vonlanthen, D.; Bürkle, M.; Pauly, F.; Cuevas, J. C.; Mayor, M.; Wandlowski, T. *J. Am. Chem. Soc.* **2010**, *133*, 184–187.

[82] Kamenetska, M.; Quek, S. Y.; Whalley, A. C.; Steigerwald, M. L.; Choi, H. J.; Louie, S. G.; Nuckolls, C.; Hybertsen, M. S.; Neaton, J. B.; Venkataraman, L. *J. Am. Chem. Soc.* **2010**, *132*, 6817–6821.

[83] Whelan, C. M.; Kinsella, M.; Carbonell, L.; Meng Ho, H.; Maex, K. *Microelectronic Engineering* **2003**, *70*, 551–557.

[84] Chen, H.; Heng, C. K.; Puiu, P. D.; Zhou, X. D.; Lee, A. C.; Lim, T. M.; Tan, S. N. *Anal. Chim. Acta* **2005**, *554*, 52–59.

[85] Castellana, E. T.; Cremer, P. S. *Surf. Sci. Rep.* **2006**, *61*, 429–444.

[86] Bonanni, B.; Bizzarri, A. R.; Cannistraro, S. *J. Phys. Chem. B* **2006**, *110*, 14574–14580.

[87] Tour, J. M. *Acc. Chem. Res.* **2000**, *33*, 791–804.

[88] Brust, M.; Walker, M.; Bethell, D.; Schiffrin, D. J.; Whyman, R. *Chem. Commun.* **1994**, 801–802.

[89] Love, J. C.; Estroff, L. A.; Kriebel, J. K.; Nuzzo, R. G.; Whitesides, G. M. *Chem. Rev.* **2005**, *105*, 1103–1170.

[90] Vericat, C.; Vela, M. E.; Benitez, G.; Carro, P.; Salvarezza, R. C. *Chem. Soc. Rev.* **2010**, *39*, 1805–1834.

[91] Rajwar, D.; Sun, X.; Cho, S. J.; Grimsdale, A. C.; Fichou, D. *CrystEngComm* **2012**, *14*, 5182–5187.

[92] Ohira, A.; Sakata, M.; Hirayama, C.; Kunitake, M. *Org. Biomol. Chem.* **2003**, *1*, 251–253.

[93] Yoshimoto, S.; Suto, K.; Tada, A.; Kobayashi, N.; Itaya, K. *J. Am. Chem. Soc.* **2004**, *126*, 8020–8027.

[94] Höger, S.; Bonrad, K.; Mourran, A.; Beginn, U.; Möller, M. *J. Am. Chem. Soc.* **2001**, *123*, 5651–5659.

[95] Gong, J.-R.; Wan, L.-J.; Yuan, Q.-H.; Bai, C.-L.; Jude, H.; Stang, P. J. *Proc. Natl. Acad. Sci. U.S.A.* **2005**, *102*, 971–974.

[96] Kudernac, T.; Lei, S.; Elemans, J. A. A. W.; De Feyter, S. *Chem. Soc. Rev.* **2009**, *38*, 402–421.

[97] Theobald, J. A.; Oxtoby, N. S.; Phillips, M. A.; Champness, N. R.; Beton, P. H. *Nature* **2003**, *424*, 1029–1031.

[98] Theobald, J. A.; Oxtoby, N. S.; Champness, N. R.; Beton, P. H.; Dennis, T. J. S. *Langmuir* **2005**, *21*, 2038–2041.

[99] Perdigão, L. M. A.; Perkins, E. W.; Ma, J.; Staniec, P. A.; Rogers, B. L.; Champness, N. R.; Beton, P. H. *J. Phys. Chem. B* **2006**, *110*, 12539–12542.

[100] Staniec, P. A.; Perdigão, L. M. A.; Saywell, A.; Champness, N. R.; Beton, P. H. *ChemPhysChem* **2007**, *8*, 2177–2181.

[101] Perdigão, L. M. A.; Saywell, A.; Fontes, G. N.; Staniec, P. A.; Goretzki, G.; Phillips, A. G.; Champness, N. R.; Beton, P. H. *Chem. Eur. J.* **2008**, *14*, 7600–7607.

[102] Saywell, A.; Magnano, G.; Satterley, C. J.; Perdigão, L. M. A.; Champness, N. R.; Beton, P. H.; O'Shea, J. N. *J. Phys. Chem. C* **2008**, *112*, 7706–7709.

[103] Slater (née Phillips), A. G.; Beton, P. H.; Champness, N. R. *Chem. Sci.* **2011**, *2*, 1440–1448.

[104] Blunt, M. O.; Russell, J. C.; Gimenez-Lopez, M. d. C.; Taleb, N.; Lin, X.; Schröder, M.; Champness, N. R.; Beton, P. H. *Nat. Chem.* **2011**, *3*, 74–78.

[105] Madueno, R.; Räisänen, M. T.; Silien, C.; Buck, M. *Nature* **2008**, *454*, 618–621.

[106] Silien, C.; Räisänen, M.; Buck, M. *Angew. Chem. Int. Ed.* **2009**, *48*, 3349–3352.

[107] Silien, C.; Räisänen, M. T.; Buck, M. *Small* **2010**, *6*, 391–394.

[108] Räisänen, M. T.; Slater (née Phillips), A. G.; Champness, N. R.; Buck, M. *Chem. Sci.* **2012**, *3*, 84.

[109] Lu, J.; Lei, S.-b.; Zeng, Q.-d.; Kang, S.-z.; Wang, C.; Wan, L.-j.; Bai, C.-l. *J. Phys. Chem. B* **2004**, *108*, 5161–5165.

[110] *Angew. Chem. Int. Ed.* **2007**, *46*, 2831–2834.

[111] Stepanow, S.; Lingenfelder, M.; Dmitriev, A.; Spillmann, H.; Delvigne, E.; Lin, N.; Deng, X.; Cai, C.; Barth, J. V.; Kern, K. *Nat. Mater.* **2004**, *3*, 229–233.

[112] Räisänen, M. T.; Slater (née Phillips), A. G.; Champness, N. R.; Buck, M. *Chem. Sci.* **2012**, *3*, 84.

[113] Bertrand, H.; Silly, F.; Teulade-Fichou, M.-P.; Tortech, L.; Fichou, D. *Chem. Commun.* **2011**, *47*, 10091.

[114] Wintjes, N.; Bonifazi, D.; Cheng, F.; Kiebele, A.; Stöhr, M.; Jung, T.; Spillmann, H.; Diederich, F. *Angew. Chem. Int. Ed.* **2007**, *46*, 4089–4092.

[115] Qiu, X. H.; Nazin, G. V.; Ho, W. *Science* **2003**, *299*, 542–546.

[116] Dong, Z.-C.; Guo, X.-L.; Trifonov, A. S.; Dorozhkin, P. S.; Miki, K.; Kimura, K.; Yokoyama, S.; Mashiko, S. *Phys. Rev. Lett.* **2004**, *92*, 086801.

[117] Marquardt, C. W.; Grunder, S.; Baszczyk, A.; Dehm, S.; Hennrich, F.; Löhneysen, H. v.; Mayor, M.; Krupke, R. *Nat. Nanotechnol.* **2010**, *5*, 863–867.

[118] Grunder, S.; Muñoz Torres, D.; Marquardt, C.; Blaszczyk, A.; Krupke, R.; Mayor, M. *Eur. J. Org. Chem.* **2011**, *2011*, 478–496.

[119] Błaszczyk, A.; Mayor, M. *Helv. Chim. Acta* **2006**, 1986–2005.

[120] Vollmann, H.; Becker, H.; Corell, M.; Streeck, H. *Justus Liebig's Annalen der Chemie* **1937**, *531*, 1–159.

[121] Rehahn, M.; Schlüter, A.-D.; Feast, W. J. *Synthesis* **1988**, *1988*, 386–388.

[122] Kukula, H.; Veit, S.; Godt, A. *Eur. J. Org. Chem.* **1999**, *1999*, 277–286.

[123] Grunder, S. New Functional Molecules in Molecular Junctions. Ph.D. thesis, University of Basel, 2009.

[124] Anderson, S. *Chem. Eur. J.* **2001**, *7*, 4706–4714.

[125] Würthner, F. *Chem. Commun.* **2004**, 1564–1579.

[126] Kobayashi, N.; Kijima, M. *J. Mater. Chem.* **2008**, *18*, 1037.

[127] Villgerodt, C.; Arnold, E. *Ber. Dtsch. Chem. Ges.* **1901**, *34*, 3343–3354.

[128] Krasnokutskaya, E.; Semenischeva, N.; Filimonov, V.; Knochel, P. *Synthesis* **2007**, 81–84.

[129] Diercks, R.; Armstrong, J. C.; Boese, R.; Vollhardt, K. P. C. *Angew. Chem. Int. Ed.* **1986**, *25*, 268–269.

[130] Aviram, A.; Ratner, M. A. *Chem. Phys. Lett.* **1974**, *29*, 277–283.

[131] Ng, M.-K.; Yu, L. *Angew. Chem. Int. Ed.* **2002**, *41*, 3598–3601.

[132] Díez-Pérez, I.; Hihath, J.; Lee, Y.; Yu, L.; Adamska, L.; Kozhushner, M. A.; Oleynik, I. I.; Tao, N. *Nat. Chem.* **2009**, *1*, 635–641.

[133] Metzger, R. M. In *Introducing Molecular Electronics*; Cuniberti, G., Richter, K., Fagas, G., Eds.; Springer Berlin Heidelberg, 2005; Vol. 680; pp 313–349.

[134] Elbing, M.; Ochs, R.; Koentopp, M.; Fischer, M.; Hänisch, C. v.; Weigend, F.; Evers, F.; Weber, H. B.; Mayor, M. *Proc. Natl. Acad. Sci. U.S.A.* **2005**, *102*, 8815–8820.

[135] Lörtscher, E.; Gotsmann, B.; Lee, Y.; Yu, L.; Rettner, C.; Riel, H. *ACS Nano* **2012**, *6*, 4931–4939.

[136] Wenner, W. *J. Org. Chem.* **1952**, *17*, 523–528.

[137] Takahashi, M.; Nishizawa, N.; Ohno, S.; Kakita, M.; Fujita, N.; Yamashita, M.; Sengoku, T.; Yoda, H. *Tetrahedron* **2009**, *65*, 2669–2677.

[138] Durola, F.; Hanss, D.; Roesel, P.; Sauvage, J.-P.; Wenger, O. S. *Eur. J. Org. Chem.* **2007**, *2007*, 125–135.

[139] Rodriguez, J.; Martin-Villamil, R.; Lafuente, A. *Tetrahedron* **2003**, *59*, 1021–1032.

Curriculum Vitae

David Muñoz Torres

13 April 1983 (Fribourg, CH)
Spanish nationality
david.munoz@unibas.ch

EDUCATION

PhD Degree in Chemistry - *October 2008 - September 2012*
University of Basel, Switzerland
Specialization: Synthetic Organic Chemistry
Supervisor: Prof. Marcel Mayor
Master Degree in Chemistry - *October 2005 - August 2007*
University of Fribourg, Switzerland
Specialization: Synthetic Organic Chemistry
Supervisor: Prof. Titus A. Jenny
Bachelor Degree in Chemistry - *October 2002 - July 2005*
University of Fribourg, Switzerland

LANGUAGES

French, Spanish - Mother Tongue
English - Proficient User
German - Independent User

EXPERIENCE

Students' Assistant in Chemistry - *Mai 2004 - September 2012*
Private classes, exercises and lab courses,

Universities of Fribourg and Basel, Switzerland
Internship in Organic Chemistry - *September 2007 - February 2008*
Philips Electronics Nederland B.V., Biomolecular Engineering Department
Eindhoven, The Netherlands
Synthesis of contrast agents and polymers modifications
Supervisor: Dr Johan Lub
Hospitality Staff Member - *March 2006, 2007*
Fribourg International Film Festival, Switzerland
Director's chaperone
Internship in Radiochemistry - *September - October 2006*
Universidad de Buenos Aires, Buenos Aires, Argentina
Synthesis and in vivo studies of serotonin derivatives
Supervisor: Dr Arturo Vitale
Teacher of Person with Special Needs - *December 2005*
Palmarin, Senegal

MISCELLANEOUS

Chemistry Students' Representative - *June 2004 - June 2007*
Faculty of science and chemistry department councils
University of Fribourg, Switzerland
Chemistry Students' Association - *October 2003 - June 2007*
University of Fribourg, Switzerland
Member of the Young People's Jury - *March 2004*
Fribourg International Film Festival, Switzerland
Radio Presenter - *April 2001 - November 2003*
Radio Quartier d'Alt, Fribourg, Switzerland

HOBBYS

Cinema
Foreign and independent cinema
Sports
Running (half-marathon distance), aerobics, football, etc...
Travel
Argentina (November 2006)
The Netherlands (September 2007 - February 2008)
Peru - Bolivia (April 2008 - June 2008)